Los Alamos
NATIONAL LABORATORY

memorandum

X-Computational Physics Division
Monte Carlo Methods, Codes, and Applications Group

Group XCP-3, MS F663
Los Alamos, New Mexico 87545
505/667-1920

To/MS: Distribution
From/MS: Jeffrey A. Favorite / XCP-3, MS F663
Phone/Email: 7-7941 / fave@lanl.gov
Symbol: XCP-3:19–022(U) (LA–UR–19–26249)
Date: July 1, 2019 (Rev. 0)

SUBJECT: (U) SENSMG: First-Order Sensitivities of Neutron Reaction Rates, Reaction-Rate Ratios, Leakage, k_{eff}, α, and Subcritical Multiplication Using PARTISN

I. Introduction

SENSMG is a tool for computing first-order sensitivities of neutron reaction rates, reaction-rate ratios, leakage, k_{eff}, α, and subcritical multiplication using the PARTISN multigroup discrete-ordinates code.[1] SENSMG computes sensitivities to all of the transport cross sections and data (total, fission,[a] nu, chi, and all scattering moments), four edit cross sections (absorption, capture, elastic scattering, and inelastic scattering), and the density for every isotope and energy group. It also computes sensitivities to the mass density for every material and derivatives with respect to all interface locations and outer boundaries. The tool can be used for one-dimensional spherical and slab (r) and two-dimensional cylindrical (r-z) geometries. The tool can be used for fixed-source and eigenvalue problems. For most responses, the tool implements Generalized Perturbation Theory (GPT) as discussed by Williams[2] and Stacey.[3] The tool is thus limited to computing sensitivities only for GPT-allowable responses.[4] For subcritical multiplication, the tool implements sensitivities derived by O'Brien[5] and Clark.[6]

Section II of this report describes the theory behind adjoint-based sensitivities, gives the equations that SENSMG solves, and defines the sensitivities that are output. Section III describes the user interface, including the input file and command line options. Section IV describes the output. Section V gives some notes about the coding that may be of interest. Section VI presents some sample problems and discusses verification, which is ongoing. Section VII lists needs and ideas for future work. Appendix A lists most of the input files whose results are presented in Sec. VI. Appendix B provides some useful details on one of the cross-section libraries that SENSMG supports.

[a] Technically, fission is an edit cross section in PARTISN because only the product with nu is used in the transport.

II. Theory and Definitions

II.A. Reaction rates, reaction-rate ratios, and sensitivities

Define two reaction rates as

$$R_1 \equiv \int_V dV \sum_{g=1}^{G} \Sigma_1^g(r)\phi^g(r) \tag{1}$$

and

$$R_2 \equiv \int_V dV \sum_{g=1}^{G} \Sigma_2^g(r)\phi^g(r), \tag{2}$$

where V represents the problem domain and r is a point within the volume V, g is an energy group index, G is the number of energy groups, $\Sigma_1^g(r)$ and $\Sigma_2^g(r)$ are arbitrary macroscopic cross sections in group g, and $\phi^g(r)$ is the scalar flux in group g at point r, defined as

$$\phi^g(r) \equiv \int_{4\pi} d\hat{\mathbf{\Omega}}\, \psi^g(r,\hat{\mathbf{\Omega}}), \tag{3}$$

where $\psi^g(r,\hat{\mathbf{\Omega}})$ is the angular flux in group g at point r in direction $\hat{\mathbf{\Omega}}$. The reaction cross sections $\Sigma_1^g(r)$ and $\Sigma_2^g(r)$ are for arbitrary nuclides that need not be present in the problem. They are defined to be zero outside of a subset of V within which the reaction rates are assumed to be measured.

The ratio of the reaction rates is

$$R \equiv \frac{R_1}{R_2} = \frac{\int_V dV \sum_{g=1}^{G} \Sigma_1^g(r)\phi^g(r)}{\int_V dV \sum_{g=1}^{G} \Sigma_2^g(r)\phi^g(r)}. \tag{4}$$

The relative sensitivity $S_{R,x}^g$ of R to a transport cross section σ_x^g for reaction x in group g is defined to be

$$S_{R,x}^g \equiv \frac{\sigma_{x,0}^g}{R_0} \left.\frac{\partial R}{\partial \sigma_x^g}\right|_{\sigma_x^g = \sigma_{x,0}^g}, \tag{5}$$

where subscript 0 indicates the initial base case. The transport cross section σ_x^g is for a specific nuclide that is present in the problem.

The derivative of R with respect to σ_x^g is found by differentiating Eq. (4) with respect to σ_x^g, noting that g denotes a specific energy group. The result is

$$\begin{aligned} \frac{\partial R}{\partial \sigma_x^g} = {} & \frac{1}{R_2}\left(\int_V dV \frac{\partial \Sigma_1^g(r)}{\partial \sigma_x^g}\phi^g(r) + \int_V dV \Sigma_1^g(r)\frac{\partial \phi^g(r)}{\partial \sigma_x^g}\right) \\ & - \frac{R_1}{R_2^2}\left(\int_V dV \frac{\partial \Sigma_2^g(r)}{\partial \sigma_x^g}\phi^g(r) + \int_V dV \Sigma_2^g(r)\frac{\partial \phi^g(r)}{\partial \sigma_x^g}\right). \end{aligned} \tag{6}$$

Rearranging Eq. (6) and using the result in Eq. (5) yields

$$S_{R,x}^{g} = \left(\frac{\sigma_x^g}{R_1} \int_V dV \frac{\partial \Sigma_1^g(r)}{\partial \sigma_x^g} \phi^g(r) - \frac{\sigma_x^g}{R_2} \int_V dV \frac{\partial \Sigma_2^g(r)}{\partial \sigma_x^g} \phi^g(r) \right) + \left(\frac{\sigma_x^g}{R_1} \int_V dV \Sigma_1^g(r) \frac{\partial \phi^g(r)}{\partial \sigma_x^g} - \frac{\sigma_x^g}{R_2} \int_V dV \Sigma_2^g(r) \frac{\partial \phi^g(r)}{\partial \sigma_x^g} \right). \quad (7)$$

In Eq. (7) and the rest of this paper, we assume that all quantities are evaluated for the base configuration.

The total first-order sensitivity of R to reaction x is the sum over groups:

$$S_{R,x} = \sum_{g=1}^{G} S_{R,x}^{g}. \quad (8)$$

As shown in Eq. (7), the relative sensitivity is the sum of two components. The first term in parentheses on the right hand side is called the *direct effect* of a perturbation in σ_x^g and the second term in parentheses is called the *indirect effect*.

The derivatives in the direct effect are nonzero only when $\Sigma_1^g = N_1 \sigma_1^g = N_1 \sigma_x^g$ and/or $\Sigma_2^g = N_2 \sigma_2^g = N_2 \sigma_x^g$, where N_1 and N_2 are the atom densities for nuclides 1 and 2. The direct effect can therefore be written

$$\left(S_{R,x}^{g} \right)_{direct} = \frac{\int_V dV \Sigma_1^g(r) \phi^g(r)}{R_1} \delta_{x1} - \frac{\int_V dV \Sigma_2^g(r) \phi^g(r)}{R_2} \delta_{x2}, \quad (9)$$

where δ_{xj} (j = 1, 2) is the Kronecker delta that is equal to one when $x = j$ and 0 otherwise. Equation (9) can be readily evaluated given the forward scalar flux $\phi^g(r)$.

Rearranging the second term in parentheses in Eq. (7), the indirect effect, yields

$$\left(S_{R,x}^{g} \right)_{indirect} = \sigma_x^g \int_V dV \left(\frac{\Sigma_1^g(r)}{R_1} - \frac{\Sigma_2^g(r)}{R_2} \right) \frac{\partial \phi^g(r)}{\partial \sigma_x^g}. \quad (10)$$

This term uses the derivative of the scalar flux with respect to σ_x^g. GPT provides an economical means of computing the indirect effect.

II.B. k_{eff} eigenvalue problems

Details of applying GPT to λ-mode (k_{eff}) eigenvalue problems are given in Ref. 2; a good summary is given in Ref. 7. Very briefly, for k_{eff} calculations, the forward and adjoint neutron fluxes $\psi^g(r, \hat{\mathbf{\Omega}})$ and $\psi^{*g}(r, \hat{\mathbf{\Omega}})$ satisfy

$$(A - \lambda F)\psi = 0 \quad (11)$$

and

$$(A^* - \lambda F^*)\psi^* = 0, \quad (12)$$

respectively, where F is the fission neutron production operator, A is the neutron loss operator, $\lambda = 1/k_{eff}$, and the asterisk represents the adjoint operators. Vacuum boundary conditions apply to Eqs. (11) and (12). The indirect effect [Eq. (10)] is

$$\left(S^g_{R,x}\right)_{indirect} = \sigma^g_x \int_V dV \int_{4\pi} d\hat{\mathbf{\Omega}}\, \Gamma^{*g}(r,\hat{\mathbf{\Omega}}) \left(\lambda \frac{\delta F}{\delta \sigma^g_x} - \frac{\delta A}{\delta \sigma^g_x} \right) \psi^g(r,\hat{\mathbf{\Omega}}), \tag{13}$$

where $\Gamma^{*g}(r,\hat{\mathbf{\Omega}})$ is the generalized adjoint function that satisfies

$$\left(A^* - \lambda F^*\right)\Gamma^* = S^* \tag{14}$$

with

$$S^{*g}(r,\hat{\mathbf{\Omega}}) = \frac{1}{R}\frac{\partial R}{\partial \phi} = \frac{\Sigma^g_1(r)}{R_1} - \frac{\Sigma^g_2(r)}{R_2}, \tag{15}$$

which is an isotropic volume source. A vacuum boundary condition applies to Eq. (14). Because the operator acting on Γ^* in Eq. (14) is singular [c.f. Eq. (12)], special techniques are required to solve Eq. (14). Another way of stating this is that Eq. (14) represents a source inserted into a critical system. One technique is the method of successive approximations,[3,8] which calculates $\Gamma^{*g}(r,\hat{\mathbf{\Omega}})$ using

$$\Gamma^{*g}(r,\hat{\mathbf{\Omega}}) = \sum_{n=0}^{\infty} \Gamma^{*g}_n(r,\hat{\mathbf{\Omega}}), \tag{16}$$

where

$$\Gamma^{*g}_n(r,\hat{\mathbf{\Omega}}) = \xi^{*g}_n(r,\hat{\mathbf{\Omega}}) - \frac{\int_V dV \sum_{g=1}^{G} \int_{4\pi} d\hat{\mathbf{\Omega}}\, \xi^{*g}_n(r,\hat{\mathbf{\Omega}}) F\psi^g(r,\hat{\mathbf{\Omega}})}{\int_V dV \sum_{g=1}^{G} \int_{4\pi} d\hat{\mathbf{\Omega}}\, \psi^{*g}(r,\hat{\mathbf{\Omega}}) F\psi^g(r,\hat{\mathbf{\Omega}})} \psi^{*g}(r,\hat{\mathbf{\Omega}}). \tag{17}$$

The $\xi^{*g}_n(r,\hat{\mathbf{\Omega}})$ are generated recursively using

$$\begin{cases} A^*\xi^*_0 = S^*, \\ A^*\xi^*_n = \lambda F^* \Gamma^*_{n-1}, \; n > 0. \end{cases} \tag{18}$$

The second term on the right side of Eq. (17) is included to remove any fundamental mode contamination. Williams[2] has a thorough discussion of this issue.

The generalized adjoint for k_{eff} eigenvalue problems must satisfy[2]

$$\int_V dV \sum_{g=1}^{G} \int_{4\pi} d\hat{\mathbf{\Omega}}\, \Gamma^{*g}(r,\hat{\mathbf{\Omega}}) F\psi^g(r,\hat{\mathbf{\Omega}}) = 0. \tag{19}$$

In fact, as Cacuci has shown,[4] Eq. (19) represents a limitation of GPT and thus of SENSMG, because only those responses whose generalized adjoints satisfy Eq. (19) are GPT-allowable responses that can be treated with GPT and thus SENSMG. In Ref. 4, Cacuci has also proposed an innovative framework that alleviates the shortcomings of GPT, but that framework has not been implemented in PARTISN or in SENSMG.

In practice, of course, the sum in Eq. (16) goes until some user-defined convergence criterion is achieved. Cacuci's framework[4] avoids the use of successive approximations altogether.

A more efficient method of solving Eq. (14) was recently implemented into Oak Ridge National Laboratory's Denovo code.[9] The method takes advantage of Denovo's GMRES and Krylov solvers.

It may also be of interest to compute the sensitivity of an "absolute" reaction rate, such as R_1 of Eq. (1). There is no absolute reaction rate in a critical system unless the amplitude of the flux is

constrained. The power level is often used as a constraint on the flux, but for critical experiments the power level is generally unknown. In Williams's development,[2] the constraint is

$$P \equiv \int_V dV \sum_{g=1}^{G} \Sigma_P^g(r)\phi^g(r) \tag{20}$$

and P and Σ_P^g essentially replace R_2 and Σ_2^g in the equations of this section, particularly Eqs. (4), (9), and (15). In the SENSMG sensitivity tool, we use 1 for Σ_P^g so that P becomes the flux in the reaction-rate region. (Williams[2] uses N where we use P.)

The λ-mode forward angular flux $\psi^g(r,\hat{\mathbf{\Omega}})$ is computed to obtain the baseline ratio R from Eq. (4). It is also used in the solution for $\Gamma^{*g}(r,\hat{\mathbf{\Omega}})$ through R_1 and R_2 in Eq. (15) and through Eq. (17). In addition, Eq. (17) requires the λ-mode adjoint angular flux $\psi^{*g}(r,\hat{\mathbf{\Omega}})$. Because the forward and adjoint fluxes are both computed, k_{eff} sensitivities can always be computed with λ-mode reaction-rate ratio sensitivities.

The relative sensitivity $S_{k,x}^g$ of k_{eff} to a transport cross section σ_x^g for reaction x in group g is defined to be

$$S_{k,x}^g \equiv \frac{\sigma_{x,0}^g}{k_{eff,0}} \left.\frac{\partial k_{eff}}{\partial \sigma_x^g}\right|_{\sigma_x^g=\sigma_{x,0}^g}. \tag{21}$$

The adjoint-based formulation for $S_{k,x}^g$ is

$$S_{k,x}^g = \frac{\sigma_x^g \int_V dV \int_{4\pi} d\hat{\mathbf{\Omega}}\, \psi^{*g}(r,\hat{\mathbf{\Omega}}) \left(\lambda \frac{\delta F}{\delta \sigma_x^g} - \frac{\delta A}{\delta \sigma_x^g}\right) \psi^g(r,\hat{\mathbf{\Omega}})}{\int_V dV \sum_{g=1}^{G} \int_{4\pi} d\hat{\mathbf{\Omega}}\, \psi^{*g}(r,\hat{\mathbf{\Omega}})\, \lambda F\, \psi^g(r,\hat{\mathbf{\Omega}})}. \tag{22}$$

Again, the total sensitivity $S_{k,x}$ of k_{eff} to reaction x is the sum of $S_{k,x}^g$ over groups.

Table I lists the specific equations that are used for the indirect effect of the sensitivities in the SENSMG sensitivity tool with the label that appears in the output (Sec. IV). In Table I, subscript i indicates an isotope. In the scattering sensitivities of Table I, $\phi_l^g(r)$ and $\Gamma_l^{*g}(r)$ are the lth moments of the forward flux and generalized adjoint flux, defined as

$$\phi_l^g(r) \equiv \int_{4\pi} d\hat{\mathbf{\Omega}}\, P_l(\hat{\mathbf{\Omega}})\psi^g(r,\hat{\mathbf{\Omega}}) \tag{23}$$

and

$$\Gamma_l^{*g}(r) \equiv \int_{4\pi} d\hat{\mathbf{\Omega}}\, P_l(-\hat{\mathbf{\Omega}})\Gamma^{*g}(r,\hat{\mathbf{\Omega}}), \tag{24}$$

where $P_l(\hat{\mathbf{\Omega}})$ are Legendre and associated Legendre polynomials appropriate for the geometry.[1] Note that the generalized adjoint moments are inner product moments defined using the Legendre polynomial for the direction opposite the direction of the angular flux.[10] When λ-mode, α-mode, or fixed-source adjoint moments are needed, their definition is analogous to Eq. (24):

$$\phi_l^{*g}(r) \equiv \int_{4\pi} d\hat{\mathbf{\Omega}}\, P_l(-\hat{\mathbf{\Omega}})\psi^{*g}(r,\hat{\mathbf{\Omega}}). \tag{25}$$

Table I. Reaction-Rate Ratio Sensitivities for λ-Mode Flux,[a] Indirect Effect.

Sensitivity	Label	Equation
Total cross section	total	$\left(S^g_{R,\sigma_{t,i}}\right)_{indirect} = -\int_V dV \int_{4\pi} d\hat{\mathbf{\Omega}}\, \Gamma^{*g}(r,\hat{\mathbf{\Omega}}) N_i\, \sigma^g_{t,i} \psi^g(r,\hat{\mathbf{\Omega}})$
Absorption cross section	abs	$\left(S^g_{R,\sigma_{a,i}}\right)_{indirect} = -\int_V dV \int_{4\pi} d\hat{\mathbf{\Omega}}\, \Gamma^{*g}(r,\hat{\mathbf{\Omega}}) N_i\, \sigma^g_{a,i} \psi^g(r,\hat{\mathbf{\Omega}})$
Capture cross section	(n,g)	$\left(S^g_{R,\sigma_{c,i}}\right)_{indirect} = -\int_V dV \int_{4\pi} d\hat{\mathbf{\Omega}}\, \Gamma^{*g}(r,\hat{\mathbf{\Omega}}) N_i\, \sigma^g_{c,i} \psi^g(r,\hat{\mathbf{\Omega}})$
Chi (not normalized)[b]	chi_nn	$\left(S^g_{R,\chi_i}\right)_{indirect} = \lambda \int_V dV \sum_{g'=1}^{G} \Gamma^{*g}_0(r) \chi_i^{g'\to g} N_i\, \nu_i^{g'} \sigma^{g'}_{f,i} \phi^{g'}_0(r)$
Nu	nu	$\left(S^g_{R,\nu_i}\right)_{indirect} = \lambda \int_V dV \sum_{g'=1}^{G} \Gamma^{*g'}_0(r) \chi_i^{g\to g'} N_i\, \nu_i^{g} \sigma^{g}_{f,i} \phi^{g}_0(r)$
Fission cross section	fiss	$\left(S^g_{R,\sigma_{f,i}}\right)_{indirect} = \lambda \int_V dV \sum_{g'=1}^{G} \Gamma^{*g'}_0(r) \chi_i^{g\to g'} N_i\, \nu_i^{g} \sigma^{g}_{f,i} \phi^{g}_0(r) - \int_V dV \int_{4\pi} d\hat{\mathbf{\Omega}}\, \Gamma^{*g}(r,\hat{\mathbf{\Omega}}) N_i\, \sigma^g_{f,i} \psi^g(r,\hat{\mathbf{\Omega}})$
Elastic scattering[c]	elastic	$\left(S^g_{R,\sigma_{e.s.,i}}\right)_{indirect} = \int_V dV \sum_{\substack{g'=1 \\ \sigma^{g\to g'}_{s,0,i}>0}}^{G} \Gamma^{*g'}_0(r) N_i\, \sigma^g_{e.s.,i} \phi^g_0(r) - \int_V dV \int_{4\pi} d\hat{\mathbf{\Omega}}\, \Gamma^{*g}(r,\hat{\mathbf{\Omega}}) N_i\, \sigma^g_{e.s.,i} \psi^g(r,\hat{\mathbf{\Omega}})$
Inelastic scattering[c]	inelastic	$\left(S^g_{R,\sigma_{i.s.,i}}\right)_{indirect} = \int_V dV \sum_{\substack{g'=1 \\ \sigma^{g\to g'}_{s,0,i}>0}}^{G} \Gamma^{*g'}_0(r) N_i\, \sigma^g_{i.s.,i} \phi^g_0(r) - \int_V dV \int_{4\pi} d\hat{\mathbf{\Omega}}\, \Gamma^{*g}(r,\hat{\mathbf{\Omega}}) N_i\, \sigma^g_{i.s.,i} \psi^g(r,\hat{\mathbf{\Omega}})$
In-scattering, P_0[d]	in-scat-0	$\left(S^{g'\to g}_{R,\sigma_{s,0,i}}\right)_{indirect} = \int_V dV \sum_{\substack{g'=1 \\ g'\neq g}}^{G} \Gamma^{*g}_0(r) N_i\, \sigma^{g'\to g}_{s,0,i} \phi^{g'}_0(r) - \int_V dV \int_{4\pi} d\hat{\mathbf{\Omega}} \sum_{\substack{g'=1 \\ g'\neq g}}^{G} \Gamma^{*g'}(r,\hat{\mathbf{\Omega}}) N_i\, \sigma^{g'\to g}_{s,0,i} \psi^{g'}(r,\hat{\mathbf{\Omega}})$
Self-scattering, P_0	self-scat-0	$\left(S^{g\to g}_{R,\sigma_{s,0,i}}\right)_{indirect} = \int_V dV\, \Gamma^{*g}_0(r) N_i\, \sigma^{g\to g}_{s,0,i} \phi^g_0(r) - \int_V dV \int_{4\pi} d\hat{\mathbf{\Omega}}\, \Gamma^{*g}(r,\hat{\mathbf{\Omega}}) N_i\, \sigma^{g\to g}_{s,0,i} \psi^g(r,\hat{\mathbf{\Omega}})$
Out-scattering, P_0[d]	out-scat-0	$\left(S^{g\to g'}_{R,\sigma_{s,0,i}}\right)_{indirect} = \int_V dV \sum_{\substack{g'=1 \\ g'\neq g}}^{G} \Gamma^{*g'}_0(r) N_i\, \sigma^{g\to g'}_{s,0,i} \phi^g_0(r) - \int_V dV \int_{4\pi} d\hat{\mathbf{\Omega}} \sum_{\substack{g'=1 \\ g'\neq g}}^{G} \Gamma^{*g}(r,\hat{\mathbf{\Omega}}) N_i\, \sigma^{g\to g'}_{s,0,i} \psi^{g}(r,\hat{\mathbf{\Omega}})$

Table I (continued). Reaction-Rate Ratio Sensitivities for λ-Mode Flux,[(a)] Indirect Effect.

Sensitivity	Label	Equation
In-scattering, P_l, $1 \le l \le L$	in-scat-[l]	$\left(S^{g'\to g}_{R,\sigma_{s,l,i}}\right)_{indirect} = \int_V dV \sum_{\substack{g'=1 \\ g'\neq g}}^{G} \Gamma^{*g}_l(r) N_i (2l+1) \sigma^{g'\to g}_{s,l,i} \phi^{g'}_l(r)$
Self-scattering, P_l, $1 \le l \le L$	self-scat-[l]	$\left(S^{g\to g}_{R,\sigma_{s,l,i}}\right)_{indirect} = \int_V dV \Gamma^{*g}_l(r) N_i (2l+1) \sigma^{g\to g}_{s,l,i} \phi^{g}_l(r)$
Out-scattering, P_l, $1 \le l \le L$	out-scat-[l]	$\left(S^{g\to g'}_{R,\sigma_{s,l,i}}\right)_{indirect} = \int_V dV \sum_{\substack{g'=1 \\ g'\neq g}}^{G} \Gamma^{*g'}_l(r) N_i (2l+1) \sigma^{g\to g'}_{s,l,i} \phi^{g}_l(r)$
Source[(e)]	source	$S^{g}_{R,Q_{N_i}} = \int_V dV \, \Gamma^{*g}_0(r,\hat{\mathbf{\Omega}}) \left(Q^{g}_{s.f.,i} + N_i \frac{\partial Q^{g}_{(\alpha,n)}}{\partial N_i} \right)$
Total scattering	ssctt	$\left(S^{g}_{R,\sigma_{s,i}}\right)_{indirect} = \sum_{l=0}^{L} \int_V dV \sum_{g'=1}^{G} \Gamma^{*g'}_l(r) N_i (2l+1) \sigma^{g\to g'}_{s,l,i} \phi^{g}_l(r)$
Nuclide density[(f)]	density	$\left(S^{g}_{R,N_i}\right)_{indirect} = \left(S^{g}_{R,\nu_i}\right)_{indirect} + \left(S^{g}_{R,\sigma_{t,i}}\right)_{indirect} + \left(S^{g}_{R,\sigma_{s,i}}\right)_{indirect}$

(a) Except for density [see note (f)], these equations are also used for α-mode and fixed-source flux, but $\lambda = 1/k_{eff}$ is set to 1 and a divisor is used where needed.

(b) This equation is used when fission chi is a matrix. When fission chi is a vector, the equation is $\left(S^{g}_{R,\chi_i}\right)_{indirect} = \lambda \int_V dV \, \Xi_i \sum_{g'=1}^{G} \Gamma^{*g}_0(r) \chi^{g}_i \nu^{g'} \Sigma^{g'}_f \phi^{g'}_0(r)$, with $\Xi_i = \left(N_i \sum_{g'=1}^{G} \nu^{g'}_i \sigma^{g'}_{f,i} f^{g'}_i \right) \Big/ \left(\sum_{i=1}^{I} N_i \sum_{g'=1}^{G} \nu^{g'}_i \sigma^{g'}_{f,i} f^{g'}_i \right)$, where $f^{g'}_i$ is the spectrum weighting function when using the NDI at LANL, 1 otherwise.

(c) Only elastic and inelastic edit cross sections are presently available.

(d) In previous versions of this report and in Ref. 11, there were typos. For in-scattering, $\Gamma^{*g'}$ was Γ^{*g}. For out-scattering, Γ^{*g} was $\Gamma^{*g'}$.

(e) For leakage and subcritical multiplication problems only. See Eq. (55) and the text that follows it.

(f) For leakage and subcritical multiplication, the nuclide density sensitivity includes $S^{g}_{R,Q_{N_i}}$ as a summand.

Also note that the zeroth forward moment $\phi^{g}_0(r)$ is just $\phi^{g}(r)$ of Eq. (3). The number of moments, *L* in Table I, depends on the scattering order and the number of dimensions (it is equal to the scattering expansion order in one dimension).[1]

The sensitivity to the total cross section and all contributors to the total cross section have an angle integral of the product of angular fluxes. For α calculations, the integrals in Eq. (34) do as well. If discrete-ordinates angular fluxes are available, then these integrals are computed using

$$\int_{4\pi} d\hat{\mathbf{\Omega}} \Gamma^{*g}(r,\hat{\mathbf{\Omega}}) \psi^{g}(r,\hat{\mathbf{\Omega}}) \approx \sum_{m=1}^{M} \omega_m \Gamma^{*g}_{-m}(r) \psi^{g}_m(r), \tag{26}$$

where *M* is the number of discrete ordinates, ω_m is the weight of ordinate *m*, and subscript –*m* denotes the ordinate that is in the opposite direction of ordinate *m*. If discrete-ordinates angular fluxes are not available, then angle integrals are estimated using a moments expansion:[10]

$$\int_{4\pi} d\hat{\mathbf{\Omega}} \Gamma^{*g}(r,\hat{\mathbf{\Omega}}) \psi^{g}(r,\hat{\mathbf{\Omega}}) \approx \sum_{l=0}^{L} (2l+1) \Gamma_l^{g*}(r) \phi_l^{g}(r). \tag{27}$$

Note that the second term in the fission cross section and P_0 scattering equations appears because these cross sections are addends in the total cross section.

The numerator of Eq. (22) is the same as Eq. (13) except that the latter has the generalized adjoint $\Gamma^{*g}(r,\hat{\mathbf{\Omega}})$ where the former has the λ-mode adjoint $\psi^{*g}(r,\hat{\mathbf{\Omega}})$. Thus, the sensitivities of k_{eff} are computed using the equations in Table I, with the following modifications: 1) k is substituted for R in the subscript on S; 2) λ-mode $\phi^{*g}(r,\hat{\mathbf{\Omega}})$ and $\phi_l^{*g}(r)$ [Eq. (25)], the solution to Eq. (12), are used instead of $\Gamma^{*g}(r,\hat{\mathbf{\Omega}})$ and $\Gamma_l^{*g}(r)$; and 3) the integrals are divided by the denominator of Eq. (22).

SENSMG also computes the relative sensitivity S_{k,ρ_n}^{g} of k_{eff} with respect to the mass density of each material defined in the SENSMG input file (Sec. III.B). The adjoint-based formulation for S_{k,ρ_n}^{g} is

$$S_{k,\rho_n}^{g} = \frac{\int_{V_n} dV \int_{4\pi} d\hat{\mathbf{\Omega}} \psi^{*g}(r,\hat{\mathbf{\Omega}}) \left(\lambda F_n - A_n\right) \psi^{g}(r,\hat{\mathbf{\Omega}})}{\int_{V} dV \sum_{g=1}^{G} \int_{4\pi} d\hat{\mathbf{\Omega}} \psi^{*g}(r,\hat{\mathbf{\Omega}}) \lambda F \psi^{g}(r,\hat{\mathbf{\Omega}})}. \tag{28}$$

The total sensitivity S_{k,ρ_n} of k_{eff} to the mass density of coarse mesh n is the sum of S_{k,ρ_n}^{g} over groups. It is important to note that the derivative in S_{k,ρ_n}^{g} is a constant-volume partial derivative.

SENSMG also computes the derivative of k_{eff} with respect to the location of each material interface location and the location of the outer boundary. The derivative, computed for each energy group, is denoted $\partial k_{eff}^{g} / \partial r_n$, where r_n is the location of the nth interface, surface S_n. The adjoint-based formulation for $\partial k_{eff}^{g} / \partial r_n$ is[12]

$$\frac{\partial k_{eff}^{g}}{\partial r_n} = \frac{k_{eff} \int_{S_n} dS \int_{4\pi} d\hat{\mathbf{\Omega}} \psi^{*g}(r,\hat{\mathbf{\Omega}}) \left(\lambda \Delta F_n - \Delta A_n\right) \psi^{g}(r,\hat{\mathbf{\Omega}})}{\int_{V} dV \sum_{g=1}^{G} \int_{4\pi} d\hat{\mathbf{\Omega}} \psi^{*g}(r,\hat{\mathbf{\Omega}}) \lambda F \psi^{g}(r,\hat{\mathbf{\Omega}})}, \tag{29}$$

where ΔF_n is the difference in the fission operator across surface S_n, defined as the operator on the negative side (left, inside, or bottom) minus the operator on the positive side (right, outside, or top), and ΔA_n is defined analogously for the transport operator. The total derivative of k_{eff} to the location of surface S_n, $\partial k_{eff} / \partial r_n$, is the sum of $\partial k_{eff}^{g} / \partial r_n$ over groups. It is important to note that $\partial k_{eff}^{g} / \partial r_n$ is a constant-density partial derivative.

For all of the problems in this paper, the constant-volume and constant-density partial derivatives can be combined (with cell volumes and interface areas) to compute constant-mass partial derivatives.[13]

II.C. α eigenvalue problems

GPT may also be used for α eigenvalue calculations. The α-mode forward and adjoint neutron fluxes $\psi^g(r,\hat{\mathbf{\Omega}})$ and $\psi^{*g}(r,\hat{\mathbf{\Omega}})$ satisfy

$$\left(\frac{\alpha}{v}+A-F\right)\psi=0 \tag{30}$$

and

$$\left(\frac{\alpha}{v}+A^*-F^*\right)\psi^*=0, \tag{31}$$

respectively, where v is the neutron speed. Vacuum boundary conditions apply to Eqs. (30) and (31). The indirect effect is

$$\left(S^g_{R,x}\right)_{indirect}=\sigma_x^g\int_V dV\int_{4\pi}d\hat{\mathbf{\Omega}}\,\Gamma^{*g}(r,\hat{\mathbf{\Omega}})\left(\frac{\delta F}{\delta\sigma_x^g}-\frac{\delta A}{\delta\sigma_x^g}\right)\psi^g(r,\hat{\mathbf{\Omega}}), \tag{32}$$

where now $\Gamma^{*g}(r,\hat{\mathbf{\Omega}})$ satisfies

$$\left(\frac{\alpha}{v}+A^*-F^*\right)\Gamma^*=S^* \tag{33}$$

with S^* given by Eq. (15). A vacuum boundary condition applies to Eq. (33). The method of successive approximations can be used to solve Eq. (33) using Eq. (16) with

$$\Gamma_n^{*g}(r,\hat{\mathbf{\Omega}})=\xi_n^{*g}(r,\hat{\mathbf{\Omega}})-\frac{\displaystyle\int_V dV\sum_{g=1}^{G}\int_{4\pi}d\hat{\mathbf{\Omega}}\,\xi_n^{*g}(r,\hat{\mathbf{\Omega}})\frac{1}{v^g}\psi^g(r,\hat{\mathbf{\Omega}})}{\displaystyle\int_V dV\sum_{g=1}^{G}\int_{4\pi}d\hat{\mathbf{\Omega}}\,\psi^{*g}(r,\hat{\mathbf{\Omega}})\frac{1}{v^g}\psi^g(r,\hat{\mathbf{\Omega}})}\psi^{*g}(r,\hat{\mathbf{\Omega}}), \tag{34}$$

where v^g is the neutron speed associated with energy group g. The $\xi_n^{*g}(r,\hat{\mathbf{\Omega}})$ are generated recursively using

$$\begin{cases}\left(\dfrac{\alpha}{v}+A^*\right)\xi_0^*=S^*,\\ \left(\dfrac{\alpha}{v}+A^*\right)\xi_n^*=F^*\Gamma_{n-1}^*,\ n>0.\end{cases} \tag{35}$$

The second term on the right side of Eq. (34) is included to remove any fundamental mode contamination.

It can be shown that the generalized adjoint for α eigenvalue problems must satisfy

$$\int_V dV\sum_{g=1}^{G}\int_{4\pi}d\hat{\mathbf{\Omega}}\,\Gamma^{*g}(r,\hat{\mathbf{\Omega}})\frac{1}{v^g}\psi^g(r,\hat{\mathbf{\Omega}})=0. \tag{36}$$

Like k_{eff} calculations, in α calculations, the α-mode forward and adjoint angular fluxes are computed to apply GPT for reaction-rate ratios, so α sensitivities can always be computed with α-mode reaction-rate ratio sensitivities. The relative sensitivity $S^g_{\alpha,x}$ of the α eigenvalue to a transport cross section σ_x^g for reaction x in group g is defined to be

$$S^g_{\alpha,x} \equiv \frac{\sigma^g_{x,0}}{\alpha_0}\frac{\partial\alpha}{\partial\sigma^g_x}\bigg|_{\sigma^g_x=\sigma^g_{x,0}}. \tag{37}$$

The adjoint-based formulation for $S^g_{\alpha,x}$ is

$$S^g_{\alpha,x} = \frac{1}{\alpha}\frac{\sigma^g_x \int_V dV \int_{4\pi} d\hat{\mathbf{\Omega}} \psi^{*g}(r,\hat{\mathbf{\Omega}})\left(\frac{\delta F}{\delta\sigma^g_x} - \frac{\delta A}{\delta\sigma^g_x}\right)\psi^g(r,\hat{\mathbf{\Omega}})}{\int_V dV \sum_{g=1}^{G}\int_{4\pi} d\hat{\mathbf{\Omega}}\psi^{*g}(r,\hat{\mathbf{\Omega}})\frac{1}{v^g}\psi^g(r,\hat{\mathbf{\Omega}})}. \tag{38}$$

Again, the total sensitivity $S_{\alpha,x}$ of α to reaction x is the sum of $S^g_{\alpha,x}$ over groups.

The equations of Table I are also used for reaction-rate ratios of the α-mode flux, except that k_{eff} is set to 1 (and the appropriate fluxes are used).

The numerator of Eq. (38) is the same as Eq. (13) except that the latter has the generalized adjoint $\Gamma^{*g}(r,\hat{\mathbf{\Omega}})$ where the former has the α-mode adjoint $\psi^{*g}(r,\hat{\mathbf{\Omega}})$. Thus, the sensitivities of α are computed using the equations in Table I, with the following modifications: 1) λ is set to 1; 2) α is substituted for R in the subscript on S; 3) α-mode $\phi^{*g}(r,\hat{\mathbf{\Omega}})$ and $\phi^{*g}_l(r)$ [Eq. (25)], the solution to Eq. (31), are used instead of $\Gamma^{*g}(r,\hat{\mathbf{\Omega}})$ and $\Gamma^{*g}_l(r)$; and 4) the integrals are divided by the denominator of Eq. (38) and (including the factor of α).

SENSMG also computes the relative sensitivity S^g_{α,ρ_n} of α with respect to the mass density of each material defined in the SENSMG input file (Sec. III.B). The adjoint-based formulation for S^g_{α,ρ_n} is

$$S^g_{\alpha,\rho_n} = \frac{1}{\alpha}\frac{\int_{V_n} dV \int_{4\pi} d\hat{\mathbf{\Omega}}\psi^{*g}(r,\hat{\mathbf{\Omega}})\left(F_n - A_n\right)\psi^g(r,\hat{\mathbf{\Omega}})}{\int_V dV\sum_{g=1}^{G}\int_{4\pi} d\hat{\mathbf{\Omega}}\psi^{*g}(r,\hat{\mathbf{\Omega}})\frac{1}{v^g}\psi^g(r,\hat{\mathbf{\Omega}})}. \tag{39}$$

The total sensitivity S_{α,ρ_n} of α to the mass density of coarse mesh n is the sum of S^g_{α,ρ_n} over groups. It is important to note that the derivative in S^g_{α,ρ_n} is a constant-volume partial derivative.

SENSMG also computes the derivative of α with respect to the location of each material interface location and the location of the outer boundary. The derivative, computed for each energy group, is denoted $\partial\alpha^g/\partial r_n$. The adjoint-based formulation for $\partial\alpha^g/\partial r_n$, whose derivation is similar to that of $\partial\lambda/\partial r_n$ in Ref. 12, is

$$\frac{\partial\alpha^g}{\partial r_n} = \frac{\int_{S_n} dS\int_{4\pi} d\hat{\mathbf{\Omega}}\psi^{*g}(r,\hat{\mathbf{\Omega}})\left(\Delta F_n - \Delta A_n\right)\psi^g(r,\hat{\mathbf{\Omega}})}{\int_V dV\sum_{g=1}^{G}\int_{4\pi} d\hat{\mathbf{\Omega}}\psi^{*g}(r,\hat{\mathbf{\Omega}})\frac{1}{v^g}\psi^g(r,\hat{\mathbf{\Omega}})}, \tag{40}$$

where again the Δ terms are differences across surface S_n. The total derivative of α to the location of surface S_n, $\partial\alpha/\partial r_n$, is the sum of $\partial\alpha^g/\partial r_n$ over groups. It is important to note that $\partial\alpha^g/\partial r_n$ is a constant-density partial derivative.

For α eigenvalue problems, SENSMG computes the reciprocal of the adjoint-weighted mean leakage time τ_l, defined as

$$\frac{1}{\tau_l} \equiv \frac{\int_{V_n} dV \sum_{g=1}^{G} \int_{4\pi} d\hat{\mathbf{\Omega}} \psi^{*g}(r,\hat{\mathbf{\Omega}}) \hat{\mathbf{\Omega}} \cdot \nabla \psi^{g}(r,\hat{\mathbf{\Omega}})}{\int_{V} dV \sum_{g=1}^{G} \int_{4\pi} d\hat{\mathbf{\Omega}} \psi^{*g}(r,\hat{\mathbf{\Omega}}) \frac{1}{v^g} \psi^{g}(r,\hat{\mathbf{\Omega}})}. \tag{41}$$

SENSMG computes Eq. (41) using[14]

$$\frac{1}{\tau_l} = \alpha \left[-1 + \sum_{i=1}^{I} S_{\alpha,\rho_i} \right]. \tag{42}$$

II.D. General fixed-source problems

For fixed-source calculations, the forward and adjoint neutron fluxes $\psi^{g}(r,\hat{\mathbf{\Omega}})$ and $\psi^{*g}(r,\hat{\mathbf{\Omega}})$ satisfy

$$(A - F)\psi = Q \tag{43}$$

and

$$(A^* - F^*)\psi^* = Q^*, \tag{44}$$

respectively. In SENSMG, the neutron source $Q^g(r)$ is an energy- and material-dependent intrinsic source of spontaneous fission neutrons and neutrons from (α,n) reactions occurring in a homogeneous material. It is assumed to be isotropic. The adjoint source Q^* is defined by the quantity of interest. In SENSMG, the quantity of interest for the adjoint flux $\psi^{*g}(r,\hat{\mathbf{\Omega}})$ is, for spheres and cylinders, the total neutron leakage *L* from the system, which is

$$L \equiv \int_{S_b} dS \sum_{g=1}^{G} \int_{\hat{\mathbf{\Omega}}\cdot\hat{\mathbf{n}}>0} d\hat{\mathbf{\Omega}}\, \hat{\mathbf{\Omega}} \cdot \hat{\mathbf{n}}\, \psi^{g}(r,\hat{\mathbf{\Omega}}), \tag{45}$$

where S_b represents the outer boundary and $\hat{\mathbf{n}}$ is the outward unit normal vector at each point on S_b. For slabs, the quantity of interest is the leakage from the right boundary, computed using Eq. (45) with S_b representing just the right boundary. Therefore the adjoint source Q^* is an isotropic incoming flux distribution on the outer boundary (for spheres/cylinders) or the right boundary (for slabs). Its value is $Q^{*g} = 1$ for all energy groups and directions. (An isotropic incoming distribution in the flux is equivalent, within the limits of the discrete ordinates approximation, to a cosine incoming distribution in the neutron density.) Other than that incoming flux condition for Eq. (44), vacuum boundary conditions apply to Eqs. (43) and (44).

The relative sensitivity $S^g_{L,x}$ of the leakage to a transport cross section σ^g_x for reaction *x* in group *g* is defined to be

$$S^g_{L,x} \equiv \frac{\sigma^g_{x,0}}{L_0} \left. \frac{\partial L}{\partial \sigma^g_x} \right|_{\sigma^g_x = \sigma^g_{x,0}}. \tag{46}$$

The adjoint-based formulation for $S^g_{L,x}$ is

$$S^g_{L,x} = \frac{1}{L} \sigma^g_x \int_V dV \int_{4\pi} d\hat{\mathbf{\Omega}} \left\{ \psi^{*g}(r,\hat{\mathbf{\Omega}}) \frac{\partial Q}{\partial \sigma^g_x} + \psi^{*g}(r,\hat{\mathbf{\Omega}}) \left(\frac{\delta F}{\delta \sigma^g_x} - \frac{\delta A}{\delta \sigma^g_x} \right) \psi^{g}(r,\hat{\mathbf{\Omega}}) \right\}. \tag{47}$$

The intrinsic neutron source rate density Q depends on isotopic (α,n) cross sections. However, SENSMG presently considers only neutron reaction cross sections. Therefore the derivative $\partial Q/\partial \sigma_x^g$ is zero, and SENSMG uses

$$S_{L,x}^g = \frac{1}{L}\sigma_x^g \int_V dV \int_{4\pi} d\hat{\mathbf{\Omega}} \psi^{*g}(r,\hat{\mathbf{\Omega}}) \left(\frac{\delta F}{\delta \sigma_x^g} - \frac{\delta A}{\delta \sigma_x^g} \right) \psi^g(r,\hat{\mathbf{\Omega}}). \tag{48}$$

Again, the total sensitivity $S_{L,x}$ of L to reaction x is the sum of $S_{L,x}^g$ over groups.

For reaction-rate ratios, the indirect effect of Eq. (10) is

$$\left(S_{R,x}^g\right)_{indirect} = \sigma_x^g \int_V dV \int_{4\pi} d\hat{\mathbf{\Omega}} \left\{ \Gamma^{*g}(r,\hat{\mathbf{\Omega}}) \frac{\partial Q}{\partial \sigma_x^g} + \Gamma^{*g}(r,\hat{\mathbf{\Omega}}) \left(\frac{\delta F}{\delta \sigma_x^g} - \frac{\delta A}{\delta \sigma_x^g} \right) \psi^g(r,\hat{\mathbf{\Omega}}) \right\}. \tag{49}$$

Again, SENSMG considers only neutron reaction cross sections, so $\partial Q/\partial \sigma_x^g = 0$ and the indirect effect is

$$\left(S_{R,x}^g\right)_{indirect} = \sigma_x^g \int_V dV \int_{4\pi} d\hat{\mathbf{\Omega}} \Gamma^{*g}(r,\hat{\mathbf{\Omega}}) \left(\frac{\delta F}{\delta \sigma_x^g} - \frac{\delta A}{\delta \sigma_x^g} \right) \psi^g(r,\hat{\mathbf{\Omega}}). \tag{50}$$

In Eqs. (49) and (50), $\Gamma^{*g}(r,\hat{\mathbf{\Omega}})$ satisfies

$$\left(A^* - F^*\right)\Gamma^* = S^* \tag{51}$$

with S^* given by Eq. (15). A vacuum boundary condition applies to Eq. (51). For fixed-source problems, the operator on $\Gamma^{*g}(r,\hat{\mathbf{\Omega}})$ in Eq. (51) is not singular, so Eq. (51) is solved directly, without the need for successive approximations.

For fixed-source problems, Eq. (51) is the same form as Eq. (44) (the sources are different). For reaction-rate ratios, we are following the convention of Stacey[3] in referring to the adjoint function as a "generalized" adjoint and using the symbol Γ^*. We use ψ^* for the neutron leakage adjoint so that the discussion in this section parallels somewhat the discussion of eigenvalue problems in Secs. II.B and II.C. However, for reaction-rate ratios in fixed-source problems, only one adjoint is needed, Γ^*. Therefore, in this case, the neutron leakage sensitivity does require an extra adjoint transport calculation beyond what the reaction-rate ratios sensitivities require, unlike in the eigenvalue case.

For fixed-source problems, the magnitude of the neutron flux is fixed, and an absolute reaction rate R_1 of Eq. (1) can be computed. In this case, S^* is

$$S^{*g}(r,\hat{\mathbf{\Omega}}) = \frac{1}{R_1}\frac{\partial R_1}{\partial \phi} = \frac{\Sigma_1^g(r)}{R_1}. \tag{52}$$

For a reaction-rate ratio in fixed-source problems, the generalized adjoint must satisfy

$$\int_V dV \sum_{g=1}^{G} \int_{4\pi} d\hat{\mathbf{\Omega}} \Gamma^{*g}(r,\hat{\mathbf{\Omega}}) Q^g(r) = 0. \tag{53}$$

For an absolute reaction rate in fixed-source problems, the generalized adjoint must satisfy

$$\int_V dV \sum_{g=1}^{G} \int_{4\pi} d\hat{\mathbf{\Omega}} \Gamma^{*g}(r,\hat{\mathbf{\Omega}}) Q^g(r) = 1. \tag{54}$$

With one exception, the equations of Table I are also used for reaction-rate ratios of a fixed-source flux, except that k_{eff} is set to 1 (and the appropriate fluxes are used). The exception is that the sensitivity of the reaction-rate ratio to the density of nuclide i, N_i, in a fixed-source problem requires the derivative $\partial Q^g / \partial N_i$ (but $\partial Q / \partial \sigma_x^g$ is still zero). The contribution of the source sensitivity to the sensitivity of R to the density of isotope i is

$$S^g_{R,Q_{N_i}} = N_i \int_V dV \int_{4\pi} d\hat{\mathbf{\Omega}} \Gamma^{*g}(r, \hat{\mathbf{\Omega}}) \frac{\partial Q^g}{\partial N_i}. \tag{55}$$

The sensitivity $S^g_{R,Q_{N_i}}$ of Eq. (55) is included as another addend on the right side of the equation for S^g_{R,N_i} in Table I. The source Q^g is the sum of the spontaneous fission source in group g and the (α,n) source in group g:

$$Q^g = Q^g_{s.f.} + Q^g_{(\alpha,n)} \tag{56}$$

For spontaneous fission sources, the source rate density in group g for isotope i is

$$Q^g_{s.f.,i} = \lambda_i N_i \chi^g_{s.f.,i}, \tag{57}$$

where λ_i is the decay constant for isotope i and $\chi^g_{s.f.,i}$ includes a spectrum function and the spontaneous fission branching ratio,[15] neither of which depend on any isotopic densities. Note that $\chi^g_{s.f.,i}$ is not a normalized spectrum. The total spontaneous fission source rate density in group g is the sum over fissioning isotopes:

$$Q^g_{s.f.} = \sum_{j=1}^{J} Q^g_{s.f.,j} = \sum_{j=1}^{J} \lambda_j N_j \chi^g_{s.f.,j}. \tag{58}$$

The derivative of the spontaneous fission neutron source rate density in group g with respect to the density of spontaneous-fissioning isotope i is

$$\frac{\partial Q^g_{s.f.}}{\partial N_i} = \frac{\partial Q^g_{s.f.,i}}{\partial N_i} = \frac{Q^g_{s.f.,i}}{N_i}. \tag{59}$$

Whether MISC (Ref. 16) or SOURCES4C (Ref. 15) is used to compute spontaneous fission sources, the overall spontaneous-fission neutron spectrum is applied for each spontaneous-fissioning isotope i.

For (α,n) sources, the source rate density in group g for α-emitting isotope j due to target isotope k is[15]

$$Q^g_{(\alpha,n),j,k} = \lambda_j N_j \chi^g_{(\alpha,n),j,k}, \tag{60}$$

where $\chi^g_{(\alpha,n),j,k}$ depends on the density of the target isotope but also on the density of every isotope in the material because they all contribute to the α stopping power of the material. Note that $\chi^g_{(\alpha,n),j,k}$ is not a normalized spectrum. The total (α,n) source rate density in group g is the sum over α-emitting isotopes and target isotopes:

$$Q^g_{(\alpha,n)} = \sum_{j=1}^{J} \sum_{k=1}^{K} Q^g_{(\alpha,n),j,k} = \sum_{j=1}^{J} \lambda_j N_j \sum_{k=1}^{K} \chi^g_{(\alpha,n),j,k}. \tag{61}$$

The derivative of the (α,n) neutron source rate density in group g with respect to the density of isotope i is

$$\frac{\partial Q^g_{(\alpha,n)}}{\partial N_i} = \delta_{ij} \lambda_j \sum_{k=1}^{K} \chi^g_{(\alpha,n),j,k} + \sum_{j=1}^{J} \lambda_j N_j \sum_{k=1}^{K} \frac{\partial \chi^g_{(\alpha,n),j,k}}{\partial N_i}. \tag{62}$$

The derivative of $\chi^g_{(\alpha,n),j,k}$ is too complicated to present here, but it has been worked out[17] and implemented in SENSMG.

Using Eqs. (56) and (59) and the left-hand side of Eq. (62), Eq. (55) becomes

$$S^g_{R,Q_{N_i}} = \int_V dV \int_{4\pi} d\hat{\mathbf{\Omega}}\, \Gamma^{*g}(r,\hat{\mathbf{\Omega}}) \left(Q^g_{s.f.,i} + N_i \frac{\partial Q^g_{(\alpha,n)}}{\partial N_i} \right). \tag{63}$$

The neutron sources are isotropic, so only the zeroth moment of $\Gamma^{*g}(r,\hat{\mathbf{\Omega}})$ is needed.

SOURCES4C prints the neutron spectrum of the spontaneous fission source for each isotope, so $Q^g_{s.f.,i}$ in Eq. (63) is known. When using MISC for the spontaneous fission source, however, SENSMG makes an approximation for $Q^g_{s.f.,i}$. The total spontaneous fission source rate density for each isotope $Q_{s.f.,i}$ is known, but the spontaneous fission spectrum calculated for the material (the mixture of isotopes) is applied to approximate $Q^g_{s.f.,i}$:

$$Q^g_{s.f.,i} \approx Q_{s.f.,i} \frac{\sum_{j=1}^{J} Q^g_{s.f.,j}}{\sum_{g=1}^{G}\sum_{j=1}^{J} Q^g_{s.f.,j}}, \tag{64}$$

where *j* indexes spontaneously fissioning isotopes.

The derivative of the (α,n) source rate density in group *g* with respect to isotope *i* is the sum of the derivative over all α emitters and targets:[17]

$$\frac{\partial Q^g_{(\alpha,n)}}{\partial N_i} = \sum_{j=1}^{J}\sum_{k=1}^{K} \frac{\partial Q^g_{(\alpha,n),j,k}}{\partial N_i} \approx \sum_{j=1}^{J}\sum_{k=1}^{K} \frac{Q^g_{(\alpha,n),j,k}}{Q_{(\alpha,n),j,k}} \frac{\partial Q_{(\alpha,n),j,k}}{\partial N_i}, \tag{65}$$

where *j* indexes α emitters and *k* indexes target isotopes. SOURCES4C prints all the information needed to compute Eq. (65).

The numerator of Eq. (47) is the same as Eq. (13) except that the latter has the generalized adjoint $\Gamma^{*g}(r,\hat{\mathbf{\Omega}})$ where the former has the fixed-source adjoint $\psi^{*g}(r,\hat{\mathbf{\Omega}})$. Thus, the sensitivities of the leakage are computed using the equations in Table I, with the following modifications: 1) λ is set to 1; 2) *L* is substituted for *R* in the subscript on *S*; 3) the fixed-source $\phi^{*g}(r,\hat{\mathbf{\Omega}})$ and $\phi^{*g}_l(r)$ [Eq. (25)], the solution to Eq. (44), are used instead of $\Gamma^{*g}(r,\hat{\mathbf{\Omega}})$ and $\Gamma^{*g}_l(r)$; 4) $S^g_{R,Q_{N_i}}$ of Eq. (63) is included (see #3); and 5) the integrals are divided by *L* of Eq. (45).

SENSMG also computes the relative sensitivity S^g_{L,ρ_n} of *L* with respect to the mass density of each material defined in the SENSMG input file (Sec. III.B). The adjoint-based formulation for S^g_{L,ρ_n} is

$$S^g_{L,\rho_n} = \frac{1}{L} \int_{V_n} dV \int_{4\pi} d\hat{\mathbf{\Omega}} \left\{ \psi^{*g}(r,\hat{\mathbf{\Omega}}) Q_n + \psi^{*g}(r,\hat{\mathbf{\Omega}}) \left(F_n - A_n \right) \psi^g(r,\hat{\mathbf{\Omega}}) \right\}. \tag{66}$$

The total sensitivity S_{L,ρ_n} of L to the mass density of coarse mesh n is the sum of S^g_{L,ρ_n} over groups. The derivative of $\chi^g_{(\alpha,n),j}$ with respect to the material mass density is zero.[17] It is important to note that the derivative in S^g_{L,ρ_n} is a constant-volume partial derivative.

SENSMG also computes the derivative of L with respect to the location of each material interface location and the location of the outer boundary. The derivative, computed for each energy group, is denoted $\partial L^g/\partial r_n$. The adjoint-based formulation for $\partial L^g/\partial r_n$ is[18]

$$\frac{\partial L^g}{\partial r_n} = \int_{S_n} dS \int_{4\pi} d\hat{\mathbf{\Omega}} \left\{ \psi^{*g}(r,\hat{\mathbf{\Omega}}) \Delta Q_n + \psi^{*g}(r,\hat{\mathbf{\Omega}}) \left(\Delta F_n - \Delta A_n \right) \psi^g(r,\hat{\mathbf{\Omega}}) \right\}, \tag{67}$$

where again the Δ terms are differences across surface S_n. The total derivative of L to the location of surface S_n, $\partial L/\partial r_n$, is the sum of $\partial L^g/\partial r_n$ over groups. It is important to note that $\partial L^g/\partial r_n$ is a constant-density partial derivative.

II.E. Subcritical multiplication fixed-source problems

The Feynman Y asymptote is[19]

$$Y = \frac{C_2}{C_1}, \tag{68}$$

and Sm2 is[20,21,22,6]

$$\mathrm{Sm}_2 = \frac{C_2}{2C_1^2} = \frac{Y}{2C_1}. \tag{69}$$

In Eqs. (68) and (69), C_1 is the mean detector count rate and C_2 is the "excess variance" of the count rate distribution, where "excess" means "more than a Poisson distribution contributes." C_2 is also the second factorial moment of the counting distribution.

The mean detector count rate C_1 is computed by introducing detector efficiency functions into Eq. (45):

$$C_1 \equiv \int_{S_b} dS \sum_{g=1}^{G} \int_{\hat{\mathbf{\Omega}}\cdot\hat{\mathbf{n}}>0} d\hat{\mathbf{\Omega}}\, \hat{\mathbf{\Omega}}\cdot\hat{\mathbf{n}} \Sigma^g_d \Sigma_\Omega \psi^g(r,\hat{\mathbf{\Omega}}), \tag{70}$$

where Σ_Ω is a geometry factor that converts the leakage through S_b into the current that actually crosses the face of the detector[23,24] and Σ^g_d is an energy efficiency function that converts the current in group g to a detector count rate. Thus, Eq. (44) uses an adjoint source Q^* that is an isotropic incoming flux distribution on the outer boundary (for spheres/cylinders) or the right boundary (for slabs) and its value is $Q^{*g} = \Sigma^g_d \Sigma_\Omega$. Presently, SENSMG is hard-wired to use efficiency functions (both Σ^g_d and Σ_Ω) for LANL's NPOD detector. (In the future, cylinders will be treated more realistically.)

The excess variance C_2 is computed as the sum of the excess variance contributed by neutrons from induced fissions, ${}_2S$, and the excess variance contributed by neutrons from spontaneous fissions, ${}_2S_{s.f.}$:

$$C_2 = {}_2S + {}_2S_{s.f.}, \tag{71}$$

where

$$ {}_2S = \int dV \sum_{g=1}^{G} Q_2^{*g}(r)\phi_0^g(r) \tag{72} $$

and

$$ {}_2S_{s.f.} = \int dV \sum_{g=1}^{G} Q_{2,s.f.}^{*g}(r) S_{s.f.}^{g}(r). \tag{73} $$

In Eq. (72), $\phi_0^g(r)$ is the scalar flux of Eq. (3) when $\psi^g(r)$ is the solution of Eq. (43), and

$$ Q_2^{*g}(r) \equiv \overline{\nu(\nu-1)}\,\Sigma_f^g(r)\left[I_1(r)\right]^2 \tag{74} $$

with

$$ I_1(r) \equiv \sum_{g'=1}^{G} \chi^{g'}(r)\phi_0^{*g'}(r), \tag{75} $$

where $\phi_0^{*g'}(r)$ is the zero'th moment of the solution of Eq. (44) [computed using Eq. (25)]. In Eq. (73), $S_{s.f.}^g(r)$ is the product of the spontaneous fission rate density and outgoing neutron spectrum in the material at point *r* and energy group *g*,

$$ S_{s.f.}^g(r) = F_{s.f.}(r)\chi_{s.f.}^g(r), \tag{76} $$

where $F_{s.f.}(r)$ is the spontaneous fission rate density, such that the spontaneous fission neutron source rate density at point *r* and energy group *g* is

$$ Q_{s.f.}^g(r) = \overline{\nu}_{s.f.} S_{s.f.}^g(r). \tag{77} $$

Note that $\chi_{s.f.}^g(r)$ is a normalized spectrum. Also in Eq. (73),

$$ Q_{2,s.f.}^{*g}(r) \equiv \overline{\nu(\nu-1)}_{s.f.}\left[I_{1,s.f.}(r)\right]^2 \tag{78} $$

with

$$ I_{1,s.f.}(r) \equiv \sum_{g'=1}^{G} \chi_{s.f.}^{g'}(r)\phi_0^{*g'}(r). \tag{79} $$

The relative sensitivity $S_{Y,x}^g$ of the Feynman *Y* to a transport cross section σ_x^g for reaction *x* in group *g* is defined to be

$$ S_{Y,x}^g \equiv \frac{\sigma_{x,0}^g}{Y_0}\frac{\partial Y}{\partial \sigma_x^g}\bigg|_{\sigma_x^g=\sigma_{x,0}^g}. \tag{80} $$

Using Eq. (68), Eq. (80) becomes

$$ S_{Y,x}^g = S_{C_2,x}^g - S_{C_1,x}^g. \tag{81} $$

Similarly, the relative sensitivity $S_{\mathrm{Sm}_2,x}^g$ of Sm_2 to a transport cross section σ_x^g for reaction *x* in group *g* is defined to be

$$ S_{\mathrm{Sm}_2,x}^g \equiv \frac{\sigma_{x,0}^g}{\mathrm{Sm}_{2,0}}\frac{\partial \mathrm{Sm}_2}{\partial \sigma_x^g}\bigg|_{\sigma_x^g=\sigma_{x,0}^g}. \tag{82} $$

Using Eq. (69), Eq. (82) becomes

$$ S_{\mathrm{Sm}_2,x}^g = S_{C_2,x}^g - 2S_{C_1,x}^g. \tag{83} $$

The relative sensitivity $S^g_{C_1,x}$ of the mean count rate C_1 to a transport cross section σ^g_x for reaction x in group g is given by the equations of Table I with the modifications discussed in Sec. II.D and using C_1 instead of L. For Feynman Y and Sm_2 sensitivities, sensitivities of C_2 are needed. The rest of this section discusses these sensitivities.

The relative sensitivity of the excess variance C_2 requires the functions $\Phi^g_1(r,\hat{\Omega})$ and $\psi^{*g}_2(r,\hat{\Omega})$ satisfying

$$\left(A-F\right)\Phi_1 = Q_1 \tag{84}$$

and

$$\left(A^*-F^*\right)\psi^*_2 = Q^*_2, \tag{85}$$

respectively. The source Q_1 for Eq. (84) is

$$Q^g_1(r) \equiv I_1(r)Q^g_{f1}(r) + I_{1,s.f.}(r)Q^g_{f1,s.f.}(r), \tag{86}$$

where $I_1(r)$ and $I_{1,s.f.}(r)$ are given by Eqs. (75) and (79), respectively, and

$$Q^g_{f1}(r) \equiv \chi^g(r)\sum_{g'=1}^{G}\overline{\nu(\nu-1)}\Sigma^{g'}_f(r)\phi^{g'}_0(r) \tag{87}$$

and

$$Q^g_{f1,s.f.}(r) \equiv \chi^g_{s.f.}(r)\sum_{g'=1}^{G}\overline{\nu(\nu-1)}_{s.f.}S^{g'}_{s.f.}(r). \tag{88}$$

In Eq. (87), $\chi^g(r)$ is the normalized induced-fission spectrum at point r. In Eq. (88), $\chi^g_{s.f.}(r)$ is the normalized spontaneous-fission spectrum at point r. The source $Q^g_1(r)$ is isotropic. The source for Eq. (85) is $Q^{*g}_2(r)$ of Eq. (74), which is isotropic.

The excess variances ${}_2S$ and ${}_2S_{s.f.}$ of Eqs. (72) and (73) and the sources $Q^g_{f1}(r)$ and $Q^g_{f1,s.f.}(r)$ of Eqs. (87) and (88) require material values of $\overline{\nu(\nu-1)}\Sigma^g_f$ and $\overline{\nu(\nu-1)}_{s.f.}/\overline{\nu}_{s.f.}Q^g_{s.f.}$ [using Eq. (77)], respectively, to be constructed from isotopic values. These are

$$\overline{\nu(\nu-1)}\Sigma^g_f = \sum_{i=1}^{I}N_i\overline{\nu(\nu-1)}_i\sigma^g_{f,i} \tag{89}$$

if $\sigma^g_{f,i}$ is available separately from $\nu\sigma^g_{f,i}$ and

$$\overline{\nu(\nu-1)}\Sigma^g_f = \sum_{i=1}^{I}N_i\left(\frac{\overline{\nu(\nu-1)}}{\overline{\nu}}\right)_i\nu\sigma^g_{f,i} \tag{90}$$

otherwise, and

$$\left(\frac{\overline{\nu(\nu-1)}}{\overline{\nu}}\right)_{s.f.}Q^g_{s.f.} = \sum_{i=1}^{I}N_i\left(\frac{\overline{\nu(\nu-1)}}{\overline{\nu}}\right)_{s.f.,i}Q^g_{s.f.,i}. \tag{91}$$

The factorial moments of the fission distributions are measured and evaluated isotopic nuclear data; for example, see Refs. 25 and 26.

The general form for the relative sensitivity of C_2 to input parameter σ^g_x in group g is[6]

$$S^g_{C_2,x} = \frac{1}{C_2}\sigma_x^g \int_V dV \int_{4\pi} d\hat{\mathbf{\Omega}} \left\{ \psi_2^{*g}(r,\hat{\mathbf{\Omega}}) \frac{\partial Q^g(r)}{\partial \sigma_x^g} + \psi_2^{*g}(r,\hat{\mathbf{\Omega}}) \left(\frac{\delta F}{\delta \sigma_x^g} - \frac{\delta A}{\delta \sigma_x^g} \right) \psi^g(r,\hat{\mathbf{\Omega}}) \right\}$$
$$+ \frac{2}{C_2}\sigma_x^g \int_V dV \int_{4\pi} d\hat{\mathbf{\Omega}} \left\{ \Phi_1^g(r,\hat{\mathbf{\Omega}}) \frac{\partial Q^{*g}(r,\hat{\mathbf{\Omega}})}{\partial \sigma_x^g} + \Phi_1^g(r,\hat{\mathbf{\Omega}}) \left(\frac{\delta F^*}{\delta \sigma_x^g} - \frac{\delta A^*}{\delta \sigma_x^g} \right) \psi^{*g}(r,\hat{\mathbf{\Omega}}) \right\} \tag{92}$$
$$+ \frac{1}{C_2}\sigma_x^g \int_V dV \int_{4\pi} d\hat{\mathbf{\Omega}} \left\{ \frac{\partial Q_2^{*g}(r)}{\partial \sigma_x^g} \psi^g(r,\hat{\mathbf{\Omega}}) + \frac{\partial Q_{2,s.f.}^{*g}(r)}{\partial \sigma_x^g} S^g(r,\hat{\mathbf{\Omega}}) + Q_{2,s.f.}^{*g}(r,\hat{\mathbf{\Omega}}) \frac{\partial S^g(r)}{\partial \sigma_x^g} \right\}.$$

As in Sec. II.D, the derivative $\partial Q / \partial \sigma_x^g$ is zero. For the same reasons, the derivative $\partial S / \partial \sigma_x^g$ is zero. Also, in SENSMG the detector response function is independent of all input parameters, so $\partial Q^{*g} / \partial \sigma_x^g$ is also zero. Equation (92) becomes

$$S^g_{C_2,x} = \frac{1}{C_2}\sigma_x^g \int_V dV \int_{4\pi} d\hat{\mathbf{\Omega}}\, \psi_2^{*g}(r,\hat{\mathbf{\Omega}}) \left(\frac{\delta F}{\delta \sigma_x^g} - \frac{\delta A}{\delta \sigma_x^g} \right) \psi^g(r,\hat{\mathbf{\Omega}})$$
$$+ \frac{2}{C_2}\sigma_x^g \int_V dV \int_{4\pi} d\hat{\mathbf{\Omega}}\, \Phi_1^g(r,\hat{\mathbf{\Omega}}) \left(\frac{\delta F^*}{\delta \sigma_x^g} - \frac{\delta A^*}{\delta \sigma_x^g} \right) \psi^{*g}(r,\hat{\mathbf{\Omega}}) \tag{93}$$
$$+ \frac{1}{C_2}\sigma_x^g \int_V dV \int_{4\pi} d\hat{\mathbf{\Omega}} \left\{ \frac{\partial Q_2^{*g}(r)}{\partial \sigma_x^g} \psi^g(r,\hat{\mathbf{\Omega}}) + \frac{\partial Q_{2,s.f.}^{*g}(r)}{\partial \sigma_x^g} S^g(r,\hat{\mathbf{\Omega}}) \right\}.$$

It should be noted that the derivatives $\partial Q_2^{*g}(r) / \partial \sigma_x^g$ and $\partial Q_{2,s.f.}^{*g}(r) / \partial \sigma_x^g$ in Eqs. (92) and (93) include only the derivatives of the material properties of Eqs. (74) [and (75)] and (78) [and (79)]. They do not include the derivative of the adjoint function in $I_1(r)$ of Eq. (75) and $I_{1,s.f.}(r)$ of Eq. (79). The derivative of the adjoint flux with respect to the cross section is the reason that a new forward flux, $\Phi_1^g(r,\hat{\mathbf{\Omega}})$ of Eq. (84), is required to have an adjoint-based sensitivity with no derivatives of the flux with respect to the cross sections.

Table II lists the specific equations that are used for the indirect effect of the sensitivities of C_2 in the SENSMG sensitivity tool with the label that appears in the output (Sec. IV). The sensitivities of C_2 are combined with the sensitivities of C_1 using Eq. (81) or (83) and do not appear on their own. In Table II, subscript *i* indicates an isotope. The moments of the solutions of Eqs. (84) and (85) are defined analogously with Eqs. (23) and (24):

$$\Phi_{1,l}^g(r) = \int_{4\pi} d\hat{\mathbf{\Omega}}\, P_l(\hat{\mathbf{\Omega}}) \Phi_1^g(r,\hat{\mathbf{\Omega}}) \tag{94}$$

and

$$\phi_{2,l}^{*g}(r) = \int_{4\pi} d\hat{\mathbf{\Omega}}\, P_l(-\hat{\mathbf{\Omega}}) \psi_2^{*g}(r,\hat{\mathbf{\Omega}}). \tag{95}$$

It is convenient to define, analogously with $I_1(r)$ of Eq. (75),

$$I_2(r) \equiv \sum_{g'=1}^{G} \chi^{g'}(r) \phi_{2,0}^{*g'}(r), \tag{96}$$

where $\phi_{2,0}^{*g'}(r)$ is the zeroth moment of the solution of Eq. (85), computed using Eq. (95).

Table II. C_2 Relative Sensitivities, Indirect Effect.

Sensitivity	Label	Equation
Total cross section	total	$\left(S^g_{C_2,\sigma_{t,i}}\right)_{indirect} = -\frac{1}{C_2}\int_V dV \int_{4\pi} d\hat{\mathbf{\Omega}}\, \psi_2^{*g}(r,\hat{\mathbf{\Omega}}) N_i \sigma^g_{t,i} \psi^g(r,\hat{\mathbf{\Omega}})$ $-2\frac{1}{C_2}\int_V dV \int_{4\pi} d\hat{\mathbf{\Omega}}\, \Phi_1^g(r,\hat{\mathbf{\Omega}}) N_i \sigma^g_{t,i} \psi^{*g}(r,\hat{\mathbf{\Omega}})$
Absorption cross section	abs	$\left(S^g_{C_2,\sigma_{a,i}}\right)_{indirect} = -\frac{1}{C_2}\int_V dV \int_{4\pi} d\hat{\mathbf{\Omega}}\, \psi_2^{*g}(r,\hat{\mathbf{\Omega}}) N_i \sigma^g_{a,i} \psi^g(r,\hat{\mathbf{\Omega}})$ $-2\frac{1}{C_2}\int_V dV \int_{4\pi} d\hat{\mathbf{\Omega}}\, \Phi_1^g(r,\hat{\mathbf{\Omega}}) N_i \sigma^g_{a,i} \psi^{*g}(r,\hat{\mathbf{\Omega}})$
Capture cross section	(n,g)	$\left(S^g_{C_2,\sigma_{c,i}}\right)_{indirect} = -\frac{1}{C_2}\int_V dV \int_{4\pi} d\hat{\mathbf{\Omega}}\, \psi_2^{*g}(r,\hat{\mathbf{\Omega}}) N_i \sigma^g_{c,i} \psi^g(r,\hat{\mathbf{\Omega}})$ $-2\frac{1}{C_2}\int_V dV \int_{4\pi} d\hat{\mathbf{\Omega}}\, \Phi_1^g(r,\hat{\mathbf{\Omega}}) N_i \sigma^g_{c,i} \psi^{*g}(r,\hat{\mathbf{\Omega}})$
Chi (not normalized)[a]	chi_nn	$\left(S^g_{C_2,\chi_i}\right)_{indirect} = \frac{1}{C_2}\int_V dV\, \Xi_i \sum_{g'=1}^{G} \phi_{2,0}^{*g}(r) \chi_i^g \nu^{g'} \Sigma_f^{g'} \phi_0^{g'}(r)$ $+2\frac{1}{C_2}\int_V dV\, \Xi_i \sum_{g'=1}^{G} \Phi_{1,0}^{g'}(r) \chi_i^g \nu^{g'} \Sigma_f^{g'} \phi_0^{*g}(r)$ $+2\frac{1}{C_2}\int_V dV\, I_1(r) \phi_0^{*g}(r) \Xi_i \sum_{g'=1}^{G} \chi_i^g \overline{\nu(\nu-1)}^{g'} \Sigma_f^{g'} \phi_0^{g'}(r)$
Nu	nu	$\left(S^g_{C_2,\nu_i}\right)_{indirect} = \frac{1}{C_2}\int_V dV\, I_2(r) N_i \nu_i^g \sigma^g_{f,i} \phi_0^g(r)$ $+2\frac{1}{C_2}\int_V dV\, I_1(r) N_i \nu_i^g \sigma^g_{f,i} \Phi_{1,0}^g(r)$
Nu × (nu – 1)[b]	nu(nu-1)	$\left(S^g_{C_2,\nu(\nu-1)_i}\right)_{indirect} = \frac{1}{C_2}\int_V dV \left[I_1(r)\right]^2 N_i \overline{\nu(\nu-1)}_i^g \sigma^g_{f,i} \phi_0^g(r)$
Fission cross section	fiss	$\left(S^g_{C_2,\sigma_{f,i}}\right)_{indirect} = \frac{1}{C_2}\int_V dV\, I_2(r) N_i \nu_i^g \sigma^g_{f,i} \phi_0^g(r)$ $+2\frac{1}{C_2}\int_V dV\, I_1(r) N_i \nu_i^g \sigma^g_{f,i} \Phi_{1,0}^g(r)$ $-\frac{1}{C_2}\int_V dV \int_{4\pi} d\hat{\mathbf{\Omega}}\, \psi_2^{*g}(r,\hat{\mathbf{\Omega}}) N_i \sigma^g_{f,i} \psi^g(r,\hat{\mathbf{\Omega}})$ $-2\frac{1}{C_2}\int_V dV \int_{4\pi} d\hat{\mathbf{\Omega}}\, \Phi_1^g(r,\hat{\mathbf{\Omega}}) N_i \sigma^g_{f,i} \psi^{*g}(r,\hat{\mathbf{\Omega}})$ $+\frac{1}{C_2}\int_V dV \left[I_1(r)\right]^2 N_i \overline{\nu(\nu-1)}_i^g \sigma^g_{f,i} \phi_0^g(r)$
Elastic scattering[c]	elastic	$\left(S^g_{C_2,\sigma_{e.s.,i}}\right)_{indirect} = \frac{1}{C_2}\int_V dV \sum_{\substack{g'=1 \\ \sigma_{s,0,i}^{g\to g'}>0}}^{G} \phi_{2,0}^{*g'}(r) N_i \sigma^g_{e.s.,i} \phi_0^g(r)$ $+2\frac{1}{C_2}\int_V dV \sum_{\substack{g'=1 \\ \sigma_{s,0,i}^{g\to g'}>0}}^{G} \Phi_{1,0}^g(r) N_i \sigma^g_{e.s.,i} \phi_0^{*g'}(r)$ $-\frac{1}{C_2}\int_V dV \int_{4\pi} d\hat{\mathbf{\Omega}}\, \psi_2^{*g}(r,\hat{\mathbf{\Omega}}) N_i \sigma^g_{e.s.,i} \psi^g(r,\hat{\mathbf{\Omega}})$ $-2\frac{1}{C_2}\int_V dV \int_{4\pi} d\hat{\mathbf{\Omega}}\, \Phi_1^g(r,\hat{\mathbf{\Omega}}) N_i \sigma^g_{e.s.,i} \psi^{*g}(r,\hat{\mathbf{\Omega}})$

Table II (continued). C_2 Relative Sensitivities, Indirect Effect.

Sensitivity	Label	Equation
Inelastic scattering[c]	inelastic	$\left(S^{g}_{C_2,\sigma_{i.s.,i}}\right)_{indirect} = \frac{1}{C_2}\int_V dV \sum_{\substack{g'=1 \\ \sigma^{g\to g'}_{s,0,i}>0}}^{G} \phi^{*g'}_{2,0}(r) N_i \sigma^{g}_{i.s.,i} \phi^{g}_{0}(r)$ $+2\frac{1}{C_2}\int_V dV \sum_{\substack{g'=1 \\ \sigma^{g\to g'}_{s,0,i}>0}}^{G} \Phi^{g}_{1,0}(r) N_i \sigma^{g}_{i.s.,i} \phi^{*g'}_{0}(r)$ $-\frac{1}{C_2}\int_V dV \int_{4\pi} d\hat{\mathbf{\Omega}}\, \psi^{*g}_{2}(r,\hat{\mathbf{\Omega}}) N_i \sigma^{g}_{i.s.,i} \psi^{g}(r,\hat{\mathbf{\Omega}})$ $-2\frac{1}{C_2}\int_V dV \int_{4\pi} d\hat{\mathbf{\Omega}}\, \Phi^{g}_{1}(r,\hat{\mathbf{\Omega}}) N_i \sigma^{g}_{i.s.,i} \psi^{*g}(r,\hat{\mathbf{\Omega}})$
In-scattering, P_0	in-scat-0	$\left(S^{g'\to g}_{C_2,\sigma_{s,0,i}}\right)_{indirect} = \frac{1}{C_2}\int_V dV \sum_{\substack{g'=1 \\ g'\neq g}}^{G} \phi^{*g}_{2,0}(r) N_i\, \sigma^{g'\to g}_{s,0,i} \phi^{g'}_{0}(r)$ $+2\frac{1}{C_2}\int_V dV \sum_{\substack{g'=1 \\ g'\neq g}}^{G} \Phi^{g'}_{1,0}(r) N_i\, \sigma^{g'\to g}_{s,0,i} \phi^{*g}_{0}(r)$ $-\frac{1}{C_2}\int_V dV \int_{4\pi} d\hat{\mathbf{\Omega}} \sum_{\substack{g'=1 \\ g'\neq g}}^{G} \psi^{*g'}_{2}(r,\hat{\mathbf{\Omega}}) N_i\, \sigma^{g'\to g}_{s,0,i} \psi^{g'}(r,\hat{\mathbf{\Omega}})$ $-2\frac{1}{C_2}\int_V dV \int_{4\pi} d\hat{\mathbf{\Omega}} \sum_{\substack{g'=1 \\ g'\neq g}}^{G} \Phi^{g'}_{1}(r,\hat{\mathbf{\Omega}}) N_i\, \sigma^{g'\to g}_{s,0,i} \psi^{*g'}(r,\hat{\mathbf{\Omega}})$
Self-scattering, P_0	self-scat-0	$\left(S^{g\to g}_{C_2,\sigma_{s,0,i}}\right)_{indirect} = \frac{1}{C_2}\int_V dV\, \phi^{*g}_{2,0}(r) N_i\, \sigma^{g\to g}_{s,0,i} \phi^{g}_{0}(r)$ $+2\frac{1}{C_2}\int_V dV\, \Phi^{g}_{1,0}(r) N_i\, \sigma^{g\to g}_{s,0,i} \phi^{*g}_{0}(r)$ $-\frac{1}{C_2}\int_V dV \int_{4\pi} d\hat{\mathbf{\Omega}}\, \psi^{*g}_{2}(r,\hat{\mathbf{\Omega}}) N_i\, \sigma^{g\to g}_{s,0,i} \psi^{g}(r,\hat{\mathbf{\Omega}})$ $-2\frac{1}{C_2}\int_V dV \int_{4\pi} d\hat{\mathbf{\Omega}}\, \Phi^{g}_{1}(r,\hat{\mathbf{\Omega}}) N_i\, \sigma^{g\to g}_{s,0,i} \psi^{*g}(r,\hat{\mathbf{\Omega}})$
Out-scattering, P_0	out-scat-0	$\left(S^{g\to g'}_{C_2,\sigma_{s,0,i}}\right)_{indirect} = \frac{1}{C_2}\int_V dV \sum_{\substack{g'=1 \\ g'\neq g}}^{G} \phi^{*g'}_{2,0}(r) N_i\, \sigma^{g\to g'}_{s,0,i} \phi^{g}_{0}(r)$ $+2\frac{1}{C_2}\int_V dV \sum_{\substack{g'=1 \\ g'\neq g}}^{G} \Phi^{g}_{1,0}(r) N_i\, \sigma^{g\to g'}_{s,0,i} \phi^{*g'}_{0}(r)$ $-\frac{1}{C_2}\int_V dV \int_{4\pi} d\hat{\mathbf{\Omega}} \sum_{\substack{g'=1 \\ g'\neq g}}^{G} \psi^{*g}_{2}(r,\hat{\mathbf{\Omega}}) N_i\, \sigma^{g\to g'}_{s,0,i} \psi^{g}(r,\hat{\mathbf{\Omega}})$ $-2\frac{1}{C_2}\int_V dV \int_{4\pi} d\hat{\mathbf{\Omega}} \sum_{\substack{g'=1 \\ g'\neq g}}^{G} \Phi^{g}_{1}(r,\hat{\mathbf{\Omega}}) N_i\, \sigma^{g\to g'}_{s,0,i} \psi^{*g}(r,\hat{\mathbf{\Omega}})$

Table II (continued). C_2 Relative Sensitivities, Indirect Effect.

Sensitivity	Label	Equation
In-scattering, P_l, $1 \le l \le L$	in-scat-[l]	$\left(S^{g'\to g}_{C_2,\sigma_{s,l,i}}\right)_{indirect} = \frac{1}{C_2}\int_V dV \sum_{\substack{g'=1\\ g'\neq g}}^{G} \phi^{*g}_{2,l}(r) N_i (2l+1)\sigma^{g'\to g}_{s,l,i}\phi^{g'}_l(r)$ $+2\frac{1}{C_2}\int_V dV \sum_{\substack{g'=1\\ g'\neq g}}^{G} \Phi^{g'}_{1,l}(r) N_i (2l+1)\sigma^{g'\to g}_{s,l,i}\phi^{*g}_l(r)$
Self-scattering, P_l, $1 \le l \le L$	self-scat-[l]	$\left(S^{g\to g}_{C_2,\sigma_{s,l,i}}\right)_{indirect} = \frac{1}{C_2}\int_V dV\, \phi^{*g}_{2,l}(r) N_i (2l+1)\sigma^{g\to g}_{s,l,i}\phi^{g}_l(r)$ $+2\frac{1}{C_2}\int_V dV \sum_{\substack{g'=1\\ g'\neq g}}^{G} \Phi^{g}_{1,l}(r) N_i (2l+1)\sigma^{g\to g}_{s,l,i}\phi^{*g}_l(r)$
Out-scattering, P_l, $1 \le l \le L$	out-scat-[l]	$\left(S^{g\to g'}_{C_2,\sigma_{s,l,i}}\right)_{indirect} = \int_V dV \sum_{\substack{g'=1\\ g'\neq g}}^{G} \phi^{*g'}_{2,l}(r) N_i (2l+1)\sigma^{g\to g'}_{s,l,i}\phi^{g}_l(r)$ $+2\frac{1}{C_2}\int_V dV \sum_{\substack{g'=1\\ g'\neq g}}^{G} \Phi^{g}_{1,l}(r) N_i (2l+1)\sigma^{g\to g'}_{s,l,i}\phi^{*g'}_l(r)$
Source	source	$S^{g}_{C_2,Q_{N_i}} = \frac{1}{C_2}\int_V dV\, \phi^{*g}_{2,0}(r,\hat{\mathbf{\Omega}})\left(Q^{g}_{s.f.,i} + N_i \frac{\partial Q^{g}_{(\alpha,n)}}{\partial N_i}\right)$ $+\frac{1}{C_2}\int_V dV \left[I_{1,s.f.}(r)\right]^2 \overline{\nu(\nu-1)}^{g}_{i,s.f.} Q^{g}_{s.f.,i}$
Total scattering	ssctt	$\left(S^{g}_{C_2,\sigma_{s,i}}\right)_{indirect} = \frac{1}{C_2}\sum_{l=0}^{L}\int_V dV \sum_{g'=1}^{G} \phi^{*g'}_{2,l}(r) N_i (2l+1)\sigma^{g\to g'}_{s,l,i}\phi^{g}_l(r)$ $+2\frac{1}{C_2}\sum_{l=0}^{L}\int_V dV \sum_{g'=1}^{G} \Phi^{g}_{1,l}(r) N_i (2l+1)\sigma^{g\to g'}_{s,l,i}\phi^{*g'}_l(r)$
Nuclide density	density	$\left(S^{g}_{C_2,N_i}\right)_{indirect} = \left(S^{g}_{C_2,\nu_i}\right)_{indirect} + \left(S^{g}_{C_2,\sigma_{t,i}}\right)_{indirect} + \left(S^{g}_{C_2,\sigma_{s,i}}\right)_{indirect} + \left(S^{g}_{C_2,Q_{N_i}}\right)_{indirect}$ $+\frac{1}{C_2}\int_V dV \left[I_1(r)\right]^2 \overline{\nu(\nu-1)}^{g}_{i} N_i \sigma^{g}_{f,i}\phi^{g}_0(r)$

(a) It is not yet clear how to apply the equations of Ref. 19 when the induced-fission χ is a matrix, so SENSMG always uses a fission χ vector for subcritical multiplication sensitivities; $\Xi_i = \left(N_i \sum_{g'=1}^{G} \nu^{g'}_i \sigma^{g'}_{f,i} f^{g'}_i\right) \Big/ \left(\sum_{i=1}^{I} N_i \sum_{g'=1}^{G} \nu^{g'}_i \sigma^{g'}_{f,i} f^{g'}_i\right)$, where $f^{g'}_i$ is the spectrum weighting function when using the NDI at LANL, 1 otherwise.

(b) The sensitivity with respect to $\overline{\nu(\nu-1)}$ is not yet calculated or printed.

(c) Only elastic and inelastic edit cross sections are presently available.

The sensitivities of C_2 to $\bar{\nu}$ and $\overline{\nu(\nu-1)}$ assume that these parameters are independent.

SENSMG also computes the relative sensitivity S^{g}_{Y,ρ_n} of Y with respect to the mass density of each material defined in the SENSMG input file (Sec. III.B). The adjoint-based formulation for $S^{g}_{C_2,\rho_n}$ is

$$S^g_{C_2,\rho_n} = \frac{1}{C_2}\int_V dV \int_{4\pi} d\hat{\mathbf{\Omega}} \left\{ \psi^{*g}_2(r,\hat{\mathbf{\Omega}}) Q_n + \psi^{*g}_2(r,\hat{\mathbf{\Omega}}) \left(F_n - A_n\right) \psi^g(r,\hat{\mathbf{\Omega}}) \right\}$$
$$+ \frac{2}{C_2}\int_V dV \int_{4\pi} d\hat{\mathbf{\Omega}}\, \Phi^g_1(r,\hat{\mathbf{\Omega}}) \left(F^*_n - A^*_n\right) \psi^{*g}(r,\hat{\mathbf{\Omega}}) \tag{97}$$
$$+ \frac{1}{C_2}\int_V dV \int_{4\pi} d\hat{\mathbf{\Omega}} \left\{ Q^{*g}_2(r) \psi^g(r,\hat{\mathbf{\Omega}}) + Q^{*g}_{2,s.f.}(r) S^g(r,\hat{\mathbf{\Omega}}) \right\}$$

[note from Eq. (78) that $\partial Q^{*g}_{2,s.f.} / \partial \rho_n = 0$]. The total sensitivity S_{C_2,ρ_n} of C_2 to the mass density of coarse mesh n is the sum of $S^g_{C_2,\rho_n}$ over groups. It is important to note that the derivative in $S^g_{C_2,\rho_n}$ is a constant-volume partial derivative. Sensitivities of C_1 and C_2 are combined as in Eq. (81). Calculations of the relative sensitivity $S^g_{\mathrm{Sm}_2,\rho_n}$ of Sm_2 are completely analogous.

SENSMG also computes the derivative of Y with respect to the location of each material interface location and the location of the outer boundary. The derivative, computed for each energy group, is denoted $\partial Y^g / \partial r_n$. The adjoint-based equation for $\partial C^g_2 / \partial r_n$ has yet to be formally derived. The equation SENSMG presently uses is

$$\frac{\partial C^g_2}{\partial r_n} = \int_{S_n} dS \int_{4\pi} d\hat{\mathbf{\Omega}} \left\{ \psi^{*g}_2(r,\hat{\mathbf{\Omega}}) \Delta Q_n + \psi^{*g}_2(r,\hat{\mathbf{\Omega}}) \left(\Delta F_n - \Delta A_n\right) \psi^g(r,\hat{\mathbf{\Omega}}) \right\}$$
$$+2\int_{S_n} dS \int_{4\pi} d\hat{\mathbf{\Omega}}\, \Phi^g_1(r_n,\hat{\mathbf{\Omega}}) \left(\Delta F^*_n - \Delta A^*_n\right) \psi^{*g}(r_n,\hat{\mathbf{\Omega}})$$
$$+\int_{S_n} dS \int_{4\pi} d\hat{\mathbf{\Omega}}\, \Delta\left[\overline{\nu(\nu-1)}\Sigma^g_f\right]_n \left[I_1(r_n)\right]^2 \psi^g(r_n,\hat{\mathbf{\Omega}}) \tag{98}$$
$$+\int_{S_n} dS \int_{4\pi} d\hat{\mathbf{\Omega}}\, \Delta\left[\overline{\nu(\nu-1)}_{s.f.}\right]_n \left[I_{1,s.f.}(r_n)\right]^2 S^g(r_n,\hat{\mathbf{\Omega}}),$$

where again the Δ terms are differences across surface S_n. The total derivative of C_2 to the location of surface S_n, $\partial C_2 / \partial r_n$, is the sum of $\partial C^g_2 / \partial r_n$ over groups. It is important to note that $\partial C^g_2 / \partial r_n$ is a constant-density partial derivative. To compute $\partial Y / \partial r_n$, the derivatives of C_1 and C_2 are combined using

$$\frac{\partial Y}{\partial r_n} = \frac{1}{C_1}\frac{\partial C_2}{\partial r_n} - \frac{C_2}{C_1^2}\frac{\partial C_1}{\partial r_n}. \tag{99}$$

To compute $\partial \mathrm{Sm}_2 / \partial r_n$, the derivatives of C_1 and C_2 are combined using

$$\frac{\partial \mathrm{Sm}_2}{\partial r_n} = \frac{1}{2C_1^2}\frac{\partial C_2}{\partial r_n} - \frac{C_2}{C_1^3}\frac{\partial C_1}{\partial r_n} = \frac{1}{C_1}\left(\frac{1}{2C_1}\frac{\partial C_2}{\partial r_n} - \frac{C_2}{C_1^2}\frac{\partial C_1}{\partial r_n}\right). \tag{100}$$

There may be terms missing from Eq. (98). For this reason, the output file warns that results for interfaces are preliminary. However, the results in Sec. VI.I are encouraging.

It is not clear how to treat (α,n) neutron sources in the formalism of Ref. 19. A system with a substantial (α,n) neutron source rate density, relative to the total, may not be computed accurately.

III. User Interface

The SENSMG sensitivity tool is run by invoking the name of a Python control script with options. On the LANL high-performance computing (HPC) machines, the control script is `/usr/projects/data/nuclear/working/sensitivities/bin/sensmg.py`.

There are four ways to input information into SENSMG: 1) through preset environment variables; 2) through an input file; 3) through the command line; and 4) in special cases, through the Python script itself. These are discussed in the following subsections.

III.A. Environment variables

SENSMG checks the environment variable SENS_PARTISN for the specific executable version of PARTISN to run. If that variable is not set, SENSMG will use (in C-shell notation) `/usr/projects/lindet/rel8_27/8_27_15/${HN}-intel-17.0.4-openmpi-2.1.2/partisn`, where `${HN}` is derived from the HOSTNAME describing the computer that the user is on. See the PARTISN documentation for available versions and systems. SENSMG loads the appropriate modules for the supported PARTISN versions.

When using the Nuclear Data Interface (NDI) at LANL, the user should have environment variable NDI_GENDIR_PATH set. If there is none, SENSMG will use `/usr/projects/data/nuclear/ndi/2.1.3/share/gendir.all`.

III.B. Input file

The default input file name is `sensmg_inp`, but this can be changed with the `-i` parameter on the command line (Sec. III.C). There are two input file options: All materials and geometry are specified in one input file, or materials and geometry are specified in PARTISN `redoin` and `lnk3dnt` files.

III.B.1. Option 1: All materials and geometry in one input file

The input file tells what type of calculation to run, fully specifies the geometry and materials, and lists the reaction-rate ratios of interest.

A forward slash ("/") designates that the rest of the line is a comment. Forward slashes are required to end material composition lines and reaction-rate ratio lines. Each line of the input file is free-format, but the lines must be in a prescribed order. In some cases, the entries on a line must also be in a prescribed order. This section describes the order.

SENSMG computes one-dimensional (*r*) spheres or slabs or two-dimensional (*r*-*z*) cylinders. The input file for a spherical geometry is described in Table III. The first card is a title line. (It must not be in Fortran 5E6 format with the integers between 0 and 9, inclusive; see Sec. III.B.2.) The second card has `sph` or `sphere` for a sphere and it also tells the type of calculation to run, either k_{eff} (`keff`), α (`alpha`), neutron leakage (`lkg`), Feynman-Y asymptote (`feyny`), or Sm_2 (`sm2`). The order of these words is not important.

The third card tells the LIBNAME used to specify cross sections to PARTISN.

The fourth and fifth cards describe materials. The number of materials (NM) is given, and then the composition for each material is specified (each material on a single line) by ZAID and weight fraction (negative entry) or atom fraction (positive entry). Numeric ZAIDs, not the full cross-section-specification ZAIDs, are used to identify nuclides. After the material specifications, the material densities are listed in order on a single line, either mass density (negative entry) or atom density (positive entry) for each material. The same material can appear at more than one density but only if it is listed each time (once for each density) in the material list.

It is at this point that sphere/slab and cylinder input files differ. For a spherical or slab input, the sixth card tells the number of radial shells or slabs (NR) and the seventh card specifies the location (not the thickness) of each shell or slab, i.e., the outer radius or surface location. The eighth card assigns materials to spherical shells or slab layers in order.

The rest of the spherical input file tells where the reaction-rate ratios are to be calculated (i.e., in what regions) and what they are. The ninth card tells the number of edit points—i.e., coarse meshes—in which reaction-rate ratios will be computed. If the number of edit points is greater than zero, then the next card lists the indices of the radial shells in which the ratios are calculated. All reaction rates and fluxes are computed in the same locations. The tenth card tells the number of reaction-rate ratios, and the next set of lines gives the reaction-rate ratios in ZAID-reaction pairs; see below in this section for details. If the number of edit points or reaction-rate ratios is zero, SENSMG will only compute k_{eff}, α, or leakage sensitivities. No reaction rates are allowed for subcritical multiplication problems.

Table III. Spherical or Slab Input File Description.

Card	Description	Number of entries per line
1	Title	Max. 120 characters
2	[`sphere`|`sph`|`slab`] [`keff`|`alpha`|`lkg`|`feyny`|`sm2`]	2 (words)
3	LIBNAME	1
4.0	Number of materials (NM)	1
4.1–4.NM	Specification for each material. Each line has an index followed by a list of pairs of ZAID and weight fraction (negative entry) or atom fraction (positive entry). End each line with "/".	Variable
5	Mass density (g/cm^3; negative entry) or atom density (atoms/b·cm; positive entry) of each material	NM
6	Number of radial shells (NR)	1
7	Radius of each shell (cm)[(a)]	NR or NR+1[(a)]
8	Material assignments to radial shells (0 means void)	NR
9.0	Number of edit points (NEDPOINTS)	1
9.1–9.NEDPOINTS	Indices of coarse meshes to use to compute reaction rates[(b)]	NEDPOINTS
10.0	Number of reaction-rate ratios (NRRR)	1
10.1–10.NRRR	Reaction-rate ratios. End each line with "/".	2 or 4

(a) For spheres, the innermost surface is assumed to be 0. For slabs, the leftmost surface is entered.
(b) For spheres, enter radial mesh indices.

The input file for a cylindrical geometry is described in Table IV. The first five cards are the same as described above and in Table III for a sphere/slab geometry. The sixth card tells not just the number of radial shells but also the number of axial layers. The outer radius of each shell is given on the seventh card. The eighth card gives the height of each axial layer, starting at the bottom. The number of axial surfaces to specify is thus one plus the number of layers.

Next, materials are assigned to two-dimensional regions. The layout here is somewhat graphical in that each line has an entry for each radial shell (in order), and there is a line for each axial layer in order from top to bottom.

The tenth card tells the number of edit points. If the number of edit points is greater than zero, then the next card lists the mesh indices of the coarse meshes in which to compute reaction-rate ratios. The mesh indices are given using the equation in footnote (b) of Table IV.

The rest of the input file is the same as in the sphere/slab case.

Table IV. Cylindrical Input File Description.

Card	Description	Number of entries per line
1	Title	Max. 120 characters
2	[`cyl`|`cylinder`] [`keff`|`alpha`|`lkg`|`feyny`|`sm2`]	2 (words)
3	LIBNAME	1
4.0	Number of materials (NM)	1
4.1–4.NM	Specification for each material. Each line has an index followed by a list of pairs of ZAID and weight fraction (negative entry) or atom fraction (positive entry). End each line with "/".	Variable
5	Mass density (g/cm^3; negative entry) or atom density (atoms/b·cm; positive entry) of each material	NM
6	Number of radial shells (NR) and axial layers (NZ)	2
7	Radius of each shell (cm)[(a)]	NR
8	Height of each axial layer starting with the bottom of the first layer (cm).	NZ+1
9.1–9.NZ	Material assignments to radial zones for each axial layer (0 means void). Axial layers are listed top to bottom.	NR
10.0	Number of edit points (NEDPOINTS)	1
10.1–10.NEDPOINTS	Indices of coarse meshes to use to compute reaction rates[(b)]	NEDPOINTS
11.0	Number of reaction-rate ratios (NRRR)	1
11.1–11.NRRR	Reaction-rate ratios. End each line with "/".	2 or 4

(a) For cylinders, the innermost surface is assumed to be 0.
(b) For cylinders, each mesh index *n* is $n = (j-1)\times NR + i$, where $i = 1,\ldots,NR$ and $j = 1,\ldots,NZ$ are the (*r*,*z*) indices of the coarse mesh.

Cross sections are specified using the LIBNAME given in the input file. As when PARTISN is run on its own, the LIBNAME library must exist in the `gendir` file specified in the environment variable NDI_GENDIR_PATH (Sec. III.A). SENSMG searches for LIBNAME in the `gendir` file to set the cross sections. For each isotope in the problem, including edit isotopes (those only used in reaction rates), SENSMG sets the full ZAID (and therefore the cross sections) using the first instance of the isotope found with the specified LIBNAME in NDI_GENDIR_PATH. As when PARTISN is run on its own, the isotopes in the input file must match those available in the specified LIBNAME and NDI_GENDIR_PATH.

In addition to the libraries available through the NDI at LANL, SENSMG can use the Kynea3 cross sections developed by Varley and Mattingly.[27] The Kynea3 cross sections are in 79 groups and have upscattering in the lower 35 groups. Use `kynea3` for LIBNAME in the input file. The code will automatically set the number of energy groups to 79. Because the Kynea3 cross sections do not have a full set of edit reactions, this capability is generally applicable only to k_{eff}, α, leakage, and subcritical multiplication sensitivities. (The Kynea3 set does include the first four edit positions of Table V, discussed below.) The isotopes available in the Kynea3 set are listed with their ZAIDs in Appendix B. The Kynea3 cross sections have only an induced-fission χ vector, not a matrix, and the same χ vector is applied to all fissionable isotopes.

SENSMG can support users who do not have access to the NDI or Kynea3. If the word `special` is used for LIBNAME in the input file, SENSMG will look in directory SENS_DATA (see Sec. III.D) for four files from a forward run (`for_macrxs`, `for_snxedt`, `for_ndxsrf`, and `for_znatdn`), four files from a cross-section run (`xs1_macrxs`, `xs1_snxedt`, `xs1_ndxsrf`, and `xs1_znatdn`), and a file called `spc_gendir`, copied from the `sensmg.log` file (see Sec. IV; below "diagnostics from rdgendir" or "diagnostics from rdbxslib"), that gives the ZAIDs and atomic weights used in the problem. These nine files must correspond exactly to the end user's input file. The eight cross-section files must be created with the end user's PARTISN version. SENSMG is presently hard-wired to accept MENDF71X cross sections using this capability. The `spc_gendir` file may also contain the isotopic spectrum weighting functions $f_i^{g'}$ used to compute the material fission chi vector. If present, these must be given under the title "spectrum weight function". For each isotope, list the full zaid, then its spectrum weighting function with energy index, starting with group 1.

Using $\Sigma_1 = N_1\sigma_{x1}$ and $\Sigma_2 = N_2\sigma_{x2}$ in Eqs. (1), (2), and (4), reaction-rate ratios are specified as

```
ZAID1    x1    ZAID2    x2        /
```

Note that the forward slash at the end of the line is required. For k_{eff} and α, problems, if `ZAID2` and `x2` are not present, it means to use 1 for Σ_2, as discussed in Sec. II.B. Numeric ZAIDS are used to specify nuclides (i.e., the full cross-section specification is not used here). Reactions `x1` and `x2` are given as integers indicating the position of the desired cross section in the PARTISN edit tables. Available edit positions when the NDI is used are given in Table V. Note from Table V that the location of certain edit reactions changed with PARTISN version 8.

Table V. Edit Reactions Available from the NDI.

	PARTISN 7 and earlier		PARTISN 8 and later	
Position	Description	Name	Description	Name
1	fission spectrum	chi	fission spectrum	chi
2	effective nusigf	nusigf	effective nusigf	nusigf
3	total	total	total	total
4	absorption	abs	absorption	abs
5	chi	chi	chi	chi
6	elastic	mend1	elastic	(n,n)
7	inelastic	mend2	inelastic	(n,n')
8	(n,2n)	mend3	(n,2n)	(n,2n)
9	(n,3n)	mend4	(n,3n)	(n,3n)
10	(n,gamma)	mend5	(n,gamma)	(n,g)
11	(n,alpha)	mend6	(n,proton)	(n,p)
12	(n,proton)	mend7	(n,alpha)	(n,a)
13	(n,deuteron)	mend8	1st-chance fission	(n,f)
14	(n,triton)	mend9	2nd-chance fission	(n,n')f
15	(n,3He)	mend10	3rd-chance fission	(n,2n)f
16	sum of all fission	n-fiss	sum of all fission	(n,F)
17	prompt fission spectrum	mend12	prompt fission spectrum	chi_pr
18	total fission spectrum	mend13	total fission spectrum	chi_tot
19	—	—	(n,deuteron)	(n,d)
20	—	—	(n,triton)	(n,t)

An example of a spherical input file follows. (Note that though the composition of material 1 wraps here, it should be on a single line.)

```
   Pu-Flattop (PU-MET-FAST-006)
   keff sph
   mt71x / libname
   2 / no of materials
   1 94239 -9.38001E-01 94240 -4.79988E-02 94241 -2.99996E-03 31069 -6.53652E-03
31071 -4.46355E-03 / Pu-alloy
   2 92234 -5.40778E-05 92235 -7.10966E-03 92238 -9.92836E-01 / Flattop natural U
   -15.53 -19.00 / densities
   3 / no of shells
   0.155 4.5332 24.142  / outer radii
    1    1      2       / material nos
    1          / number of edit points
    1          / index of coarse mesh to use for reaction rates
    3          / number of reaction-rate ratios
    92238 16   92235 16 /numerator and denominator
    93237 16   92235 16 /numerator and denominator
    92235 10            /numerator and flux
```

An example of a cylindrical input file follows.

```
   HEU-MET-FAST-001-02 Godiva-II
   keff cyl
   mt71x / libname
   1 / no of materials
   1 92234 -1.01999E-02 92235 -9.37100E-01 92238 -5.27004E-02 / Godiva
```

```
-18.74 / densities
2 3 / no of r layers, no of z layers
  0.635 7.62  / outer radii
  0. 7.86 9.13 16.99  / heights
 1  1    / material nos, top
 1  1    / material nos
 1  1    / material nos, bottom
 1          / number of edit points
 3          / indices of coarse meshes to use for reaction rates
 1          / number of reaction-rate ratios
 92238 16   92235 16 /numerator and denominator
```

More examples are given in Appendix A and discussed in Sec. VI.

III.B.2. Option 2: `redoin` and `lnk3dnt` files

The `redoin` and `lnk3dnt` are files written by PARTISN and/or MCNP in a previous run. For SENSMG, the `redoin` file can have any name, and that is the file name specified with the `-i` parameter on the command line (Sec. III.C). SENSMG recognizes it as a `redoin` file because the first line is that of a PARTISN input in NAMELIST format: It has five one-digit integers each preceded by five spaces (Fortran 5I6 format), and the fourth integer is 1 (NPASS in the PARTISN manual[1]). Once SENSMG recognizes a `redoin` file, it expects to find a `lnk3dnt` file. The `lnk3dnt` file must be named "lnk3dnt" but it can be a symbolic link to a file with a different name. The `lnk3dnt` file is a binary file that contains the geometry specifications and the material in each mesh.[1]

The `redoin` file has the geometry type (slab, sphere, or cylinder) as `igeom` in block 1; the number of radial and axial coarse meshes as `im` and `jm`, respectively, in block 1; the number of materials as `mt` in block 1; LIBNAME as `libname` in block 3; the number of isotopes as `matls_size` in block 4; the materials and isotopes in the correct order in block 4; and the type of calculation (i.e., eigenvalue or fixed-source) as `ievt` in block 5. It has any reaction rates or reaction-rate ratios in block 6 (in the format given below).

If materials are specified in the `redoin` file rather than the `lnk3dnt` file, then the `matls` keyword in block 4 should have all materials in order. It is assumed that `matspec` is the same for all materials (only the first one is read). If materials are specified in the `lnk3dnt` file rather than the `redoin` file, then the `matls` keyword in block 4 should have one isotope per material, with its density given as 1, and `assign="matls"` (including the quotation marks). In both cases, material names must be given as `mNNNNNN` and zone names as `znNNNNNN`, where NNNNNN is at most a six-digit material number (fewer digits can be used). SENSMG does not have the generic input parser that PARTISN has.

In block 6, use "`/ nrrr=`" to set the number of reaction rates or reaction-rate ratios (NRRR in Table III and Table IV). Use `points_size` to set the number of fine-mesh points in the reaction-rate volume integral. Use `edisos` to specify isotopes involved in the desired reaction rates, and use `edxs` to specify reactions. Unlike in the regular `redoin` input, in this case the number of entries on these two lines is significant. As in the regular SENSMG input, two entries on a line are treated as a ratio and one entry is divided by the flux. Use `points` to specify the fine-mesh points used in the reaction rate integrals. Use the regular PARTISN convention to convert a fine mesh index (i,j) to an index n in a one-dimensional list:

$$n = (j-1)\times IT + i, \quad i = 1,\ldots,IT, \quad j = 1,\ldots,JT, \tag{101}$$

where *IT* and *JT* are the number of fine meshes in the radial and axial directions, respectively. (For a one-dimensional sphere or slab, *JT* = 1.)

MCNP6 can write regular PARTISN input files (not `redoin` format) and `lnk3dnt` files.[28] To convert MCNP6's PARTISN input `partinp` to the correct format to use with SENSMG to run `lnk3dnt` files, simply run it with PARTISN. The resulting `redoin` file is then the SENSMG input file. It only needs to be modified to include any reaction-rate ratios as described above.

SENSMG is not set up to run a `lnk3dnt` file that specifies more than one fine mesh per coarse mesh unless there is also only one material (usually comprising multiple isotopes) specified in each fine mesh. In this case, SENSMG accepts the `redoin`/`lnk3dnt` input but treats it like a regular input, after it checks to ensure that every coarse mesh has only one material (all fine meshes within each coarse mesh have the same material). This is the type of `lnk3dnt` file that PARTISN writes when `wrlnk3d=1` in block 1. Also in this case, the points to list for reaction rates should use the coarse-mesh indices rather than the fine-mesh indices in Eq. (101).

The number of groups, number of angles, scattering order, etc. are also present in the `redoin` file but these are ignored (except that warnings are issued if they differ from the SENSMG command-line inputs [Sec. III.C]).

The `redoin` file need not have "`fmmix=1`" in block 1 to tell PARTISN to read the geometry and materials from the `lnk3dnt` file.[1] That keyword is written to SENSMG's PARTISN input file.

The `redoin`/`lnk3dnt` capability is only implemented for k_{eff} or α eigenvalue problems. If `ievt` = 0 in the `redoin` file, specifying a fixed-source problem to PARTISN, SENSMG will do an α eigenvalue problem instead.

To reiterate, the `redoin`/`lnk3dnt` capability is invoked from the format of the first line of the input file. This slightly limits the type of title that should be used in a regular SENSMG input file (Sec. III.B.1).

III.C. Command line

The available command line options are listed and described in Table VI beginning on the next page.

If PARTISN version 7 or earlier is used, then spherical and slab problems should be run using a single processor (`-np 1`). The reason is that Eq. (26) is more accurate than Eq. (27), and PARTISN's angular fluxes are readily available for one-dimensional problems, except that MPI runs of PARTISN 7 (and earlier) cannot print the angular flux file. If PARTISN version 8 or later is used, then spherical and slab problems can be run with as many processors as are available.

Because of memory limitations, cylindrical problems approximate the volume inner product of angular fluxes with a moments expansion [Eq. (27)]. Therefore, cylindrical problems can always be run with as many processors as are available. (This approximation is too crude for surface integrals, so the `-rplane` and `-zplane` options discussed below were developed.)

Table VI. Command Line Options.

Flag	Description	Default
`-i`	Input file name	`sensmg_inp`
`-np`	Number of mpi processes to use for PARTISN	1
`-ngroup`	Number of energy groups	30
`-isn`	S_N order	32
`-isct`	Legendre scattering expansion order	3
`-epsi`	Convergence criterion for PARTISN calculations (PARTISN's `epsi`[1])	1E-06
`-epsig`	Convergence criterion for GPT adjoint calculations in the method of successive approximations	1E-05
`-chinorm`	`full`/`partial`/`none` constrained normalization for the chi matrix	`full`
`-fissdata`	`0`/`1`/`2` use fission transfer matrix/chi matrix/chi vector (PARTISN's `fissdata`[1])	`0`
`-chieff`	`0`/`1` don't/do include the derivative of the material χ with respect to isotope density, ν, and σ_f	`0`
`-fissneut`	`0`/`1` use prompt/total nu-bar (PARTISN's `fissneut`[1])	`1`
`-aflxfrm`	`0`/`1` no/yes use an α-eigenvalue search method that may help for subcritical problems (PARTISN's `aflxfrm`[1]; ignored for versions before 7.72)	`0`
`-trcor`	`no`/`diag`/`bhs`/`cesaro` (PARTISN's `trcor`[1])[(a)]	`no`
`-alpha_n`	`yes`/`no` use/ignore (α,n) neutron sources	`yes`
`-misc`	`yes`/`no` use MISC/use SOURCES4C for spontaneous fission sources	`yes`
`-nag`	Number of α-particle energy groups in SOURCES4C	100
`-srcacc_no`	`none`/`for`/`adj`/`for+adj` turn off source acceleration for neither/forward/adjoint/both	`none`
`-use_existing`	`yes`/`no` use/don't use PARTISN output files that have already been calculated.	`no`
`-my_modules`	`yes`/`no` use/don't use user's own loaded module files. "yes" skips automatic module file loading, used to override defaults or if the user's system does not use modules.	`no`
`-rplane`	Radial surface on which to compute angular fluxes	–1 (i.e. do not use)
`-zplane`	Axial surface on which to compute angular fluxes	–1 (i.e. do not use)

Table VI (continued). Command Line Options.

`-xsecs`	`no/yes` don't/do compute sensitivities with respect to cross sections	`yes`
`-plotg`	`no/yes` don't/do write an MCNP input file for plotting the geometry	`no`
`-wrxsecs`	`no/yes` don't/do write an output file of cross sections called `xsecs`	`no`
`-wrsensmg`	`no/yes` don't/do write a SENSMG input file from information in `redoin` and `lnk3dnt` files	`no`
`-h`	Show options (i.e., help)	None

(a) Computed sensitivities do not include the effect of diagonal and BHS transport corrections.[29] These transport corrections should not be used with `isct` < 3. The Cesàro transport correction should not be used at all.

The number of energy groups "`-ngroup` [*G*]" available when using the NDI at LANL is *G* = 618, 301, 250, 141, 133, 130, 91, 75, 70, 49, 47, 30, 21, 16, 14, 13, 12, 10, 9, 8, 7, 6, 5, 4, 3, 2, and 1. Not every value is available for all possible values of LIBNAME (Sec. III.B). (The 130-group library[30] is particularly limited.) The 79-group Kynea3 set[27] is also available (Sec. III.B). Detector efficiency functions, used for computing subcritical multiplication, are presently only available for *G* = 618, 130, 79, 70, 44, 30, 2, and 1.

For spheres and slabs, the "traditional" S_N constants are used (`iquad=1` in PARTISN lingo[1]). For cylinders, the square Chebychev-Legendre built-in set is used (`iquad=6`). For both geometries, any even S_N quadrature order can be used[1]; set with the `-isn` parameter.

The `-epsig` parameter is the convergence criterion for the sum in Eq. (16). Before the latest $\Gamma_n^{*g}(r,\hat{\mathbf{\Omega}})$ is added to the current sum up to $n-1$, each element of $\Gamma_n^{*g}(r,\hat{\mathbf{\Omega}})$ (radial fine mesh, axial fine mesh, energy group, and either moment or discrete ordinate) is divided by the corresponding element in the current sum. If the absolute value of the largest ratio is smaller than `epsig`, the sum is considered to be converged. The latest $\Gamma_n^{*g}(r,\hat{\mathbf{\Omega}})$ is then added to the current sum (whether the sum is converged or not).

The `-chinorm` parameter controls constrained normalization for induced-fission χ sensitivities. Constrained normalization is described in Ref. 31 for material compositions, but SENSMG uses the same equations for the normalization of χ sensitivities. The `-chinorm` parameter is similar to the CONSTRAIN keyword on MCNP6's KSEN card.[28] In MCNP6, "CONSTRAIN = yes" gives full normalization[32] and is the default, as in SENSMG. "CONSTRAIN = no" is the same as "`-chinorm none`". MCNP6 does not have a partial normalization option.

The material induced-fission χ vector or matrix is computed from isotopic χ vectors or matrices using isotopic densities and $\nu\sigma_{f,i}^{g}$ cross sections. (The material χ vector also includes an isotopic spectrum weight function f_i^g when the NDI is used.) The `-chieff` parameter controls whether the computed sensitivities include the derivative of the material χ values with respect to the isotopic data. These derivatives are expected to be very small.

For fixed-source neutron leakage problems (keyword `lkg` in the input file; Sec. III.B), SENSMG uses the MISC code[16] to compute spontaneous fission sources and the SOURCES4C code[15] to compute (α,n) sources. "`-misc no`" can be used to have SENSMG use SOURCES4C rather than MISC for spontaneous fission sources. "`-alpha_n no`" can be used to ignore (α,n) sources altogether.

The `-srcacc_no` parameter is useful if the PARTISN iterations for the forward or adjoint files are observed to "flip flop" between two states or otherwise have trouble converging. If that happens, turn off source acceleration for the difficult calculation. Source acceleration is always turned off for the generalized adjoint functions.

The `-use_existing` option is a quick way to see the effect of a change in the χ sensitivity normalization using the `-chinorm` parameter or the effect of including the derivative of the material χ with respect to other parameters using the `-chieff` parameter. It is also a quick way to write an MCNP geometry plot file using the `-plotg` option or the cross sections using the `-wrxsecs` option, both described below.

The `-rplane` and `-zplane` options activate PARTISN's ASLEFT/ASRITE and ASBOTT/ASTOP keywords[1] to write surface angular flux files on the specified surfaces. The radial surfaces are indexed from 1 to NR, and the axial surfaces are indexed from 0 to NZ (bottom to top). Without this option, in cylindrical problems, the surface fluxes appearing in Eqs. (29), (40), and (67) are approximated using mesh-centered moments. This feature is intended for PARTISN versions before 8.27. Those versions allow only one surface in each coordinate direction to have all angular fluxes written. The default value for both directions is –1, which deactivates this feature.

Beginning with version 8.27, PARTISN is able to write surface angular fluxes for a user-input list of surfaces using the AFLUXX and AFLUXY keywords.[1] For cylindrical problems, SENSMG automatically generates that list.

The `-xsecs` option allows the user to skip calculating and outputting the cross-section sensitivities if geometry (i.e., mass densities and interface locations) is the only interest.

The `-plotg` option writes an MCNP input file called `inpi` and plot command file called `com` to use for plotting the SENSMG geometry with MCNP. It does not actually call MCNP to create the plot. The files are created before any PARTISN calculations are run, and sensitivities are not computed.

The `-wrxsecs` option writes an output file called `xsecs` that contains the material macroscopic cross sections and isotope microscopic cross sections. The file is written after the forward transport calculation finishes, but sensitivities are not computed.

The `-wrsensmg` option writes a SENSMG input file, named `tmp_sensmg_inp`, from information in the `redoin` and `lnk3dnt` files. This capability can be used to see what geometry and materials are actually in the `redoin` and `lnk3dnt` files. The SENSMG file can then be plotted with the `-plotg` option. With this option, sensitivities are not computed.

The execution command for SENSMG at LANL is
`/usr/projects/data/nuclear/working/sensitivities/bin/sensmg.py`

III.D. Python control script

The full path specifying the executable code for SENSMG is set in the Python control script as a local variable. The paths to the SOURCES4C code[15] and its data files, used in fixed-source problems, are also set in the script (as local variables). The path to the MISC code[16] and its data files, also used in fixed-source problems, are also set in the script (as local variable `misc_exe` for the code and environment variable ISCDATA for the data).

The path to the directory containing group-structure files, Kynea3 cross sections, and special cross-section files (LIBNAME = `special`; see Sec. III.B) is set in the script as environment variable SENS_DATA.

The main reason that a user might want a local copy of the Python script is to set different locations for the executable code (including different versions) or data files.

The path and file variables set in the Python script are listed in Table VII.

Table VII. Variables Set in the Python Script.

Variable	Description
`sensmg_exe`	SENSMG executable name including full path
`sources_exe`	SOURCES4C executable name including full path
`sources_dir`	Full path to directory containing SOURCES4C data (tape files)
`misc_exe`	MISC executable name including full path
ISCDATA	Full path to directory containing MISC data
SENS_DATA	Full path to directory containing SENSMG data (group-structure files, detector efficiency files, etc.)
SENS_PARTISN	A default value to use if the user does not have one set (Sec. III.A); it is `/usr/projects/lindet/rel8_27/8_27_15/snow-intel-17.0.4-openmpi-2.1.2/partisn`
NDI_GENDIR_PATH	A default value if to use the user does not have one set (Sec. III.A); it is `/usr/projects/data/nuclear/ndi/2.1.3/share/gendir.all`

IV. Output

The main output of SENSMG consists of five files. The first two are `sens_rr_x` and one of `sens_k_x`, `sens_a_x`, or `sens_l_x`, which contain the sensitivities of the specified reaction rates and k_{eff} or α or neutron leakage, respectively, to all cross sections, as shown in Table I. For subcritical multiplication problems, the file `sens_s_x` containing the sensitivities of the Feynman Y or Sm_2 is printed in addition to `sens_l_x`. In these files, sensitivities are given in units of %/%. The sensitivity to the total cross section (denoted "total" in the output tables) is the relative change in the ratio or the eigenvalue if *only* the total cross section for each isotope changes. This notion of the sensitivity to the total cross section is different from the way it is understood in MCNP6 (Ref. 28) and SCALE 6.2 (Ref. 33). There, the total cross section is the sum of all other cross sections and the sensitivity to the total cross section is the same as the sensitivity to the isotopic density.[31] In PARTISN, it is possible for the total cross section to change independently of all other cross sections and densities. SENSMG uses the label "density" to denote the sensitivity to the total cross section or density as it is understood in MCNP and SCALE (Table I). This explains why it is possible to have an energy-dependent sensitivity to the density in PARTISN (see the equation for the sensitivity to the density in Table I and Table II).

The file `sens_rr_x` includes a block of data for each reaction-rate ratio. Each "ratio block" includes the indirect effect as a block for each isotope in each material, the direct effect as a single block that includes the numerator and the denominator, and the total (indirect plus direct) as a block for each unique isotope in the problem. If an isotope appears in more than one material, the total will include all of its appearances and include indirect and direct effects, if any.

The file `sens_k_x` or `sens_a_x` or `sens_l_x` or `sens_s_x` includes a single "k_{eff} block" or "α block" or "leakage block" or "subcritical multiplication block," respectively, that includes the result of Eq. (22), (38), (47), or (81) [or (83)], respectively, as a block for each isotope in each material and the total as a block for each unique isotope in the problem. If each isotope only appears in one material, then the "total isotope" block will be the same as the "isotope by material" block.

The isotope blocks begin with an isotope "summary," which is just the sum over groups of each sensitivity of Table I or Table II. The group-dependent sensitivities follow. The isotope blocks include the full matrix of sensitivities to chi, each element of which is, for example,

$$S_{R,\chi_i}^{g'\to g} = \frac{1}{k_{eff}} \int_V dV\, \Gamma_0^{*g}(r)\chi_i^{g'\to g} N_i \nu_i^{g'} \sigma_{f,i}^{g'} \phi_0^{g'}(r), \tag{102}$$

and the full matrix of sensitivities to scattering, each element of which is, for example,

$$S_{R,\sigma_{s,l,i}}^{g'\to g} = \int_V dV\, \Gamma_l^{*g}(r) N_i (2l+1) \sigma_{s,l,i}^{g'\to g} \phi_l^{g'}(r) \tag{103}$$

for $l > 0$. [For α and leakage calculations, k_{eff} is set to 1 in Eq. (102).] The zeroth-moment scattering elements include the effect on the total cross section as shown in the entries on Table I and Table II. In the chi and scattering matrices that are printed, columns are "from" groups [g' in Eqs. (102) and (103)] and rows are "to" groups (g).

The normalization of chi is indicated in the label for chi: `chi_(nn)` is used for no normalization, `chi_(fn)` for full normalization, and `chi_(pn)` for partial normalization. In full normalization, the sum over groups is analytically zero, but the output may have very small nonzero values due to numerical imprecision.

Using Eq. (9), it can easily be shown that the sum over groups of the direct effect should be one.

The third and fourth main output files are `sens_rr_r` and one of `sens_k_r`, `sens_a_r`, or `sens_l_r`. These are the sensitivities of the specified reaction rates and k_{eff} or α or neutron leakage, respectively, to the mass densities, as given by Eqs. (28), (39), or (66), respectively, and the derivatives with respect to the interface locations, as given by Eq. (29), (40), or (67), respectively. For subcritical multiplication problems, the file `sens_s_r` containing the sensitivities of the Feynman Y or Sm_2 with respect to mass densities as given by Eq. (97) and derivatives with respect to interface locations as given by Eq. (98) is printed in addition to `sens_l_r`. The sensitivities have units of %/% and the derivatives have units of (units of quantity of interest)/cm. This output file has a block for the density sensitivities, followed by a block for the radial surface derivatives, followed by a block for the axial surface derivatives (for cylinders).

For cylinders, the derivative for each surface of each coarse mesh is output individually. The block for radial surface derivatives has an entry for each of the NR radial coarse mesh surfaces and each of the NZ axial zones (in the notation of Table IV). The block for axial surface derivatives has an entry for each of the NR radial zones and each of the NZ + 1 axial surfaces.

If the material is the same on both sides of the coarse mesh, the derivatives on the surface will be zero, but they will still be output.

For the `redoin`/`lnk3dnt` capability, each mesh is considered to have a different material (or void). The relative sensitivity of the response to the density of the material in each mesh is output.

The fifth main output file is `sensmg.log`, which has all of the input parameters, any warnings that were generated, and information from SENSMG's reading of NDI_GENDIR_PATH. Diagnostic information about the forward and adjoint transport calculations and the iterations for the generalized adjoint functions is printed as the calculations are run. For example, the normalization of Eq. (19), (36), (53), or (54) is checked at each iteration. It is difficult to monitor the progress of the iterations in the foreground window because the PARTISN screen output is constantly scrolling. The user can `cat` the contents of the log file in another window in order to monitor progress. A convergence monitor can be extracted with a command like "`grep convergence sensmg.log`".

For leakage calculations, this file also includes $\partial Q_{(\alpha,n)} / \partial N_i$, the derivative of the total (α,n) source rate density with respect to each isotope, labeled as "dQ/dN for (alpha,n) sources", separated into contributions from each nuclide as a target, stopping element, and α-emitter.

SENSMG also keeps all input files, all text output files from transport and source calculations, and all binary cross-section and flux files.

V. Some Notes on the Coding

SENSMG is a combination of a Python script and a Fortran code. The Python script runs MISC and/or SOURCES4C (for fixed-source problems). It runs PARTISN and controls the iterations in the solution of Eqs. (14) and (33). The Fortran code writes MISC, SOURCES4C, and PARTISN input files and reads MISC, SOURCES4C, and PARTISN output files, including cross-section files. The Fortran code computes and writes the final sensitivities. The Fortran code can probably be replaced with Python, but the author is not adept enough at Python to do this cost-effectively.

For fixed-source calculations, SENSMG first computes the intrinsic neutron source using the MISC code[16] and/or the SOURCES4C code.[15] The energy group structure is needed for this input before it is available from the PARTISN output files. Thus, the available energy group structures are listed in data files in the `sensmg/data` directory (set with the SENS_DATA environment variable in the `sensmg.py` script; see Sec. III.D). The available energy-group structures are those listed under the heading "NDI group structure" at <https://xweb.lanl.gov/projects/data/nuclear/ndi_data/transport/group_structure.html> as [*G*]`_lanl`. The 79-group Kynea3 library is also available. See the `ngroup` keyword in Sec. III.C. (The "special" 16-, 12-, and 2-group structures exist but are not available because there is no logic to use these in PARTISN. The group structures 87_llnl, 17_llnl, 16_llnl, 105_awe, and 16_hr also exist but are not available for the same reason.)

To add a new group structure, follow the example in source file `set_ebins.F`. Increase the number of available group-structure files and add the file name to the DATA statement. Add logic to select the correct file name. Finally, put the group structure data file in the `sensmg/data` directory. If it is to be available through the NDI, the data file name is [*G*]`_lanl`; otherwise, it is [*G*]_[LIBNAME].

SENSMG gets cross sections from PARTISN outputs. It writes a special PARTISN input file with one problem or edit isotope per zone, with atom density equal to 1 atom/(b·cm), and runs it with `nosolv=1`, a PARTISN block 1 input entry[1] that turns off the solver module but not before PARTISN writes a `macrxs` macroscopic cross-section file and an `snxedt` microscopic edit cross-section file. The `macrxs` file now has microscopic transport data for every isotope. The fission and capture cross sections for every isotope are read from the `snxedt` file.

It has been suggested to use existing tools to use the NDI to read cross-section files directly. However, the present scheme allows SENSMG to compute sensitivities for any cross-section library, not just those available through the NDI. The ability to use the Kynea3 library has been very useful.

After computing the neutron source rate density (if necessary), SENSMG runs PARTISN for the forward input file and the special cross-section input file. In subsequent adjoint and generalized adjoint calculations, SENSMG uses the cross-section files from the forward run with PARTISN's "`lib=macrxs`" option.[1] This saves a lot of time.

The adjoint k_{eff} or α from Eq. (12) or (31) is read from the adjoint output file and compared with the forward value; the comparison is printed in the log file. For fixed-source calculations, the adjoint-based leakage is computed using

$$L = \int dV \sum_{g=1}^{G} \int_{4\pi} d\hat{\mathbf{\Omega}} \psi^{*g}(r, \hat{\mathbf{\Omega}}) Q^{g}(r)$$
$$= \int dV \sum_{g=1}^{G} \phi^{*g}(r) Q^{g}(r)$$
$$= \sum_{n=1}^{N_z} \sum_{g=1}^{G} \phi_n^{*g}(r) Q_n^{g}(r), \quad (104)$$

where n is an index representing coarse meshes and N_z is the number of coarse meshes (zones). Equation (104) is evaluated using PARTISN's edit module for the adjoint calculation, with the forward source $Q_n^g(r)$ in coarse mesh n used as the response function in coarse mesh n.

SENSMG supports older versions of PARTISN (5.69 and 7.72) as well as newer (8, currently up to 8.31). One place in the Fortran code that depends on the PARTISN version is where the code writes the forward input file. Because it might be of interest to the user, all available reaction-rate edits are specified for the edit isotopes. There are 18 available in PARTISN version 7 (and earlier) but 20 in version 8 (see Table V). For now, it appears to be an easy thing to support this difference, but if it becomes a burden, then the code will be changed to print only the reaction rates specified in the input file. If an unsupported PARTISN version is used, SENSMG will simply not specify edits in the forward input file.

SENSMG automatically loads the correct modules for the specified PARTISN version and the detected host. As modules, PARTISN versions, and computers get updated and deprecated, this logic will have to be maintained. The "`-use_existing yes`" option is intended for use when the user knows that his modules are the correct ones.

New cross-section libraries that become available through the NDI should work automatically. Stand-alone libraries such as Kynea3 can be accommodated with a small amount of effort, using the coding for Kynea3 as an example.

To add a new detector efficiency file, follow the example in source file `set_deteff.F`. Increase the number of available efficiency files and add the file name to the DATA statement. Add logic to select the correct file name. Finally, put the group structure data file in the `sensmg/data` directory. The file name is [`detname`]_[*G*], where variable `detname` is the detector name. The detector name "npod" is presently hard-coded in source file `rdmdl.F`. It will eventually become a user input, either on the command line or in the input file.

SENSMG is generally LANL-HPC-centric, but it should be straightforward to generalize it to other platforms. In the Python script, modify the default value of SENS_PARTISN and the construction of PARTISN_EXE, which uses the variable MACH, derived from the environment variable HOSTNAME. If your system does not use modules, set the default MY_MODULES to yes (for convenience). Modify the location of your cross-section data files. The Fortran code does not need to be modified.

PARTISN solves Eqs. (18) and (35) using "`nosigf=1`" to inhibit fission multiplication. PARTISN solves Eq. (35) using "`anorm`=[α]" to put the α/v term on the left-hand side. For Eqs. (18), (35), and (51), the sources are input to PARTISN using the `fixsrc` file rather than the standard input file.

As noted, SOURCES4C is used to compute the intrinsic neutron source for fixed-source problems. A special version of SOURCES4C was made that does not stop on certain errors (namely, "Target nuclide not found in tape3", "Target nuclide not found in tape4", "Source nuclide not found in tape5", "S.F. source nuclide not found on tape5", and "D.N. source nuclide not found on tape5"). Also, more digits are written to the SOURCES4C output files in certain places. These digits are not improving the accuracy of the simulation, but they are needed so that sources are balanced correctly, particularly for the central-difference calculations used for verification. In addition, SOURCES4C was modified to print the quantities that are needed to compute Eq. (62).[17]

VI. Sample Problems and Verification

This section provides a few results for a few problems. Default values of the input parameters (Sec. III.C) were used unless otherwise stated. A more thorough verification by comparison with adjoint-based sensitivity results from MCNP6 (Ref. 28) has been performed for k_{eff} problems for fast spherical systems.[34,35]

VI.A. Comparison with MCNP6 and SCALE 6.2 for k_{eff} sensitivities for a cylinder

A test problem was documented in Ref. 31 in which the sensitivities of k_{eff} to isotopic densities in a homogeneous cylinder were computed using MCNP6 (Ref. 28), SCALE 6.2 (Ref. 33), and PARTISN. Results are repeated here. The fuel is similar to that used in the Transient Reactor Test Facility[36] (TREAT) at Idaho National Laboratory. The height and radius of the reactor are 240 cm and 60 cm, respectively. The atom density and the mass density of the fuel are 0.113705 atoms/b·cm and 2.27 g/cm^3, respectively. The composition of the fuel is given in Table VIII. The enrichment is 92.9168 wt.% ^{235}U. The input file for SENSMG is listed in Appendix A. The calculations used S_{64} angular quadrature and a P_7 scattering expansion.

Table VIII. Composition of TREAT Fuel.

Nuclide	Atom Density (atoms/b·cm)	Weight Fraction
^{1}H	1.13694E-4	8.38215E-5
^{10}B	5.68468E-7	4.16390E-6
C (nat.)	1.13579E-1	9.97955E-1
^{235}U	1.05735E-5	1.81803E-3
^{238}U	7.95855E-7	1.38591E-4

In MCNP6, the $S(\alpha,\beta)$ table grph.20t was associated with the fuel. Otherwise, ENDF/B-VII.1 cross sections were used. In SCALE, the cross section table for carbon in graphite was associated with natural carbon, and ENDF/B-VII.1 cross sections were used. (Chris Perfetti ran the SCALE calculations at Oak Ridge National Laboratory.) SENSMG used Kynea3 with the "C(gph)" $S(\alpha,\beta)$ data for carbon and it used S_{64} angular quadrature and a P_7 scattering expansion. Also it used 16 processors.

Results are shown in Table IX. The deterministic sensitivities are in excellent agreement with the Monte Carlo sensitivities. They are within 1.4% of the MCNP6 results, except for the sensitivity to ^{1}H, for which the deterministic sensitivity is 11% smaller. It is likely that the deterministic neutron flux spectrum, with only 79 groups, is not quite as thermal as the continuous-energy Monte Carlo spectrum.

Table IX. Sensitivity S_{k,N_j} to Constituents of TREAT Fuel.

Nuclide	MCNP	SCALE	PARTISN
^{1}H	4.0059E-03 ± 4.37%	4.0194E-03 ± 1.63%	3.5619E-03
^{10}B	–2.0248E-01 ± 0.02%	–2.0235E-01 ± 0.00%	–2.0292E-01
C (nat.)	5.9836E-01 ± 0.46%[(a)]	5.8209E-01 ± 1.58%	5.9970E-01
^{235}U	3.5071E-01 ± 0.04%	3.5032E-01 ± 0.01%	3.4584E-01
^{238}U	–2.5392E-03 ± 0.50%	–2.5494E-03 ± 0.14%	–2.5535E-03
$S(\alpha,\beta)$	2.3217E-01 ± 0.82%	N/A[(b)]	N/A[(b)]

(a) Includes the $S(\alpha,\beta)$ sensitivity for the grph table.
(b) Not applicable—$S(\alpha,\beta)$ scattering is not calculated separately in SCALE or PARTISN.

VI.B. Comparison with MCNP6 KSEN results for a sphere

Results from SENSMG were compared with results from the KSEN card[28] of MCNP6 for a one-dimensional spherical Flattop-Pu model.[37] The SENSMG input file and the MCNP6 input file are listed in Appendix A. The PARTISN sensitivities used 30 groups, S_{32} angular quadrature, and a P_3 scattering expansion.

The sensitivity profiles of k_{eff} to the density of ^{235}U in the reflector are compared in Figure 1. The agreement is excellent.

Group-dependent results for the unconstrained (unnormalized) sensitivity of k_{eff} to the chi distribution of ^{235}U in the reflector are compared in Figure 2, and results using full normalization are compared in Figure 3. In both cases, the agreement is excellent. The full-normalization results are in the same output file as the density results of Figure 1. The unconstrained results were obtained using the same flux files with "`-use_existing yes -chinorm none`" (Sec. III.C).

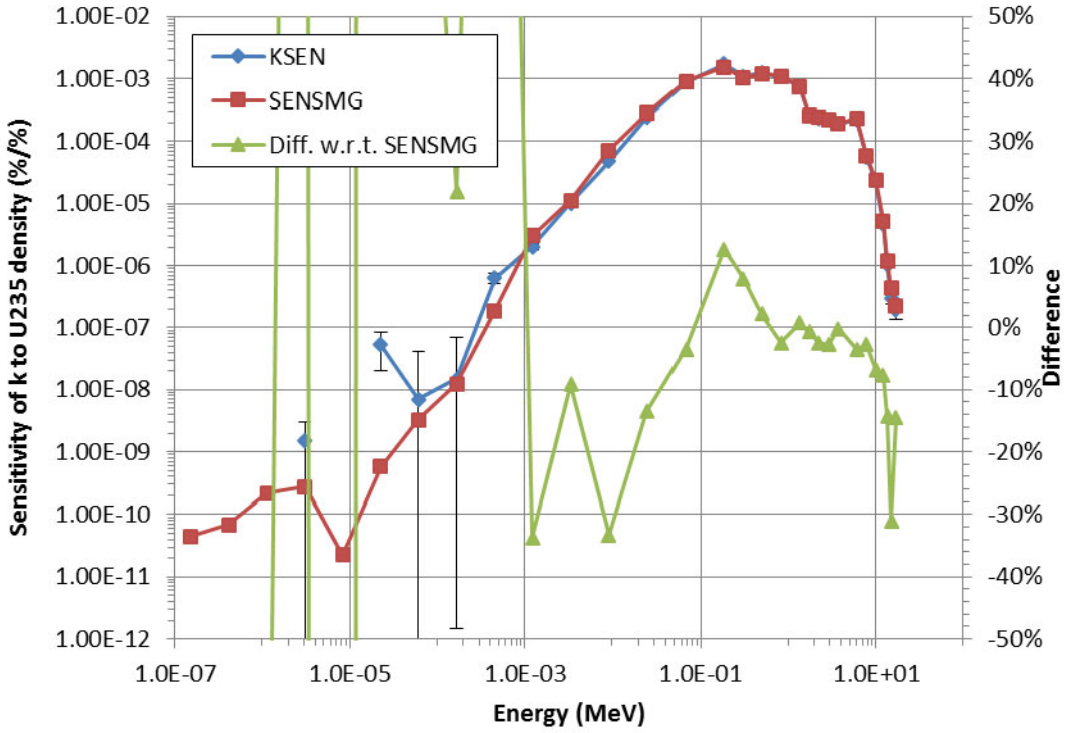

Figure 1. Sensitivity of k_{eff} to ^{235}U density in Flattop-Pu reflector.

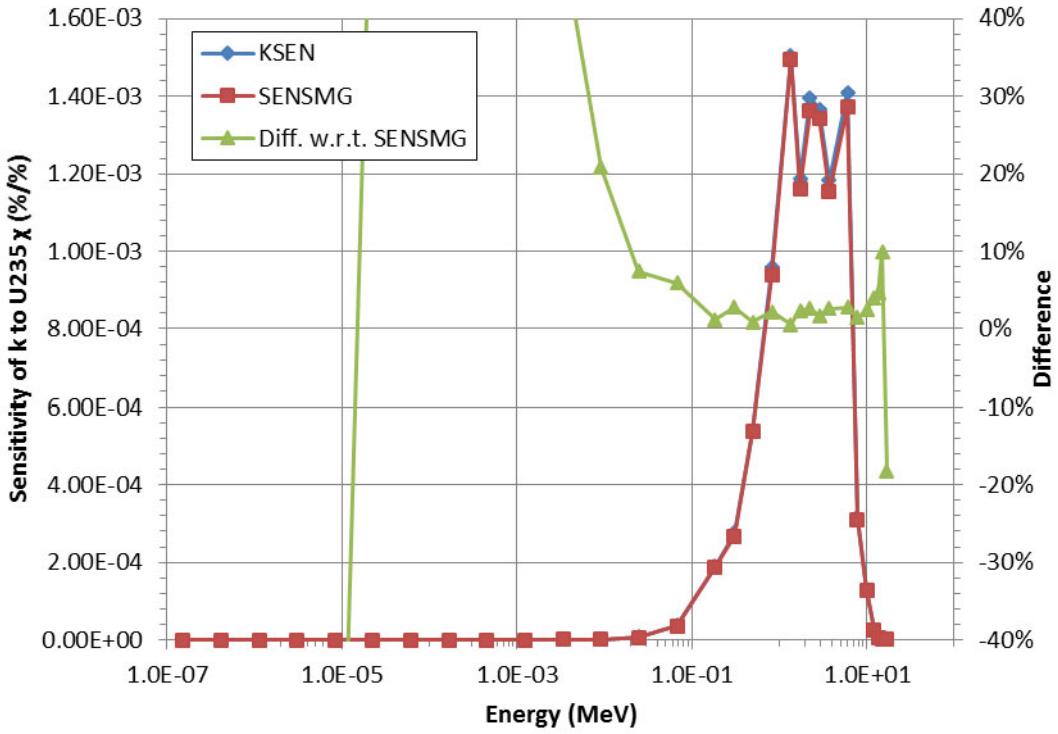

Figure 2. Sensitivity (unconstrained) of k_{eff} to ^{235}U chi in Flattop-Pu reflector.

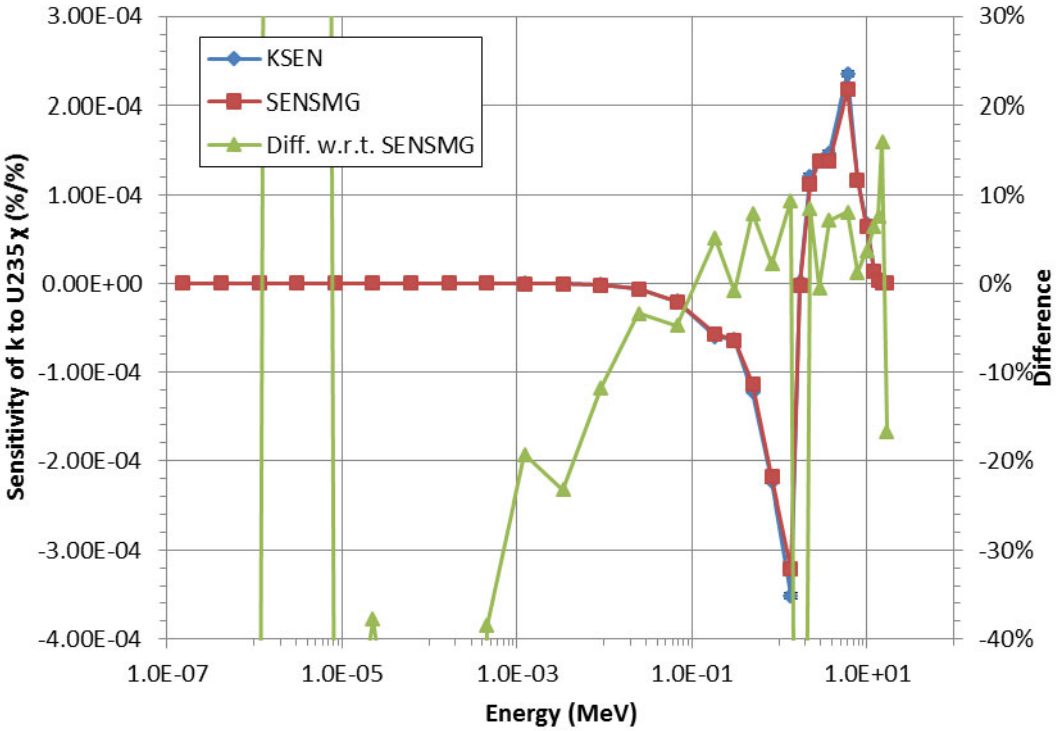

Figure 3. Sensitivity (full normalization) of k_{eff} to ^{235}U chi in Flattop-Pu reflector.

VI.C. Comparison with TSUNAMI-ID for a reaction-rate ratio with λ-mode flux

As part of a verification for a continuous-energy Monte Carlo GPT capability for SCALE, Perfetti recently published TSUNAMI-1D results.[7] The multigroup sensitivity tool SENSMG of this paper is more similar to the deterministic TSUNAMI-1D capability than to the Monte Carlo capability, so TSUNAMI-1D results were used for comparison. Reference 7 shows graphs of sensitivity profiles; Perfetti kindly provided the numerical results.[38]

The problem is the one-dimensional spherical Flattop-Pu model and the ratio of interest is the ^{237}Np fission rate (F37) to the ^{235}U fission rate (F25) in a central sphere of radius 0.155 cm (whose volume matches that of the cylindrical foil described in Ref. 7). The TSUNAMI-1D calculation used 238 energy groups and S_{16} angular quadrature.[7] It used ENDF/B-VII.0 cross sections with self-shielding and a P_5 scattering expansion.[38] SENSMG used ENDF/B-VII.1 cross sections in 70 energy groups with no self-shielding, S_{32} quadrature, and a P_3 scattering expansion. The SENSMG input file is listed in the Appendix A.

The sensitivity profiles of the ratio F37/F25 to the ^{239}Pu density and fission cross section are shown in Figure 4, where SENSMG results are compared with TSUNAMI-1D results (compare with Fig. 9 of Ref. 7, where "total" is "density" of this report; see Sec. IV). The two codes generally agree very well. The peaks in the SENSMG profiles are about 5% smaller than the peaks in the TSUNAMI-1D profiles.

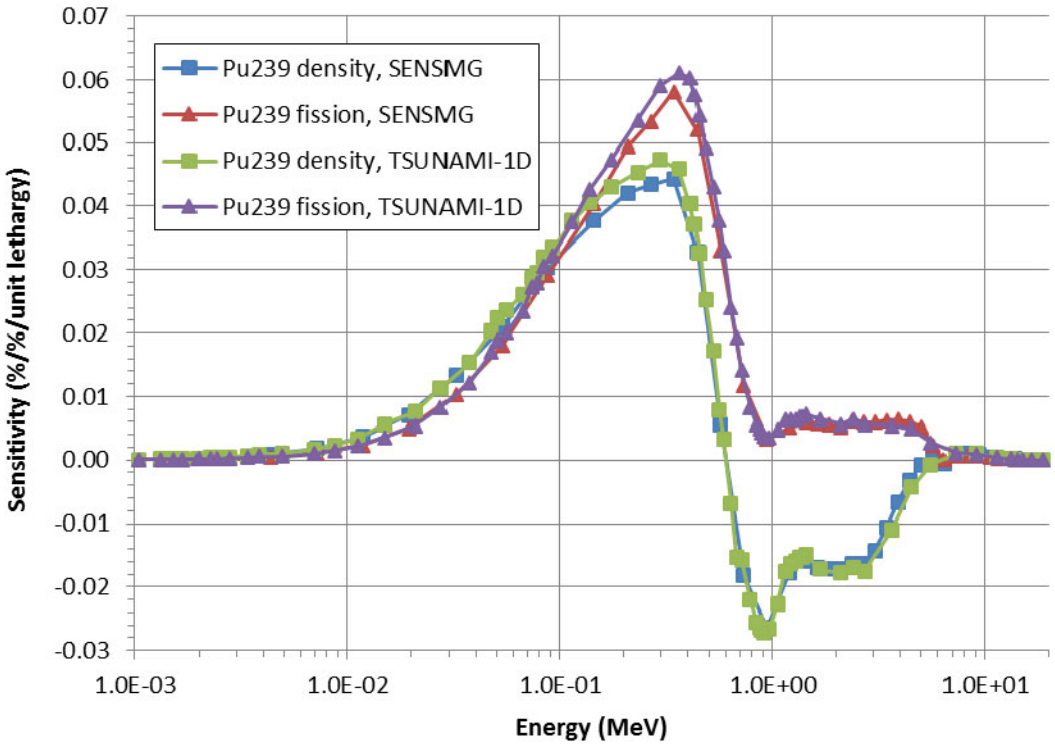

Figure 4. Sensitivity of the ^{237}Np fission to ^{235}U fission ratio to the ^{239}Pu density and fission cross section in Flattop-Pu.

VI.D. Comparison with direct perturbations for a reaction rate with λ-mode flux

A spherical Jezebel model was run. The reaction rate of interest, calculated in a central sphere with a radius of 0.5 cm, was capture in ^{239}Pu. The SENSMG input file is listed in Appendix A. As discussed in Sec. II.B, the reaction rate is put in a ratio with the flux in the reaction-rate region in the denominator. The sensitivity of this reaction rate to the ^{239}Pu capture cross section (indirect effect only, sum of groups) was computed by SENSMG to be –3.1228E-02%/%. (The direct effect, of course, is 1%/%, which was correctly calculated by SENSMG.) A chi vector was used (`-fissdata 2`) to facilitate the comparisons with direct perturbations.

A direct calculation of this reaction rate is shown in Figure 5. The reaction rate of interest, called R1, and the flux are plotted as a function of the relative change in the ^{239}Pu capture cross section in the top figure. The bottom figure plots the ratio.

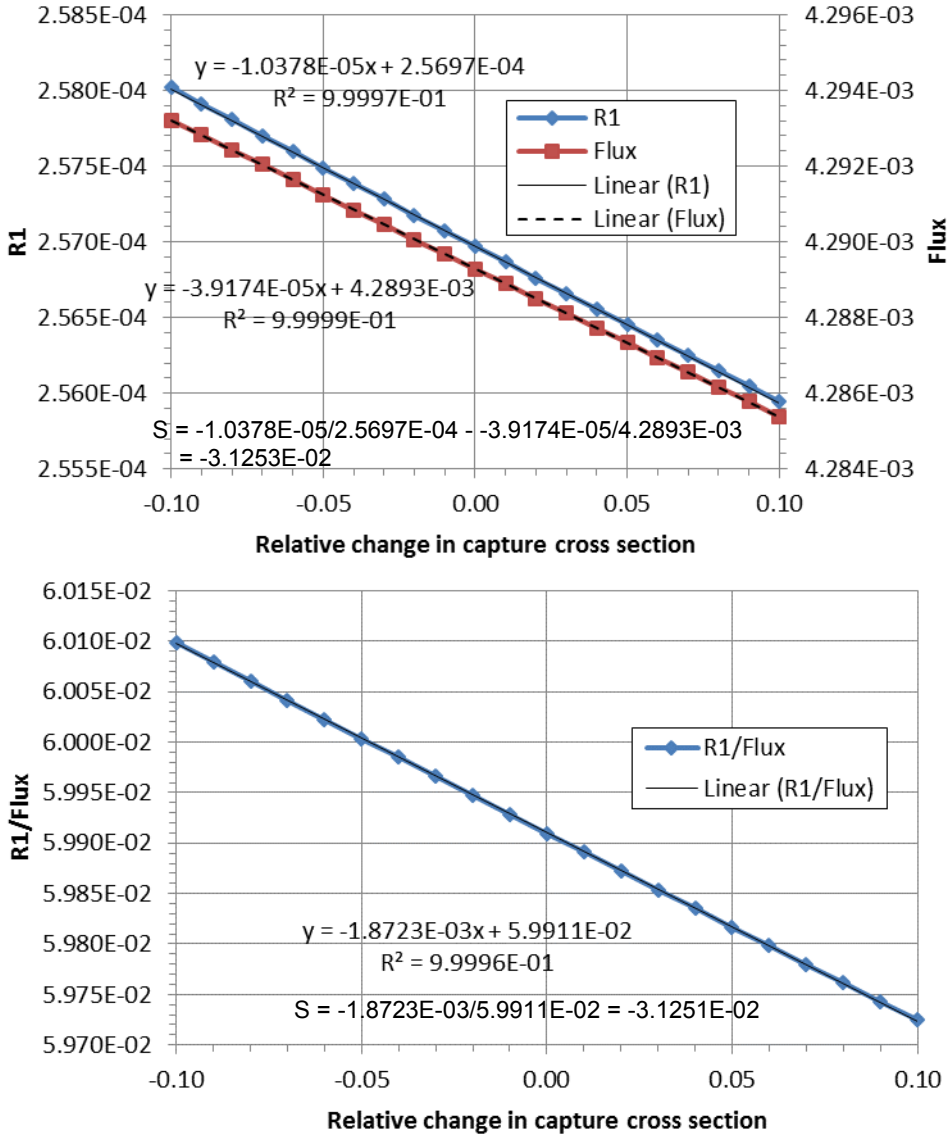

Figure 5. Sensitivity of the ratio of R1 = ^{239}Pu capture reaction rate to the flux to the ^{239}Pu capture cross section (indirect effect) in a one-dimensional Jezebel model. (Top) R1 and flux plotted separately. (Bottom) R1/Flux.

The plots show that the reaction rate, the flux, and the ratio are all very linear in this range of perturbations (±10%). The sensitivity estimated from the slopes of the reaction rate and the flux is –3.1253E-02%/%, and the sensitivity estimated from the slope of the ratio is –3.1251E-02%/%. Both are in excellent agreement with the SENSMG result.

To run the direct perturbation cases, the cross sections for each perturbed case were written directly into a PARTISN input file. A chi matrix cannot be entered this way, which is why a chi vector was used for the sensitivity calculations.

Twenty PARTISN calculations in addition to the base case were run to produce the plots of Figure 5. This seems like overkill, when only two calculations are required for a central difference. However, in verifying SENSMG, many cases were encountered in which central differences gave unreliable results. Indeed, the difficulty computing central differences is another argument for the use of GPT.

VI.E. Comparison with direct perturbations for a reaction-rate ratio with λ-mode flux

A spherical Godiva model was run. The reaction-rate ratio of interest, calculated in a central sphere with a radius of 0.574 cm, was fission in ^{238}U to fission in ^{235}U. The SENSMG input file is listed in Appendix A. The number of energy groups was 70. The sensitivity of this reaction rate to the ^{234}U fission cross section in group 30 (indirect effect only; the direct effect is zero) was computed by SENSMG to be 2.1113E-04%/%. A chi vector was used (`-fissdata 2`) to facilitate the comparisons with direct perturbations. Neither the direct perturbations nor the adjoint-based sensitivities included the effect that changing a fission cross section has on the material chi vector.

The sensitivity of the reciprocal of this reaction rate was also calculated. It was (correctly) the negative of the original sensitivity.

A direct calculation of this reaction-rate ratio is shown in Figure 6. The numerator, fission in ^{238}U, is R1 and the denominator, fission in ^{235}U, is R2. R1 and R2 are plotted as a function of the relative change in the ^{234}U fission cross section in the top figure. The bottom figure plots the ratio.

Note from the *y*-axis scales that the changes plotted are extremely small, even though the range of perturbations is ±100%. The reason that R1 is jagged is that the reaction rates were obtained from PARTISN's edit output, which prints only six significant figures. A smoother curve would be obtained by reading the binary flux file and the binary edit cross section file and constructing the reaction rates in post-processing, as SENSMG does. However, the slope would be close to the least-squares slope shown in Figure 6 and the conclusions of this section would be the same.

The plots show that R1 is fairly linear and R2 and the ratio are very linear in this range of perturbations (±100%). The sensitivity estimated from the slopes of the reaction rates is 2.3777E-04%/%, and the sensitivity estimated from the slope of the ratio is 2.3778E-04%/%. The difference between these and the SENSMG result is ~13%.

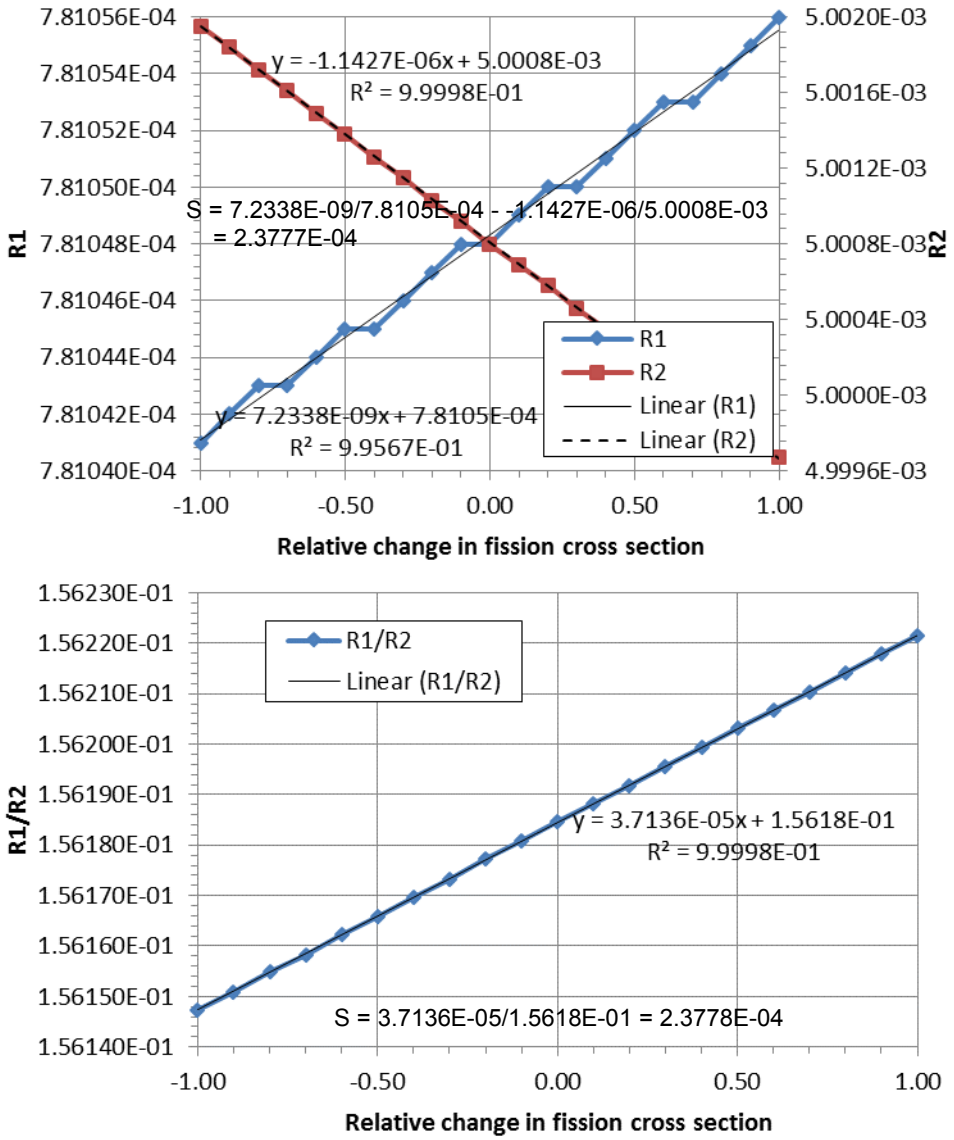

Figure 6. Sensitivity of the ratio of R1 = ^{238}U fission to R2 = ^{235}U fission to the ^{234}U fission cross section in group 30 in a one-dimensional Godiva model. (Top) R1 and R2 plotted separately. (Bottom) R1/R2.

The sensitivity for each of the 70 groups was computed directly as in Figure 6 (20 PARTISN calculations in addition to the base case and a least-squares fit for the slope of the ratio). The sensitivities from SENSMG are compared with the direct sensitivities in Figure 7. The average energy of group 30, whose result is shown in Figure 6, is 0.732 MeV; the sensitivity there is the largest in both curves.

Figure 7 shows the difference discussed previously in this section for group 30 and also differences for other energies. The shapes of the curves are similar, but the adjoint-based sensitivities are more negative by ~10-15%.

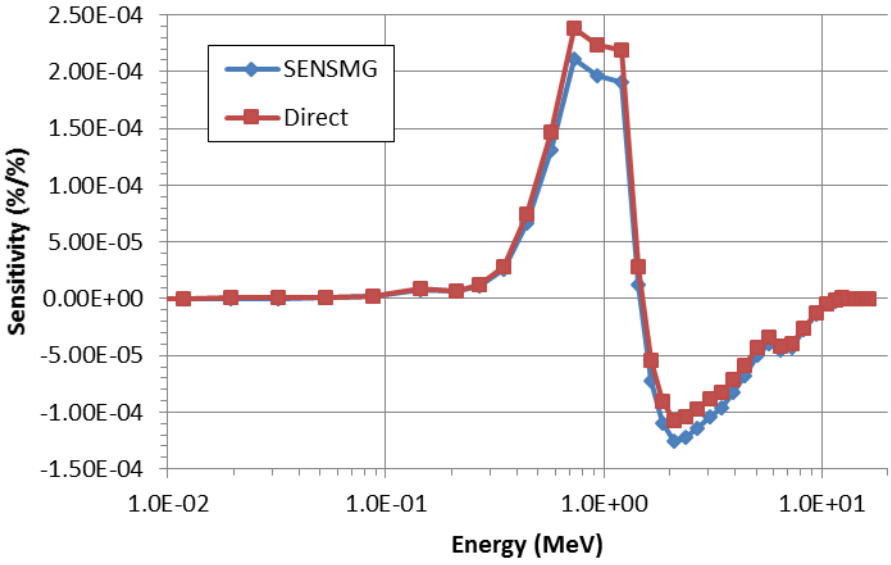

Figure 7. Sensitivity profile of the ratio of R1 = ^{238}U fission to R2 = ^{235}U fission to the ^{234}U fission cross section in a one-dimensional Godiva model.

Since the energy-dependent sensitivities are both positive and negative, these differences strongly affect the total (sum over groups). The total adjoint-based sensitivity is –2.6119E-04%/% and the total direct sensitivity is 3.3178E-05%/%. The direct sensitivity obtained by perturbing the ^{234}U fission cross section in all 70 groups is 2.6441E-05, indicating either nonlinear behavior or inaccuracies in the methodology used to compute direct sensitivities.

It should be noted that the sensitivities computed and discussed in this section are extremely small.

VI.F. Comparison with direct perturbations for α and a reaction-rate ratio with α-mode flux

This is an α eigenvalue problem. The problem is the one-dimensional Jezebel model with the benchmark radius (6.39157 cm) but the realistic Pu-alloy density (15.82 g/cm^3) rather than the benchmark density (15.61 g/cm^3). The reaction-rate ratio of interest, fission in ^{238}U to fission in ^{235}U, was computed in a central sphere of radius 0.5 cm. The SENSMG input file is listed in Appendix A. Thirty-group MENDF71X cross sections, S_{32} angular quadrature, and P_3 scattering were used. A chi vector was used (`-fissdata 2`) to facilitate comparisons with direct perturbations. The α eigenvalue for this model was 0.0373818 /sh.

The sensitivities of the α eigenvalue and the reaction-rate ratio to the P_0 and P_1 (separately) ^{239}Pu self-scattering cross sections in every group (simultaneously) are compared with central differences (computed using cross section perturbations of ±1%) in Table X. The agreement is excellent.

Table X. Sensitivity to ^{239}Pu Self-Scattering for the High-Density Jezebel Model.

	α			Reaction-Rate Ratio		
Scattering Order	SENSMG	Central Diff.	Diff.	SENSMG	Central Diff.	Diff.
0	1.63687E+01	1.6338E+01	0.186%	7.96962E-02	7.9501E-02	0.246%
1	–9.49096E+00	–9.4800E+00	0.116%	–9.73175E-02	–9.7199E-02	0.122%

VI.G. Comparison with direct perturbations for leakage and a reaction-rate ratio in a fixed-source problem

This is a fixed-source problem. The problem is a simplified model of the BeRP ball reflected by 3.81 cm of polyethylene.[39,40] The simplified model has only α-phase plutonium and polyethylene, no steel can or gas fill. The ratio of fission in ^{238}U to fission in ^{235}U was computed in a central sphere of radius 0.25 cm (the actual BeRP ball does not have a cavity for samples). The absolute fission rate in ^{238}U was also computed. The SENSMG input file is listed in Appendix A. Thirty-group MENDF71X cross sections, S_{32} and S_{128} angular quadrature, and P_3 scattering were used. A chi vector was used (`-fissdata 2`). The neutron leakage for this model [using MISC for spontaneous fission and SOURCES4C for (α,n)] was 1.81174×10^6 /s using S_{32} and 1.80663×10^6 /s using S_{128}. A slightly modified version of this problem is discussed in detail Ref. 17, but without the reaction rates.

The sensitivities of the leakage to the two material densities and to the ^{9}Be and ^{240}Pu atom densities in the plutonium are shown in Table XI. They are compared with central differences. The results of Table XI used S_{32} quadrature. The agreement is excellent.

Table XI. Sensitivity of the Leakage to Density for the BeRP Ball Model.

Density	Adjoint	Central Diff.	Diff.
Pu bulk mass density	7.20992E+00	7.21712E+00	–0.100%
Poly bulk mass density	1.56066E+00	1.56032E+00	0.022%
^{9}Be atom density	1.15770E-02	1.15836E-02	–0.057%
^{240}Pu atom density	1.18230E+00	1.18305E+00	–0.064%

The sensitivities of the ratio of fission in ^{238}U to fission in ^{235}U and the absolute fission rate in ^{238}U to the ^{240}Pu density are shown in Table XII, where they are compared with central differences. These calculations were done with S_{32} and S_{128} quadrature, as shown in the table. When going from S_{32} to S_{128} quadrature, the relative differences are reduced by a factor of about 10.

Table XII. Sensitivity of Reaction Rates to ^{240}Pu Density for the BeRP Ball Model.

Reaction	S_N	Adjoint	Central Diff.	Diff.
^{238}U(n,f)/^{235}U(n,f)	32	–1.11391E-02	–1.14502E-02	–2.717%
	128	–1.14238E-02	–1.14488E-02	–0.218%
^{238}U(n,f)	32	1.20874E+00	1.20539E+00	0.277%
	128	1.20497E+00	1.20461E+00	0.030%

The results of Table XII suggest that this problem is not converged with respect to angular quadrature order at S_{32}. Table XIII compares several adjoint-weighted quantities as a function of S_N order. In Table XIII, L^* is the leakage computed using the solution of Eq. (44),

$$L^* \equiv \int_V dV \sum_{g=1}^{G} \int_{4\pi} d\hat{\mathbf{\Omega}} \psi^{*g}(r,\hat{\mathbf{\Omega}}) Q^g(r)\,, \tag{105}$$

which should be equal to L of Eq. (45). Table XIII also evaluates Eq. (53) for the reaction-rate ratio and Eq. (54) for the absolute reaction rate. These quantities are all quite different from their exact values at low S_N orders but they all approach their exact values as the S_N order increases, particularly when the spatial discretization is refined as well. The PARTISN convergence criterion for all cases was 10^{-6}.

Table XIII. Adjoint-Weighted Quantities as a Function of S_N Order for the BeRP Ball Model.

S_N	Fine mesh width (cm)	$(L^* - L)/L$ (should be 0)	Eq. (53) (should be 0)	Eq. (54) (should be 1)
16	0.005	–2.3660E-03	9.0572E-04	1.009210
32	0.005	–6.0765E-04	2.7421E-04	1.002783
64	0.005	–1.5487E-04	7.7350E-05	1.000797
128	0.005	–4.5194E-05	2.1796E-05	1.000219
256	0.005	–1.6662E-05	7.8144E-06	1.000070
512	0.005	–2.4125E-06	4.3070E-06	1.000038
1024	0.005	–3.2741E-06	5.4009E-06	1.000025
1024	0.0005	3.1054E-06	1.0501E-06	1.000007

The results of this section suggest that adjoint-based sensitivities for leakage problems require larger angular quadrature orders than might be expected. See Ref. 41 for more on diagnosing convergence by comparing forward and adjoint quantities.

VI.H. Comparison with direct perturbations for leakage from a slab in a fixed-source problem

This is a fixed-source problem. The problem is a three-region slab. The left region is 1.8 cm of polyethylene, the middle region is 2 cm of a simplified version of the BeRP plutonium, and the right region is 1.8 cm of polyethylene. The only quantity of interest is the leakage from the right side of the slab. The SENSMG input file is listed in Appendix A. Thirty-group MENDF71X cross sections, S_{32} angular quadrature, and P_3 scattering were used. A chi vector was used (`-fissdata 2`). The neutron leakage for this model [using MISC for spontaneous fission; there was no (α,n)] was 1.08877×10^4 /s.

The sensitivities of the leakage to the four boundaries and internal interfaces are shown in Table XIV. They are compared with central differences. The agreement is excellent.

Table XIV. Derivative of the Leakage with Respect to Boundaries and Internal Interfaces for the BeRP Slab.

Surface Location	Adjoint	Central Diff.	Diff.
–2.8 cm	–9.58828E+03	–9.58820E+03	0.0008%
–1.0 cm	–3.25842E+04	–3.25967E+04	–0.0384%
1.0 cm	3.39701E+04	3.39837E+04	–0.0398%
2.8 cm	8.20235E+03	8.20220E+03	0.0018%

The derivatives of Table XIV are not symmetric about the slab's center because the quantity of interest is the leakage from the right side, not the total leakage.

VI.I. Feynman Y problem

The test problem for Feynman *Y* sensitivities used the BeRP ball with 1.480 in. of tungsten reflector.[42] This problem included the 0.03429-cm thickness of NO fill gas and the 0.0305-cm thickness of stainless steel. The input file for SENSMG is listed in Appendix A. Thirty-group MENDF71X cross sections, S_{128} angular quadrature, and P_3 scattering were used. A 30-group detector efficiency function for LANL's NPOD detector was applied. A chi vector was used (`-fissdata 2`). The singles count rate for this model [using SOURCES4C for spontaneous fission and (α,n)] was 2.14903×10^4 /s. The Feynman *Y* was 1.702.

This problem also tested multiple ways of inputting materials: the plutonium is specified using weight fractions and mass density; the NO is specified using atom fractions and atom density; the stainless steel is specified using atom fractions and mass density; and the tungsten is specified using weight fractions and atom density.

The sensitivity of the Feynman *Y* to the mass density of each material and the derivative with respect to each interface location are compared with central differences in Table XV and Table XVI. The agreement is excellent.

Table XV. Sensitivity (%/%) of the Feynman *Y* to Material Densities for the BeRP-W Sphere.

Material	Adjoint	Central Diff.	Diff.
Pu (BeRP Ball)	1.553353E+01	1.553154E+01	0.0128%
NO	2.464145E-05	2.464877E-05	–0.0297%
Steel	4.587978E-02	4.587098E-02	0.0192%
Tungsten	3.312836E+00	3.313388E+00	–0.0167%

Table XVI. Derivative of the Feynman *Y* with Respect to Boundaries and Internal Interfaces for the BeRP-W Sphere.

Surface Location	Adjoint	Central Diff.	Diff.
3.794 cm	1.044908E+01	1.044845E+01	0.0060%
3.82829 cm	–2.588534E+00	–2.588766E+00	–0.0090%
3.85879 cm	–6.460486E-01	–6.460850E-01	–0.0056%
7.61799 cm	6.450146E-01	6.449589E-01	0.0086%

The sensitivity of the Feynman *Y* to the density of four isotopes (representing three materials) are compared with central differences in Table XVII. The agreement is excellent.

Table XVII. Sensitivity (%/%) of the Feynman *Y* to Isotope Densities for the BeRP-W Sphere.

Isotope	Adjoint	Central Diff.	Diff.
^{239}Pu	1.488087E+01	1.488438E+01	–0.0236%
^{240}Pu	6.003422E-01	6.003187E-01	0.0039%
^{56}Fe (in steel)	2.889157E-02	2.888586E-02	0.0198%
^{56}Fe (in tungsten)	5.028331E-02	5.027259E-02	0.0213%

The sensitivity of the Feynman *Y* to the microscopic fission cross section in group 12 of three isotopes in the plutonium are compared with central differences in Table XVIII. The agreement is excellent for ^{239}Pu and ^{240}Pu, but not very good for ^{241}Am. We are analyzing this problem.

Table XVIII. Sensitivity (%/%) of the Feynman *Y* to σ_f^{12} for the BeRP-W Sphere.

Isotope	Adjoint	Central Diff.	Diff.
^{239}Pu	2.246693E+00	2.246573E+00	0.0054%
^{240}Pu	1.082759E-01	1.082696E-01	0.0058%
^{241}Am	4.666387E-03	4.639920E-03	0.5704%

This section verifies the sensitivities of the Feynman *Y* but not the Feynman *Y* (or Sm_2) itself. A one-group slab S_2 ("rod") problem has also been used for verification.[43]

VI.J. lnk3dnt file from auxiliary code

A cylindrical test problem for the `redoin`/`lnk3dnt` capability has been presented.[44] It was a k_{eff} problem with reaction-rate ratios. All of the sensitivities (cross sections, mass densities, and interfaces) from a `redoin`/`lnk3dnt` input created from an auxiliary code matched the sensitivities from an equivalent regular SENSMG input. The `redoin` input file for SENSMG is listed in Appendix A. This was from Sec. III.A.6 of Ref. 44.

VI.K. lnk3dnt file from MCNP

In another cylindrical k_{eff} test problem with reaction-rate ratios for the `redoin`/`lnk3dnt` capability, all of the sensitivities (cross sections, mass densities, and interfaces) from a `redoin`/`lnk3dnt` input created from MCNP6.2 matched the sensitivities from an equivalent regular SENSMG input. The `redoin` input file for SENSMG is listed in Appendix A. This was from Sec. III.A.4 of Ref. 44.

VI.L. Comparison with direct perturbations for k_{eff} and total neutron leakage from a cylinder

Constant-density adjoint-based derivatives of k_{eff} and total neutron leakage with respect to interface and outer boundary locations for a cylinder are compared in detail with direct perturbations in Ref. 13. These calculations used the `rplane`/`zplane` capability (Sec. III.C). General comparisons for constant-volume adjoint-based derivatives with respect to material mass density are also given in Ref. 13. The main point of Ref. 13 is to derive an equation for constant-mass derivatives with respect to interface and outer boundary locations and to make comparisons with direct perturbations. The SENSMG input files used for the neutron problems in Ref. 13 are listed in Appendix A.

For these problems, particularly the k_{eff} problem, the moments expansion approximation of the inner product of angular fluxes, Eq. (27), was extremely inaccurate. Using it lead to errors of 11%, 13%, and 15% in the sensitivity of k_{eff} to the mass density of lead, aluminum, and ^{238}U, respectively (and 0.3% in the sensitivity of k_{eff} to the mass density of ^{235}U). A 17th-order expansion was required to reduce all of the errors below 0.1%.

These results suggest that caution should be applied when using the moments expansion approximation. Better memory management in SENSMG and the ability for PARTISN to print mesh-centered angular flux files from MPI runs of cylindrical problems would obviate this problem.

VII. Summary and Future Work

SENSMG is a tool for calculating the first-order sensitivities of reaction-rate ratios, k_{eff}, and α in critical problems and reaction-rate ratios, reaction rates, leakage, and subcritical multiplication in fixed-source problems to multigroup cross sections, isotope densities, material mass densities, and interface locations using PARTISN. SENSMG treats only GPT-allowable responses.[4] It is installed at
`/usr/projects/data/nuclear/working/sensitivities/bin/sensmg.py`
For access, contact Morgan White (XCP-5). For questions, comments, bugs, suggestions for this user's manual, etc., contact Jeff Favorite (XCP-3).

For all of the problems that SENSMG can treat, the constant-volume and constant-density partial derivatives can be combined (with cell volumes and interface areas) to compute constant-mass partial derivatives.[13]

SENSMG continues to undergo verification.

Future work for SENSMG includes:
1. Implement a more efficient strategy for memory management so that larger cylindrical problems can be run and angular fluxes used.
2. Compute sensitivities consistently when diagonal or BHS transport correction is used.[29]
3. Compute cross-section sensitivities when PARTISN uses self-shielded cross sections.[45,46]
4. Treat subcritical multiplication in cylinders more realistically.
5. Develop and implement a better method for an "absolute" reaction rate for critical problems.
6. Implement a more efficient convergence scheme for the generalized adjoint calculations.
7. Extend SENSMG to compute higher-order sensitivities.
8. Implement a continue-run capability.

If SENSMG is widely used, then it might be worth making some modifications to PARTISN for more efficiency and accuracy. Two specific suggestions are:
1. Have PARTISN print more flux moments than the number used in the transport.
2. Implement a solver such as described in Ref. 4 so that the successive approximation scheme is unnecessary.

Acknowledgments

SENSMG was begun in July 2016 with encouragement from M. C. White and P. Talou (LANL) and funding from the U.S. Department of Energy Advanced Simulation and Computing (ASC) program, Physics and Engineering Models project, at LANL. Since October 2016, SENSMG has been funded by the U.S. National Nuclear Security Administration's Office of Defense Nuclear Nonproliferation Research & Development. Beginning in October 2018, parts of SENSMG have been funded by the ASC program, Primary Validation & Verification project, at LANL.

Alexander R. Clark (North Carolina State University) wrote most of the code for the sensitivities of the excess variance C_2, discussed in Sec. II.E.

References

1. R. E. Alcouffe, R. S. Baker, J. A. Dahl, E. J. Davis, T. G. Saller, S. A. Turner, R. C. Ward, and R. J. Zerr, "PARTISN: A Time-Dependent, Parallel Neutral Particle Transport Code System," Los Alamos National Laboratory report LA–UR–08–7258 (Revised September 2017).

2. M. L. Williams, "Perturbation Theory for Nuclear Reactor Analysis," in *CRC Handbook of Nuclear Reactor Calculations*, Vol. III, Y. Ronen, Ed., CRC Press, Boca Raton, Florida (1986).

3. W. M. Stacey, Jr., *Variational Methods in Nuclear Reactor Physics*, Chap. 1, Academic Press, New York, New York (1974).

4. D. G. Cacuci, "A Paradigm-Shifting Methodology for Sensitivity Analysis of Multiplying Nuclear Systems," *Nucl. Sci. Eng.*, **185**, *3*, 361–383 (2017); http://dx.doi.org/10.1080/00295639.2016.1272993.

5. Sean O'Brien, John Mattingly, and Dmitriy Anistratov, "Sensitivity Analysis of Neutron Multiplicity Counting Statistics Using First-Order Perturbation Theory and Application to a Subcritical Plutonium Metal Benchmark," *Nucl. Sci. Eng.*, **185**, *3*, 406–425 (2017); http://dx.doi.org/10.1080/00295639.2016.1272988.

6. Alexander Clark, "Sensitivity Analysis and Uncertainty Quantification Applied to the Feynman *Y* and Sm_2," Los Alamos National Laboratory report LA–UR–18–30511 (October 29, 2018).

7. Christopher M. Perfetti and Bradley T. Rearden, "Development of a Generalized Perturbation Theory Method for Sensitivity Analysis Using Continuous-Energy Monte Carlo Methods," *Nucl. Sci. Eng.*, **182**, 354–368 (2016); http://dx.doi.org/10.13182/NSE15-13.

8. Jeffrey A. Favorite, "Second-Order Reactivity Worth Estimates Using an Off-the-Shelf Multigroup Discrete Ordinates Transport Code," *Proceedings of the International Conference on the Physics of Reactors* (PHYSOR'08), CD-ROM, Interlaken, Switzerland, September 14–19 (2008).

9. R. T. Evans and D. G. Cacuci, "A Parallel Krylov-Based Adjoint Sensitivity Analysis Procedure," *Nucl. Sci. Eng.*, **172**, 216–222 (2012); http://dx.doi.org/10.13182/NSE11-110.

10. Jeffrey A. Favorite, "Flux Moments and Inner Products (U)," Los Alamos National Laboratory report X-1–RN(U)09–02 (November 25, 2008).

11. Jeffrey A. Favorite, "SENSMG: First-Order Sensitivities of Neutron Reaction Rates, Reaction-Rate Ratios, Leakage, k_{eff}, and α Using PARTISN," *Nucl. Sci. Eng.*, **192**, *1*, 80–114 (2018); http://dx.doi.org/10.1080/00295639.2018.1471296.

12. Jeffrey A. Favorite and Keith C. Bledsoe, "Eigenvalue Sensitivity to System Dimensions," *Ann. Nucl. Energy*, **37**, *4*, 522–528 (2010); http://dx.doi.org/10.1016/j.anucene.2010.01.004.

13. Jeffrey A. Favorite, "Adjoint-Based Constant-Mass Partial Derivatives," *Ann. Nucl. Energy*, **110**, 1052–1059 (2017); http://dx.doi.org/10.1016/j.anucene.2017.08.015.

14. Jeffrey A. Favorite, "(U) Adjoint-Weighted Leakage Time in SENSMG," Los Alamos National Laboratory report LA–UR–19–23677 (April 22, 2019).

15. W. B. Wilson, R. T. Perry, E. F. Shores, W. S. Charlton, T. A. Parish, G. P. Estes, T. H. Brown, E. D. Arthur, M. Bozoian, T. R. England, D. G. Madland, and J. E. Stewart, "SOURCES 4C: A Code for Calculating (alpha,n), Spontaneous Fission, and Delayed Neutron Sources and Spectra," *Proceedings of the American Nuclear Society/Radiation Protection and Shielding Division 12th Biennial Topical Meeting*, Santa Fe, New Mexico, April 14–18, 2002.

16. C. J. Solomon, "MCNP Intrinsic Source Constructor (MISC): A User's Guide," Los Alamos National Laboratory Internal Memorandum LA–UR–12–20252 (updated March 27, 2012).

17. Jeffrey A. Favorite and Sophie L. Weidenbenner, "Sensitivity of a Response to the Composition of an (α,n) Neutron Source," *20th Topical Meeting of the Radiation Protection and Shielding Division of the American Nuclear Society (RPSD-2018)*, Santa Fe, New Mexico, August 26–31 (2018).

18. Keith C. Bledsoe, Jeffrey A. Favorite, and Tunc Aldemir, "Using the Levenberg-Marquardt Method for Solutions of Inverse Transport Problems in One- and Two-Dimensional Geometries," *Nucl. Technol.*, **176**, *1*, 106–126 (2011); http://dx.doi.org/10.13182/NT176-106.

19. John Mattingly, "Computation of Neutron Multiplicity Statistics Using Deterministic Transport," *IEEE Trans. Nucl. Sci.*, **59**, *2*, 314–322 (2012); http://dx.doi.org/10.1109/TNS.2012.2185060.

20. Mark A. Smith-Nelson and Jesson D. Hutchinson, "The Sm_2 Ratio for Evaluating Neutron Multiplicity Models," Los Alamos National Laboratory Report LA–UR–07–6170 (Nov. 21, 2014); http://dx.doi.org/10.2172/1164461.

21. Alex McSpaden, Mark Nelson, and Jesson Hutchinson, "Eliminating Detector Response in Neutron Multiplicity Measurements for Model Evaluation," *Trans. Am. Nucl. Soc.*, **117**, 979–982 (2017).

22. Alexander Clark, Jeffrey A. Favorite, Alexander McSpaden, and Mark Nelson, "Sensitivity Analysis and Uncertainty Quantification of the Feynman Y and Sm_2," *Trans. Am. Nucl. Soc.*, **119**, 805–808 (2018).

23. N. Tsoulfanidis, *Measurement and Detection of Radiation*, Second Ed., Chap. 8, Taylor & Francis, Washington, DC (1995).

24. Jeffrey A. Favorite, "The Solid Angle (Geometry Factor) for a Spherical Surface Source and an Arbitrary Detector Aperture," *Nucl. Instrum. Methods Phys. Res., Sect. A*, **813**, 29–35 (2016); http://dx.doi.org/10.1016/j.nima.2015.12.060.

25. M. S. Zucker and N. E Holden, "Energy Dependence of the Neutron Multiplicity P_ν in Fast Neutron Induced Fission of $^{235,238}U$ and ^{239}Pu," Brookhaven National Laboratory report BNL-38491 (1986).

26. J. W. Boldeman and M. G. Hines, "Prompt Neutron Emission Probabilities Following Spontaneous and Thermal Neutron Fission," *Nuclear Science and Engineering*, **91**, *1*, 114–116 (1985); https://doi.org/10.13182/NSE85-A17133.

27. E. S. Varley and J. Mattingly, "Rapid Feynman-Y Synthesis: Kynea3 Cross-Section Library Development," *Trans. Am. Nucl. Soc.*, **98**, 575–576 (2008).

28. Christopher J Werner, ed., "MCNP® User's Manual, Code Version 6.2," Los Alamos National Laboratory report LA–UR–17–29981, Rev. 0 (Oct. 27, 2017).

29. Jeffrey A. Favorite, "(U) Transport Corrections in SENSMG," Los Alamos National Laboratory report LA–UR–19–24335 (May 8, 2019).

30. S. Frankle, "A Prototype Fine-Group Library for Gamma-Ray Spectroscopy, ACTI," Los Alamos National Laboratory Internal Memorandum XCI:SCF–99–19(U) (updated February 2, 2004).

31. Jeffrey A. Favorite, Zoltán Perkó, Brian C. Kiedrowski, and Christopher M. Perfetti, "Adjoint-Based Sensitivity and Uncertainty Analysis for Density and Composition: A User's Guide," *Nucl. Sci. Eng.*, **185**, *2*, 384–405 (2017); http://dx.doi.org/10.1080/00295639.2016.1272990.

32. Brian C. Kiedrowski, University of Michigan, private communication (2016).

33. B. T. Rearden and M. A. Jessee, eds., "SCALE Code System," Oak Ridge National Laboratory report ORNL/TM-2005/39, Version 6.2 (2016).

34. W. Haeck, D. K. Parsons, M. C. White, T. G. Saller, and J. A. Favorite, "A Comparison of Monte Carlo and Deterministic Solvers for k_{eff} and Sensitivity Calculations," Los Alamos National Laboratory report LA–UR–17–31177 (December 1, 2017); http://permalink.lanl.gov/object/tr?what=info:lanl-repo/lareport/LA-UR-17-31177.

35. W. Haeck, D. K. Parsons, M. C. White, T. G. Saller, and J. A. Favorite, "Comparison of Monte Carlo and Deterministic Solvers for k_{eff} and Sensitivity Calculations," *Proceedings of the International Conference on the Physics of Reactors* (PHYSOR'18), CD-ROM, Cancun, Mexico, April 22–26 (2018).

36. John D. Bess and Mark D. DeHart, "TREAT Fuel Assembly Characterization for Modern Neutronics Validation Methods," *Trans. Am. Nucl. Soc.*, **112**, 373–376 (2015).

37. R. W. Brewer, T. P. McLaughlin, and Virginia Dean, "Plutonium Sphere Reflected by Normal Uranium Using Flattop," *International Handbook of Evaluated Criticality Safety Benchmark Experiments*, PU-MET-FAST-006, Revision 1, Nuclear Energy Agency, Organization for Economic Co-Operation and Development (December 2016).

38. Christopher M. Perfetti, Oak Ridge National Laboratory, private communication (2016).

39. John Mattingly, "Polyethylene-Reflected Plutonium Metal Sphere: Subcritical Neutron and Gamma Measurements," Sandia National Laboratories report SAND2009-5804 Revision 3 (Rev. July 2012).

40. E. C. Miller, J. K. Mattingly, S. D. Clarke, C. J. Solomon, B. Dennis, A. Meldrum, and S. A. Pozzi, "Computational Evaluation of Neutron Multiplicity Measurements of Polyethylene-Reflected Plutonium Metal," *Nucl. Sci. Eng.*, **176**, 167–185 (2014); http://dx.doi.org/10.13182/NSE12-53.

41. Jeffrey A. Favorite, "On the Application of the Discrete Ordinates Method to Fixed-Source Problems (Forward and Adjoint)," Proceedings of the Advances in Nuclear Nonproliferation Technology and Policy Conference 2018 – (ANTPC-2018), CD-ROM, Orlando, Florida, November 11–15 (2018).

42. Benoit Richard, Jesson Hutchinson, Theresa Cutler, Mark Smith-Nelson, Sean Walston, Gregory Keefer, Gregory Caplin, and Wilfried Monange, "Tungsten-Reflected Plutonium-Metal-Sphere Subcritical Measurements," *International Handbook of Evaluated Criticality Safety Benchmark Experiments*, FUND-NCERC-PU-HE3-MULT-002, Revision 0, Nuclear Energy Agency, Organization for Economic Co-Operation and Development (December 2016).

43. Jeffrey A. Favorite, "(U) Analytic One-Group S_2 Slab Problem with Isotropic Scattering and Fission Applied to Neutron Multiplicity Sensitivity," Los Alamos National Laboratory report LA–UR–19–24544 (May 16, 2019).

44. Jeffrey A. Favorite, "(U) LNK3DNT Capability in SENSMG Extended," Los Alamos National Laboratory report LA–UR–19–23874 (April 29, 2019).

45. Thomas G. Saller, "(U) On the Need for Self-Shielding in PARTISN," Los Alamos National Laboratory report CCS-2:18-051 (December 4, 2018).

46. Thomas G. Saller, "Self-Shielding in PARTISN," *Proceedings of the International Conference on Mathematics and Computational Methods Applied to Nuclear Science and Engineering* (M&C 2019), Portland, Oregon, August 25–29 (2019).

JAF:jaf

Distribution:
M. W. Schraad, XCP-DO, MS B218, schraad@lanl.gov
J. E. Sweezy, XCP-3, MS A143, jsweezy@lanl.gov
J. T. Goorley, XCP-3, MS A143, jgoorley@lanl.gov
K. C. Bledsoe, Oak Ridge National Laboratory, bledsoekc@ornl.gov
T. A. Bredeweg, C-NR, MS J514, toddb@lanl.gov
J. D. Hutchinson, NEN-2, MS B228, jesson@lanl.gov
A. T. McSpaden, NEN-2, MS B228, mcspaden@lanl.gov
M. A. Nelson, NEN-2, MS B228, manelson@lanl.gov
R. S. Baker, CCS-2, MS D409, rsb@lanl.gov
J. A. Dahl, CCS-2, MS D409, dahl@lanl.gov
E. J. Davis, CCS-2, MS D409, ejdavis@lanl.gov
T. Saller, CCS-2, MS D409, tgsaller@lanl.gov
R. J. Zerr, CCS-2, MS D409, rzerr@lanl.gov
J. A. Arthur, XTD-IDA, MS T087, jennifera@lanl.gov
J. E. Fessenden-Rahn, XTD-NTA, MS T082, fessende@lanl.gov
P. J. Jaegers, XTD-NTA, MS T082, pjaegers@lanl.gov
C. D. Ahrens, XTD-PRI, MS T086, cdahrens@lanl.gov
J. W. Gibbs, XTD-PRI, MS T086, jwgibbs@lanl.gov
E. F. Shores, XTD-SS, MS T082, eshores@lanl.gov
R. C. Little, XCP-DO, MS F663, rcl@lanl.gov
J. L. Conlin, XCP-5, MS F663, jlconlin@lanl.gov
W. Haeck, XCP-5, MS P365, wim@lanl.gov
D. Neudecker, XCP-5, MS B221, dneudecker@lanl.gov
D. K. Parsons, XCP-5, MS F663, dkp@lanl.gov
P. Talou, XCP-5, MS F644, talou@lanl.gov
M. C. White, XCP-5, MS F663, morgan@lanl.gov
J. L. Alwin, XCP-3, MS A143, jalwin@lanl.gov
A. R. Clark, XCP-3, MS P363, arclark@lanl.gov
G. J. Dean, XCP-3, MS K784, gjdean@lanl.gov
M. E. Rising, XCP-3, MS F663, mrising@lanl.gov
A. Sood, XCP-3, MS F663, sooda@lanl.gov
T. J. Trahan, XCP-3, MS F663, tjtrahan@lanl.gov
J. A. Favorite, XCP-3, MS F663, fave@lanl.gov
X-archive, xarchive@lanl.gov
XCP-3 File

APPENDIX A
SENSMG and MCNP6 INPUT FILES

SENSMG Input File for Sec. VI.A
(Because of memory management issues, this file will only run if it has the title shown [line 1] and if it is named “bck01”.)

```
brian's problem, inspired by TREAT
keff cyl
kynea3
1 / no of materials
1 1001 -8.38215E-05 5010 -4.16390E-06 106012 -9.97955E-01 92235 -1.81803E-03 92238 -1.38591E-04  / TREAT
fuel
 -2.27     / densities
1 1 / no of r layers, no of z layers
  60.    / outer radii
  0. 240.    / heights
 1       / material nos
 0          / number of edit points
 0          / number of reaction-rate ratios
```

SENSMG Input File for Sec. VI.B

```
Pu-Flattop (PU-MET-FAST-006)
keff sphere
mendf71x
2 / no of materials
1 94239 -9.38001E-01 94240 -4.79988E-02 94241 -2.99996E-03 31069 -6.53652E-03 31071 -4.46355E-03 / Pu-
alloy
2 92234 -5.40778E-05 92235 -7.10966E-03 92238 -9.92836E-01 / Flattop natural U
-15.53 -19.00 / densities
3 / no of shells
0.5 4.5332 24.142  / outer radii
 1  1      2       / material nos
 0          / number of edit points
 0          / number of reaction-rate ratios
```

MCNP6 Input File for Sec. VI.B

```
Pu-Flattop (PU-MET-FAST-006)
1   1    -15.53     -1          imp:n=1
2   1    -15.53     -2   1      imp:n=1
3   2    -19.00     -3   2      imp:n=1
9   0                   3      imp:n=0

1  so   0.5
2  so   4.5332
3  so   24.142

mode n
totnu
rand gen=2 seed=100001
kcode 1200000 1.0 50 2050
prdmp j 500
sdef rad=d1 erg=d2
si1  0. 24.142
sp1  -21 2
sp2  -3 0.988 2.249
m1    94239 -9.38001E-01
      94240 -4.79988E-02
      94241 -2.99996E-03
      31069 -6.53652E-03
      31071 -4.46355E-03
m2    92234 -5.40778E-05
      92235 -7.10966E-03
      92238 -9.92836E-01
m3    77191  1.
```

```
m4    92235  1.
m5    77193  1.
m6    77193  1.
e0    1.3900E-10 1.5200E-07 4.1400E-07 1.1300E-06 3.0600E-06
      8.3200E-06 2.2600E-05 6.1400E-05 1.6700E-04 4.5400E-04
      1.2350E-03 3.3500E-03 9.1200E-03 2.4800E-02 6.7600E-02
      1.8400E-01 3.0300E-01 5.0000E-01 8.2300E-01 1.3530E+00
      1.7380E+00 2.2320E+00 2.8650E+00 3.6800E+00 6.0700E+00
      7.7900E+00 1.0000E+01 1.2000E+01 1.3500E+01 1.5000E+01
      1.7000E+01 t
f04:n  1
fm04 (1. 3 -1) $ total
sd04  1.
f14:n  1
fm14 (1. 4 -6) $ fission
sd14  1.
f24:n  1
fm24 (1. 5 -1) $ total
sd24  1.
f34:n  1
fm34 (1. 6 -2:-6) $ absorption (capture+fission)
sd34  1.
print -30
kopts   blocksize = 5
c total
ksen01   xs   cell= (1 2)
ksen02   xs   cell= (1 2)
         erg=1.3900E-10 1.5200E-07 4.1400E-07 1.1300E-06 3.0600E-06
             8.3200E-06 2.2600E-05 6.1400E-05 1.6700E-04 4.5400E-04
             1.2350E-03 3.3500E-03 9.1200E-03 2.4800E-02 6.7600E-02
             1.8400E-01 3.0300E-01 5.0000E-01 8.2300E-01 1.3530E+00
             1.7380E+00 2.2320E+00 2.8650E+00 3.6800E+00 6.0700E+00
             7.7900E+00 1.0000E+01 1.2000E+01 1.3500E+01 1.5000E+01
             1.7000E+01
c chi
ksen03   xs   cell= (1 2) rxn= -1018 constrain=yes
         erg=1.3900E-10 1.5200E-07 4.1400E-07 1.1300E-06 3.0600E-06
             8.3200E-06 2.2600E-05 6.1400E-05 1.6700E-04 4.5400E-04
             1.2350E-03 3.3500E-03 9.1200E-03 2.4800E-02 6.7600E-02
             1.8400E-01 3.0300E-01 5.0000E-01 8.2300E-01 1.3530E+00
             1.7380E+00 2.2320E+00 2.8650E+00 3.6800E+00 6.0700E+00
             7.7900E+00 1.0000E+01 1.2000E+01 1.3500E+01 1.5000E+01
             1.7000E+01
c chi
ksen04   xs   cell= (1 2) rxn= -1018 constrain=no
         erg=1.3900E-10 1.5200E-07 4.1400E-07 1.1300E-06 3.0600E-06
             8.3200E-06 2.2600E-05 6.1400E-05 1.6700E-04 4.5400E-04
             1.2350E-03 3.3500E-03 9.1200E-03 2.4800E-02 6.7600E-02
             1.8400E-01 3.0300E-01 5.0000E-01 8.2300E-01 1.3530E+00
             1.7380E+00 2.2320E+00 2.8650E+00 3.6800E+00 6.0700E+00
             7.7900E+00 1.0000E+01 1.2000E+01 1.3500E+01 1.5000E+01
             1.7000E+01
c nu
ksen05   xs   cell= (1 2) rxn= -7
         erg=1.3900E-10 1.5200E-07 4.1400E-07 1.1300E-06 3.0600E-06
             8.3200E-06 2.2600E-05 6.1400E-05 1.6700E-04 4.5400E-04
             1.2350E-03 3.3500E-03 9.1200E-03 2.4800E-02 6.7600E-02
             1.8400E-01 3.0300E-01 5.0000E-01 8.2300E-01 1.3530E+00
             1.7380E+00 2.2320E+00 2.8650E+00 3.6800E+00 6.0700E+00
             7.7900E+00 1.0000E+01 1.2000E+01 1.3500E+01 1.5000E+01
             1.7000E+01
c total
ksen11   xs   cell= 3
ksen12   xs   cell= 3
         erg=1.3900E-10 1.5200E-07 4.1400E-07 1.1300E-06 3.0600E-06
             8.3200E-06 2.2600E-05 6.1400E-05 1.6700E-04 4.5400E-04
             1.2350E-03 3.3500E-03 9.1200E-03 2.4800E-02 6.7600E-02
             1.8400E-01 3.0300E-01 5.0000E-01 8.2300E-01 1.3530E+00
             1.7380E+00 2.2320E+00 2.8650E+00 3.6800E+00 6.0700E+00
             7.7900E+00 1.0000E+01 1.2000E+01 1.3500E+01 1.5000E+01
             1.7000E+01
c chi
ksen13   xs   cell= 3 rxn= -1018 constrain=yes
         erg=1.3900E-10 1.5200E-07 4.1400E-07 1.1300E-06 3.0600E-06
```

```
             8.3200E-06 2.2600E-05 6.1400E-05 1.6700E-04 4.5400E-04
             1.2350E-03 3.3500E-03 9.1200E-03 2.4800E-02 6.7600E-02
             1.8400E-01 3.0300E-01 5.0000E-01 8.2300E-01 1.3530E+00
             1.7380E+00 2.2320E+00 2.8650E+00 3.6800E+00 6.0700E+00
             7.7900E+00 1.0000E+01 1.2000E+01 1.3500E+01 1.5000E+01
             1.7000E+01
c chi
ksen14   xs   cell= 3 rxn= -1018 constrain=no
         erg=1.3900E-10 1.5200E-07 4.1400E-07 1.1300E-06 3.0600E-06
             8.3200E-06 2.2600E-05 6.1400E-05 1.6700E-04 4.5400E-04
             1.2350E-03 3.3500E-03 9.1200E-03 2.4800E-02 6.7600E-02
             1.8400E-01 3.0300E-01 5.0000E-01 8.2300E-01 1.3530E+00
             1.7380E+00 2.2320E+00 2.8650E+00 3.6800E+00 6.0700E+00
             7.7900E+00 1.0000E+01 1.2000E+01 1.3500E+01 1.5000E+01
             1.7000E+01
c nu
ksen15   xs   cell= 3 rxn= -7
         erg=1.3900E-10 1.5200E-07 4.1400E-07 1.1300E-06 3.0600E-06
             8.3200E-06 2.2600E-05 6.1400E-05 1.6700E-04 4.5400E-04
             1.2350E-03 3.3500E-03 9.1200E-03 2.4800E-02 6.7600E-02
             1.8400E-01 3.0300E-01 5.0000E-01 8.2300E-01 1.3530E+00
             1.7380E+00 2.2320E+00 2.8650E+00 3.6800E+00 6.0700E+00
             7.7900E+00 1.0000E+01 1.2000E+01 1.3500E+01 1.5000E+01
             1.7000E+01
```

SENSMG Input File for Sec. VI.C

```
Pu-Flattop (PU-MET-FAST-006)
keff sphere
mendf71x
2 / no of materials
1 94239 -9.38001E-01 94240 -4.79988E-02 94241 -2.99996E-03 31069 -6.53652E-03 31071 -4.46355E-03 / Pu-
alloy
2 92234 -5.40778E-05 92235 -7.10966E-03 92238 -9.92836E-01 / Flattop natural U
-15.53 -19.00 / densities
3 / no of shells
0.155 4.5332 24.142  / outer radii
 1    1      2       / material nos
 1          / number of edit points
 1          / index of coarse mesh to use for reaction rates
 2          / number of reaction-rate ratios
 92238 16   92235 16 /numerator and denominator
 93237 16   92235 16 /numerator and denominator
```

SENSMG Input File for Sec. VI.D

```
Pu-239 Jezebel (PU-MET-FAST-001)
sph keff
mendf71x / libname
1 / no of materials
1 94239 -9.42090E-01 94240 -4.47189E-02 94241 -2.99354E-03 31069 -6.12984E-03 31071 -4.06790E-03 / Pu-
alloy
-15.61  / densities
2 / no of shells
0.5 6.39157        / outer radii
 1  1              / material nos
 1          / number of edit points
 1          / index of coarse mesh to use for reaction rates
 1          / number of reaction-rate ratios
 94239 10           / denominator is flux
```

SENSMG Input File for Sec. VI.E

```
HEU-MET-FAST-001-02 Godiva
sphere keff
mendf71x / libname
1 / no of materials
1 92234 -1.01999E-02 92235 -9.37100E-01 92238 -5.27004E-02 / Godiva
-18.74 / densities
2 / no of shells
0.5738912155190165 8.7407     / outer radii
 1      1          / material nos
 1          / number of edit points
 1          / index of coarse mesh to use for reaction rates
 2          / number of reaction-rate ratios
 92238 16   92235 16 /numerator and denominator
 92235 16   92238 16 /numerator and denominator
```

SENSMG Input File for Sec. VI.F

```
Pu-239 Jezebel (benchmark radius, realistic density)
alpha sph
mendf71x / libname
1 / no of materials
1 94239 -9.42090E-01 94240 -4.47189E-02 94241 -2.99354E-03 31069 -6.12984E-03 31071 -4.06790E-03 / Pu-
alloy
-15.82  / densities
2 / no of shells
0.5 6.39157        / outer radii
 1  1              / material nos
 1          / number of edit points
 1          / index of coarse mesh to use for reaction rates
 1          / number of reaction-rate ratios
 92238 16   92235 16 /numerator and denominator
```

SENSMG Input File for Sec. VI.G
(Though the composition of material 1 wraps here, it should be on a single line.)

```
BeRP ball, 38.1 mm reflector, no steel or NO
sph lkg
mendf71x
2 / no of materials
1 31069 -1.99071E-04 31071 -1.35938E-04 6000 -2.29800E-04 26054 -5.65054E-07 26056 -9.19000E-06 26057 -
2.16145E-07 26058 -2.90477E-08 20040 -2.89993E-06 20042 -2.03213E-08 20043 -4.34122E-09 20044 -6.86363E-
08 20046 -1.37596E-10 20048 -6.71243E-09 42092 -1.27960E-06 42094 -8.14938E-07 42095 -1.41752E-06 42096
-1.50082E-06 42097 -8.68256E-07 42098 -2.21645E-06 42100 -9.02647E-07 40090 -5.07075E-05 40091 -
1.11812E-05 40092 -1.72786E-05 40094 -1.78916E-05 40096 -2.94387E-06 11023 -5.00013E-05 24050 -2.08690E-
07 24052 -4.18508E-06 24053 -4.83692E-07 24054 -1.22671E-07 28058 -3.36013E-06 28060 -1.33868E-06 28061
-5.91747E-08 28062 -1.91509E-07 28064 -5.06485E-08 4009 -1.00003E-06 5010 -1.84314E-07 5011 -8.15712E-07
12024 -7.79520E-07 12025 -1.02804E-07 12026 -1.17702E-07 94238 -1.59585E-04 92234 -3.94427E-05 94239 -
9.35361E-01 92235 -7.51202E-04 94240 -5.92435E-02 92236 -1.75085E-04 94241 -6.77410E-04 95241 -2.48513E-
03 93237 -7.84266E-05 94242 -2.79593E-04 / BeRP Pu from John Mattingly
2  6000 -8.56299E-01 1001 -1.43701E-01 / HDPE, C2H4
-19.6   -0.95 / densities
3 / no of shells
 0.25 3.794  7.604  / radii
 1    1      2      / material nos
 1          / number of edit points
 1          / index of coarse mesh to use for reaction rates
 2          / number of reaction-rate ratios
 92238 16   92235 16 /numerator and denominator
 92238 16            /numerator and denominator
```

SENSMG Input File for Sec. VI.H

```
BeRP ball slab
slab lkg
mendf71x
2 / no of materials
1 94239 -9.38039E-01 94240 -5.94113E-02 31069 -1.51516E-03 31071 -1.03465E-03 / simple BeRP
2  6000 -8.56299E-01 1001 -1.43701E-01 / HDPE, C2H4
-19.6   -0.95 / densities
3 / no of shells
 -2.800 -1.000 1.000  2.800  / radii
         2     1      2      / material nos
 1          / number of edit points
 1          / index of coarse mesh to use for reaction rates
 0          / number of reaction-rate ratios
 92238 16   92235 16 /numerator and denominator
 92238 16            /numerator and denominator
```

SENSMG Input File for Sec. VI.I

```
BeRP ball, 1.480 in. W reflector (berp_w04_ndi)
sphere feyny
mendf71x
4 / no of materials
1 31069 -1.99071E-04 31071 -1.35938E-04 6000 -2.29800E-04 26054 -5.65054E-07 26056 -9.19000E-06 26057 -
2.16145E-07 26058 -2.90477E-08 20040 -2.89993E-06 20042 -2.03213E-08 20043 -4.34122E-09 20044 -6.86363E-
08 20046 -1.37596E-10 20048 -6.71243E-09 42092 -1.27960E-06 42094 -8.14938E-07 42095 -1.41752E-06 42096
-1.50082E-06 42097 -8.68256E-07 42098 -2.21645E-06 42100 -9.02647E-07 40090 -5.07075E-05 40091 -
1.11812E-05 40092 -1.72786E-05 40094 -1.78916E-05 40096 -2.94387E-06 11023 -5.00013E-05 24050 -2.08690E-
07 24052 -4.18508E-06 24053 -4.83692E-07 24054 -1.22671E-07 28058 -3.36013E-06 28060 -1.33868E-06 28061
-5.91747E-08 28062 -1.91509E-07 28064 -5.06485E-08 4009 -1.00003E-06 5010 -1.84314E-07 5011 -8.15712E-07
12024 -7.79520E-07 12025 -1.02804E-07 12026 -1.17702E-07 94238 -1.59585E-04 92234 -3.94427E-05 94239 -
9.35361E-01 92235 -7.51202E-04 94240 -5.92435E-02 92236 -1.75085E-04 94241 -6.77410E-04 95241 -2.48513E-
03 93237 -7.84266E-05 94242 -2.79593E-04 / Pu from John
2 7014 4.327249E-05 8016 1.0685167-05 / NO fill
3 24050 6.518941E-04 24052 1.257128E-02 24053 1.425319E-03 24054 3.548248E-04 26054 3.442237E-03 26056
5.351259E-02 26057 1.225230E-03 26058 1.633551E-04 28058 6.405671E-03 28060 2.448989E-03 28061
1.060310E-04 28062 3.368464E-04 28064 8.538426E-05 / SS316
4  6000 -2.50058E-05 8016 -1.65864E-05 15031 -1.10319E-04 26054 -4.97920E-04 26056 -8.02687E-03 26057 -
1.87069E-04 26058 -2.53800E-05 28058 -1.38684E-02 28060 -5.39333E-03 28061 -2.37453E-04 28062 -7.66980E-
04 28064 -1.97595E-04 29063 -4.97570E-05 29065 -2.18310E-05 39089 -3.91720E-04 42092 -1.82942E-06 42094
-1.16510E-06 42095 -2.02660E-06 42096 -2.14569E-06 42097 -1.24132E-06 42098 -3.16880E-06 42100 -
1.29049E-06 74182 -2.52813E-01 74183 -1.38025E-01 74184 -2.98357E-01 74186 -2.80976E-01 / tungsten
-19.6   5.395766E-05 -7.62    6.478894E-02 / densities
4 / no of shells
 3.794  3.82829  3.85879  7.61799  / radii
 1      2        3       4         / material nos
 0          / number of edit points
 0          / number of reaction-rate ratios
```

SENSMG Input File for Sec. VI.J

```
     3     0     0     1     0
knowles, high-density solution
input: knowles
 forward input file, keff

&block_1
   b1_inputs=12
   iquad=6
   jm=70
   niso=0
   maxscm=600000000
   jt=70
   it=50
   mt=10
   im=50
   isn=16
```

```
   nzone=10
   ngroup=30
   igeom="r-z"
   fmmix=1
/

&block_2
/
&block_2_arrays
/

&block_3
   b3_inputs=6
   libname="mendf71x"
   fissdata=0
   lib="ndilib"
   fissneut=1
   lng=30
   ebound_size=31
/
&block_3_arrays
   ebound=
      1.700000E+01  1.500000E+01  1.350000E+01  1.200000E+01  1.000000E+01  7.790000E+00  6.070000E+00
3.680000E+00  2.865000E+00  2.232000E+00
      1.738000E+00  1.353000E+00  8.230000E-01  5.000000E-01  3.030000E-01  1.840000E-01  6.760000E-02
2.480000E-02  9.120000E-03  3.350000E-03
      1.235000E-03  4.540000E-04  1.670000E-04  6.140000E-05  2.260000E-05  8.320000E-06  3.060000E-06
1.130000E-06  4.140000E-07  1.520000E-07
      1.390000E-10
/

&block_3_xsec
/

&block_4
   b4_inputs=3
   matspec_size=1
   matls_size=10
   assign_size=1
/
&block_4_arrays
   matspec=
      "atdens"
   matls=
      "m000001" "92235" 1.
      "m000002" "92238" 1.
      "m000003" "8016" 1.
      "m000004" "1001" 1.
      "m000005" "1001" 1.
      "m000006" "6000" 1.
      "m000007" "13027" 1.
      "m000008" "92238" 1.
      "m000009" "92235" 1.
      "m000010" "79197" 1.
   assign=
      "matls"
/

&block_5_int
   b5_inputs=16
   nofxup=1
   ith=0
   cellsol=1
   raflux=0
   xsectp=2
   ievt=1
   rmflux=1
   oitm=9999
   balp=0
/
&block_5_real
   epsi=1.00E-03
   norm=1.0
/
```

```
&block_5_char
/
&block_5_sizes
   isct_size=1
   iitl_size=1
   iitm_size=1
   afluxx_size=5
   afluxy_size=8
/
&block_5_arrays
   isct=
      3
   iitl=
      0
   iitm=
      999
   afluxx=
      11  21  31  41  51
   afluxy=
      1  11  21  31  41  51  61  71
/

&block_6
   b6_inputs=9
   resdnt=0
   igrped=0
   pted=1
   ajed=0
   edmats_size=4
   rsfnam_size=1
   edxs_size=4
   rsfe_size=30
   points_size=100
/  nrrr=3
/
&block_6_arrays
   edisos=
    "92238" "92235"
    "79197"
    "92235" "92238"
   rsfnam=
      "flux"
   edxs=
       "16" "16"
       "10"
       "16" "16"
   rsfe=
      1.  1.  1.  1.  1.  1.  1.  1.  1.  1.
      1.  1.  1.  1.  1.  1.  1.  1.  1.  1.
      1.  1.  1.  1.  1.  1.  1.  1.  1.  1.
   points=
1511 1512 1513 1514 1515 1516 1517 1518 1519 1520
1561 1562 1563 1564 1565 1566 1567 1568 1569 1570
1611 1612 1613 1614 1615 1616 1617 1618 1619 1620
1661 1662 1663 1664 1665 1666 1667 1668 1669 1670
1711 1712 1713 1714 1715 1716 1717 1718 1719 1720
1761 1762 1763 1764 1765 1766 1767 1768 1769 1770
1811 1812 1813 1814 1815 1816 1817 1818 1819 1820
1861 1862 1863 1864 1865 1866 1867 1868 1869 1870
1911 1912 1913 1914 1915 1916 1917 1918 1919 1920
1961 1962 1963 1964 1965 1966 1967 1968 1969 1970
/
```

SENSMG Input File for Sec. VI.K

```
     5     0     0     1     0
knowles problem, high-density solution
*****************************************************
* Input autogenerated by MCNP                       *
* Input for PARTISN kcode run for comparison to MCNP  *
*****************************************************
```

```
&block_1
   b1_inputs=14
   iquad=6
   niso=0
   mt=6
   jt=20
   it=10
   km=1
   jm=20
   fmmix=1
   im=10
   isn=16
   ngroup=30
   kt=1
   nzone=3
   igeom="r-z"
/

&block_2
   b2_inputs=0
/
&block_2_arrays
/

&block_3
   b3_inputs=3
   fissneut=1
   libname="mendf71x"
   lib="ndilib"
/
&block_3_arrays
/

&block_3_xsec
/

&block_4
   b4_inputs=3
   matspec_size=6
   matls_size=10
   assign_size=3
/
&block_4_arrays
   matspec=
      "wtfrac"
      "wtfrac"
      "wtfrac"
      "atdens"
      "atdens"
      "atdens"
   matls=
      "m000001" "92235.711nm" 3.3959000E-05
      "m000001" "92238.711nm" 9.9660400E-03
      "m000001" "8016.710nm" 8.83106001E-01
      "m000001" "1001.710nm" 1.0689400E-01
      "m000002" "1001.710nm" 1.4371600E-01
      "m000002" "6000.710nm" 8.5628400E-01
      "m000003" "13027.710nm" 1.0000000E+00
      "m000004" "92238.711nm" 1.0000000E+00
      "m000005" "92235.711nm" 1.0000000E+00
      "m000006" "79197.710nm" 1.0000000E+00
   assign=
      "zn000001" "m000001" 1.
      "zn000002" "m000002" 1.
      "zn000003" "m000003" 1.
/

&block_5_int
   b5_inputs=12
   oitm=9999
   nofxup=1
   rmflux=1
   ievt=1
/
```

```
&block_5_real
   epsi=1.000E-03
   norm=1.000E+00
/
&block_5_char
   diffsol="mg"
   trcor="no"
   srcacc="dsa"
/
&block_5_sizes
   isct_size=1
   iitl_size=1
   iitm_size=1
/
&block_5_arrays
   isct=
      3
   iitl=
      0
   iitm=
      999
/

&block_6
   b6_inputs=2
   edoutf=3
   massed=1
   points_size=1
/  nrrr=3
/
&block_6_arrays
   edisos=
    "92238" "92235"
    "79197"
    "92235" "92238"
   edxs=
       "16" "16"
       "10"
       "16" "16"
   points=
53
/
```

SENSMG Input File for Sec. VI.L (Ref. 13)
(This is the k_{eff} input file. To change to the neutron leakage input, change “keff” to “lkg”.)

```
4 material input file U235 U238 Al Pb
cyl keff
mendf70x
4 / no. of materials
1 92235 1.000000 /
2 92238 1.000000 /
3 13027 1.000000 /
4 82000 1.000000 /
-18.00 -18.00 -2.70 -11.4 /
3 7 / number of cylinders, number of heights
1.    2.  4.  /
0. 1. 1.5 2. 4. 4.5 6. 7.  / heights, bottom to top
 3 3 3  /material map, top layer
 1 1 3  /material map, next layer
 0 1 3  /material map, next layer
 0 1 4  /material map, next layer
 1 1 4  /material map, next layer
 4 4 4  /material map, next layer
 2 2 2  /material map, bottom layer
 0          / number of edit points
 0          / number of reaction-rate ratios
```

APPENDIX B
ISOTOPES AVAILABLE IN THE KYNEA3 LIBRARY

The ZAIDs listed here are the ones to enter in the input file; SENSMG converts them to the names when writing the PARTISN forward input file. The ZAIDS are intuitive except for four special ones that are needed to distinguish between pairs of the same isotope: 101001 and 1001 for "H1(H2O)" and "H1," respectively; 104009 and 4009 for "Be9(th)" and "Be9," respectively; 6012 and 106012 for "C12" and "C12(gph)," respectively; and 95242 and 195242 for "Am242" and "Am242m," respectively. Note that "H1" does have an $S(\alpha,\beta)$ association: It is "H1(CH2)" from the Vitamin-B6 library.[27]

The order listed here is the order that they appear in the library. The last seven (from "H3" through "Li7") do not have atomic weights in the library. Their atomic weights are hard-coded in the SENSMG source code. All fissionable isotopes use the same induced-fission χ vector.

The neutron group velocities in Kynea3 are in units of cm/μs, so divide by 100 to get cm/sh.

ZAID	Name	ZAID	Name	ZAID	Name	ZAID	Name	ZAID	Name
1000	H	17000	Cl	40000	Zr	74184	W184	94237	Pu237
101001	H1(H2O)	19000	K	41000	Nb	74186	W186	94238	Pu238
1001	H1	20000	Ca	41093	Nb93	75000	Re	94239	Pu239
1002	H2	22000	Ti	42000	Mo	75185	Re185	94240	Pu240
4000	Be	23000	V	47000	Ag	75187	Re187	94241	Pu241
104009	Be9(th)	24000	Cr	47107	Ag107	79000	Au	94242	Pu242
4009	Be9	24050	Cr50	47109	Ag109	79197	Au197	94243	Pu243
5000	B	24052	Cr52	48000	Cd	82000	Pb	94244	Pu244
5010	B10	24053	Cr53	49000	In	82206	Pb206	95241	Am241
5011	B11	24054	Cr54	50000	Sn	82207	Pb207	95242	Am242
6000	C	25000	Mn	56000	Ba	82208	Pb208	195242	Am242m
6012	C12	25055	Mn55	56138	Ba138	83000	Bi	95243	Am243
106012	C12(gph)	26000	Fe	63000	Eu	83209	Bi209	96241	Cm241
7000	N	26054	Fe54	63151	Eu151	90000	Th	96242	Cm242
7014	N14	26056	Fe56	63152	Eu152	90230	Th230	96243	Cm243
7015	N15	26057	Fe57	63153	Eu153	90232	Th232	96244	Cm244
8000	O	26058	Fe58	63154	Eu154	91000	Pa	96245	Cm245
8016	O16	27000	Co	63155	Eu155	91231	Pa231	96246	Cm246
8017	O17	27059	Co59	72000	Hf	91233	Pa233	96247	Cm247
9000	F	28000	Ni	72174	Hf174	92000	U	96248	Cm248
9019	F19	28058	Ni58	72176	Hf176	92232	U232	1003	H3
11000	Na	28060	Ni60	72177	Hf177	92233	U233	2000	He
11023	Na23	28061	Ni61	72178	Hf178	92234	U234	2003	He3
12000	Mg	28062	Ni62	72179	Hf179	92235	U235	2004	He4
13000	Al	28064	Ni64	72180	Hf180	92236	U236	3000	Li
13027	Al27	29000	Cu	73000	Ta	92237	U237	3006	Li6
14000	Si	29063	Cu63	73181	Ta181	92238	U238	3007	Li7
15000	P	29065	Cu65	73182	Ta182	93237	Np237		
15031	P31	31000	Ga	74000	W	93238	Np238		
16000	S	39000	Y	74182	W182	93239	Np239		
16032	S32	39089	Y89	74183	W183	94236	Pu236		